

**Mathematical modeling of the population
dynamics and optimal control of COVID-19
disease**



Jené Mercia van Schalkwyk

A project submitted in fulfillment of the requirements
for the degree of
Master of Science

UNIVERSITY of the
in the
Department of Mathematics and Applied Mathematics
WESTERN CAPE
University of the Western Cape

Supervisor: **Prof. P. J. Witbooi**

Co-supervisors: **Dr. M. U. Nsuami, Dr. S. Maku-Vyambwera**

26 September 2023

Contents

Abstract	iii
Acknowledgements	v
Declaration	vi
Index of Abbreviations	vii
Index of Symbols	vii
1 Introduction	1
1.1 History of diseases: COVID-19	1
1.2 Objectives	6
1.3 Structuring of the project	7
2 Literature review	8
3 Mathematical preliminaries	17
3.1 Fundamental measures in epidemiology	18
3.2 General first-order differential equation	19
3.3 Invariant set	19
3.4 Equilibrium solution	21
3.5 The Routh-Hurwitz criterion	23
3.6 Linearization	23

3.7	The direct method of Lyapunov	26
3.8	The second additive compound matrix	30
3.9	Compartmental modeling: spread of diseases	30
3.9.1	Model terminology	31
3.9.2	The method of the next generation matrix operator	37
3.10	Pontryagin's maximum principle	38
3.11	Optimal control method	39
3.12	Sensitivity analysis	41
4	A model of COVID-19 population dynamics	42
4.1	Mathematical model	42
4.2	Boundedness and positivity of solutions	47
4.3	Equilibria and the basic reproduction number of our <i>SIARP</i> Model	50
4.3.1	The next generation matrix operator	51
4.4	Existence of the endemic equilibrium	52
4.5	Global stability of the disease-free equilibrium	60
5	South African population during its first wave of COVID-19	64
5.1	Sensitivity analysis of R_0	65
5.2	Numerical simulations	69
5.2.1	The country under lockdown and behaviour of South Africans	70
5.2.2	Graphical representation of new and active cases	71
6	Optimal control	75
6.1	The optimal control problem	75
6.1.1	Constructing the Hamiltonian H for pointwise minimization	78
6.2	Numerical results and discussion	81
7	Conclusion	87

Abstract

Since the onset of the COVID-19 pandemic, researchers speculated that this virus would create numerous challenges in the daily lives of individuals, especially medical and governmental authorities as they are put under pressure to effectively manage the problem. Previous information gathered by researchers shows that the strain in trying to control this ongoing COVID-19 outbreak is largely due to asymptomatic infectives. This outbreak underlines just how crucial it is to find therapeutics to target this virus so that the spread of the infection and the number of fatalities can be slowed down to reduce the pressure. Further research is being done to determine possible treatments that can be beneficial in controlling the spread of the disease. In this dissertation we construct, analyse and demonstrate the utility of mathematical models of the disease dynamics of COVID-19, and in particular we consider the effect of migrants into and out of the local population, asymptomatic carriers, vaccination, and also effect of the environmental reservoir of the pathogen, the COVID-19 virus (SARS-CoV-2). Such models are useful to public health authorities for the purpose of making future projections and to test the feasibility of certain combinations of interventions for controlling the disease. For this dissertation, we provide an insight into mathematical epidemiology by developing a model that considers the effect of migrants into and out of the local population, asymptomatic carriers, vaccination, and also effect of the environmental reservoir of the pathogen, the COVID-19 virus (SARS-CoV-2). Similar work on coronavirus diseases such as Severe Acute Respiratory Syndrome (SARS), and Middle Eastern Respiratory Syndrome (MERS) assists us with describing and analysing compartmental models in epidemiology for disease trans-

mission of COVID-19. Calculations of the basic reproduction number, R_0 , will be shown as this parameter measures the ability of the disease to spread, and become endemic (if $R_0 > 1$), or ultimately vanish from the population (if $R_0 < 1$). Through our investigation R_0 yielded 0.5348. Equilibrium points of the model system are studied, and you will come to see that we ended up with a cubic equation in I^* . For this we state and prove two theorems to show that our system has a unique endemic equilibrium point X^* for cases when the influx rate of asymptotically infected migrants is positive ($B_1 > 0$), and for when the influx rate is zero ($B_1 = 0$). We then also analyse the global stability of the disease-free equilibrium with Lyapunov techniques, and prove that the disease-free equilibrium of the COVID-19 model is globally asymptotically stable. Our study includes deterministic modelling. Sensitivity analysis of the basic reproduction number R_0 is also done where we use our model to show how it fits real data during the first wave in South Africa between 20 July 2020 to 2 November 2020. We want to see how the importance of the threshold quantity R_0 is validated through our investigation. Finally, we formulate a deterministic optimal control problem and prove its existence, and solve it using Pontryagin's Maximum Principle. The numerical simulations of Euler's method and the Forward-Backward fourth-order Runge-Kutta method are then done in Octave. Through this we see that the control in the form of vaccination is more efficient in reducing the spread of the virus compared to the control of non-pharmaceutical intervention. Our dissertation is then fully rounded off with thoughtful and useful ideas for future research. All of this is done to test mathematically the feasibility, and efficiency of certain public health interventions such as different levels of lockdown, social distancing, extensive screening and testing, and vaccination.

Key words: COVID-19, Asymptomatic carrier, Environmental reservoir, Basic reproductive number, Disease-free equilibrium, Endemic equilibrium, Hamiltonian, Lockdown, Vaccination.

Acknowledgements

2 Corinthians 9:6

Remember that the person who sows few seeds will have a small crop; the one who sows many seeds will have a large crop.

First and foremost, I would like to express my deepest gratitude to God. I give Him all my thanks. Without His strength and guidance, I surely could not have done this alone - I am forever grateful.

To my supervisor Prof. P. J. Witbooi and my co-supervisors Dr. M. U. Nsuami and Dr. S. Maku-Vyambwera, thank you for taking me on as your Master's student. I am immensely grateful for the patience you have shown me, and for your invaluable feedback whilst working on my research.

Many thanks to my friends, and fellow staff members at the Department of Mathematics and Applied Mathematics for your kind and encouraging words throughout this process. Additionally, I extend a thank you to the University of Western Cape, and the Department of Mathematics and Applied Mathematics for the generous financial support through the departmental study bursary.

Lastly, to my family and friends, you have been with me through it all. I appreciate each and every one of you for your encouragement, love and support.

Many blessings to all.

Declaration

I declare that *Mathematical modeling of the population dynamics and optimal control of COVID-19 disease* is my own work, that it has not been submitted for any degree or examination in any other university, and that all the sources I have used or quoted have been indicated and acknowledged by complete references.

Jené Mercia van Schalkwyk

26 September 2023

UNIVERSITY *of the*
WESTERN CAPE

Signed:



Index of abbreviations

TB - Tuberculosis

WHO - World Health Organization

HIV/AIDS - Human immunodeficiency virus/Acquired immunodeficiency syndrome

COVID-19 - Coronavirus disease of 2019

SARS - Severe acute respiratory syndrome

SARS-Cov-2 - Severe acute respiratory syndrome coronavirus 2

MERS - Middle eastern respiratory syndrome

DE/ODE - Differential equation/Ordinary differential equations

SLE - Systemic lupus erythematosus

ACE - Angiotensin-converting enzyme

SIRS - Systemic inflammatory response syndrome

FDA - Food and Drug Administration

CDC - Centers for Disease Control and Prevention

SI - Susceptible-Infectious

SIS - Susceptible-Infectious-Susceptible

SIR - Susceptible-Infectious-Recovered

SIRS - Susceptible-Infectious-Recovered-Susceptible

PHEOC - Public Health Emergency Operations Centre

NCCC - National COVID-19 Command and Control Council

Index of symbols

(C^*, D^*) - Steady state of the equations

$D^{[2]}$ - The second additive compound matrix is a matrix of order $\binom{k}{2}$

$S(t)$ - Hosts who are susceptible to the disease at time t

$E(t)$ - Hosts exposed (latent) to the disease at time t

$I(t)$ - Hosts that are able to spread the disease through contact with susceptible hosts at time t

$R(t)$ - Hosts removed due to reinfection being possible, or for spreading the disease again, or those that have recovered successfully at time t

R_0 - The basic reproduction number

E^* - The endemic equilibrium

$H(u, z(u), v(u), \alpha(u))$ - Hamiltonian function H

$J(v(u), z(u), u)$ - Objective functional J

C^{Ro}_m - The normalized-forward sensitivity index

List of Figures

3.1	The compartmental diagram for the SI model	32
3.2	The compartmental diagram for the SIS model	34
3.3	The compartmental diagram for the SIR model	36
4.1	The flow diagram for the <i>SIARP</i> model	45
5.1	Daily new cases averaged over seven days during first wave, 105 days, in 2020 parameters as in Table 5.1, $R_0 = 0.5348$	73
5.2	Daily new cases averaged over seven days during the first wave, 105 days in 2020, for the modified model.	73
5.3	Model output of active cases averaged over seven days during the first wave, 105 days in 2020, with parameters as in Table 5.1.	74
5.4	Model output of active cases averaged over seven days during the first wave, 105 days in 2020, for the modified model.	74
6.1	Susceptible population under optimal control strategies	83
6.2	Symptomatic infectious population under optimal control strategies.	83
6.3	Asymptomatic infectious population under optimal control strategies.	84
6.4	Recovered population under optimal control strategies.	84
6.5	Pathogen population under optimal control strategies.	85
6.6	Non-pharmaceutical intervention.	85
6.7	Vaccination control.	86

6.8 Combination of non-pharmaceutical intervention u_1^* and vaccination control u_2^* 86



List of Tables

5.1 Parameters with values and their descriptions 66

5.2 Sensitivity indices of R_0 68



Chapter 1

Introduction

For this chapter, we make use of the following references: Vecchio *et al.* [2], Shahid *et al.* [3], Kukla *et al.* [5], Guan *et al.* [21], Brauer [33], Böttiger and Norrby [34], Maku-Vyambwera and Witbooi [35], Witbooi and Maku-Vyambwera [36], McNeill [37], Ellner and Gallant and Theiler [38], Glomski and Ohanian [39], Dietz [40], Hamer [41], Ross [42], McKendrick [43], Bailey [44], Centers for Disease Control and Prevention [46], Volkow [47], Bernoulli [49], En'ko [50], and Kermack and McKendrick [51].

1.1 History of diseases: COVID-19

Diseases such as measles, influenza, tuberculosis (TB), and smallpox to name a few, are considered communicable diseases. The World Health Organization (WHO) defines communicable diseases as infectious diseases caused by microorganisms such as bacteria, viruses, parasites, and fungi that can spread from one source (person, or animal) to another. Every year millions of people in the western world suffer from issues caused by respiratory infections, diarrhoea, measles, easily treatable diseases, and those considered as not threatening. Other diseases such as typhus, malaria, schistosomiasis, and cholera are endemic (a situation in which a disease is always present) in different world regions. For the most part, sources that are infected by infectious microorganisms, their bodies

build immunity against reinfection, while sources infected by diseases transmitted by bacteria, their bodies do not allow immunity against reinfection. For sexually transmitted diseases such as HIV/AIDS with homosexual, or heterosexual transmission, each sex acts as a vector whereby the disease is then transmitted between the two sexes. Information regarding the basics of the HIV/AIDS disease that can help one to avoid getting the virus, if one is HIV-negative, and avoid transferring it to someone, if one is indeed HIV-positive can be found in [33, 35, 36].

The process of disease transmission has majorly shaped and has been a topic of interest in the field of epidemiology throughout history. The word epidemiology stems from late nineteenth-century Greece, and is roughly translated as ‘the knowledge of what is over the people’. Its conventional definition is the branch of medicine, which deals with the incidence, distribution, and possible control of diseases, and other factors relating to health. Subclinical and clinical infections are caused by numerous viruses. A disease is subclinical, if it has no identifiable clinical findings; no sign of showing symptoms. This type of disease is unmistakable from its clinical counterpart where signs and symptoms can be recognized. Both of these diseases are very significant in the spread of infections. The term epidemic is defined as - the occurrence of a particular disease in a frequency exceeding that which should be expected under normal conditions. The term pandemic is denoted as - outbreak of infections of exceptional proportions, including a spread over continents. In simple terms, an epidemic is the sudden outbreak of a disease, and a pandemic is an epidemic that spreads through the human population across a large region, the continent, or worldwide [34, 37].

We want to focus on how the inflow and outflow of migrants, mainly the asymptomatic carriers of the virus, affected the South African population during the first wave of COVID-19. In our investigation we will also include the effect of the environmental reservoir of the pathogen. Studying these will give us a better understanding of COVID-19 pandemic’s evolution. In addition, our investigation will include examination of previous epidemics such as the 2002 SARS outbreak and the 2012 MERS outbreak. Both of these

occurrences elicited significant concern and piqued public curiosity. This will give us a guideline on how to approach our own investigation. We hope to provide an insight into mathematical epidemiology with the help of mathematical models for the spread of diseases mentioned above, and with tools to analyze them. Research-based investigations are generally depicted for acquiring knowledge, and for examining assumptions. Investigations in epidemiology with certain parameters are often hard to deal with, or unattainable to depict, and even when it is attainable to set out an investigation, there are important ethical inquiries involved in retaining treatment from a class of parameters. Now and then it is possible to acquire information through reports of an epidemic, or endemic disease levels, but this leaves room for inaccuracy. Additionally, information is capable of having a sufficient amount of irregularities, such that important inquiries of interpretations are raised [33, 38]. As a result, it is extremely difficult to approximate parameters and to fit models. Which leads to questioning, ‘What role does mathematical modeling have in epidemiology? Is it truly useful?’. The book of Brauer [33] states that mathematical modeling in the world of epidemiology broadens one’s understanding of the fundamental structures and the processes that determine the spread of diseases. He also suggests different strategies to control diseases. During the process of an investigation to acquire information, some models oftentimes behave in problematic ways. This is due to the information being unrepeatable, the total amount of points that contain information being restricted and then being subjected to errors in measurements. An example of this is that most mathematical models in epidemiology generally display a “threshold” behavior. This means that, if the basic reproduction number R_0 is strictly less than one a disease will die out, and if R_0 is greater than one there will be an epidemic. This principle is generally used in estimating the usefulness of vaccination policies, it may also be useful during prevention policies, and the possibility that a disease may be terminated; this principle of R_0 is one, which explains the control of the spread of diseases, see for instance in [33, 35, 36].

Thanks to historical public health physicians, numerous advancements were made in the

mathematical modelling of communicable diseases. In 1760, a member of a famous family of mathematicians called Daniel Bernoulli [49] was the first known physician to implement a defense against smallpox utilizing inoculation (a set of methods of artificially inducing immunity against various infectious diseases). He created the first compartmental model of infectious disease, and constructed and solved a differential equation (DE) detailing the dynamics of infections which is still very significant in present times. P.D. En'ko [50] was the first to largely contribute to the world of modern mathematical epidemiology between the years 1873 and 1894, and until the beginning of the 20th-century development of mathematical epidemiology was obstructed by the lack of knowledge about the spread of infectious diseases. The foundations of the entire approach to epidemiology were based on compartmental models laid by public health physicians such as Ross, Hamer, McKendrick, and Kermack between 1900 and 1935 [33, 35, 36, 39, 40]. In 1906, Hamer [41] constructed and examined a discrete-time model, because he wanted to understand the outbreak of the measles epidemic. He proposed that the spread of infection depends on the product of susceptible and infective individuals. In 1911, Ross [42] developed models of differential equations (DEs) for malaria as a host-vector disease, because he was interested in the spread and control of malaria. For his contribution; demonstrating the dynamics of the transmission of malaria between mosquitoes and humans, he was awarded the second Nobel Prize in Medicine. In 1926, McKendrick [43] developed the first stochastic theory, and by 1930 Kermack and McKendrick [51] had already established the threshold theorem which shows that the density of susceptible individuals must exceed a certain critical value for an epidemic outbreak to occur. The Kermack-McKendrick model is a compartmental susceptible-infectious-recovered (SIR) model with the population regarded as divided into three classes: individuals susceptible to disease, individuals infected by the disease, and individuals recovered from the disease. The models can be formulated as a system of ordinary differential equations (ODEs). The SIR systems have over time been expanded to include classes accommodating vaccination, latently infected carriers, quarantine, and other situations. An SIS model is used to describe a disease with no immunity against reinfection. SEIR and SEIS are models with an exposed period between being infected,

and becoming infective, and SIRS is a model, that describes short-term immunity on recovery from an infection. The models mentioned above have been cited frequently in the literature, and are formulated as differential equations (DEs) [33, 35, 36, 44]. As we stated previously, COVID-19 is a virus that mainly attacks the respiratory system of an individual, and depending on the person's age and health status is proven to be fatal. Researchers have found that this virus causes more fatalities and is especially bad for geriatrics with comorbidities (the presence of one, or more additional conditions co-occurring with a primary condition), where the most common comorbidities are diabetes, chronic kidney disease, respiratory disease, hypertension, cardiac disease, renal disease, malignancy, and pregnancy. Apart from geriatrics, individuals that have previously suffered from opioid use disorder are also more likely to be infected by the virus as they have increased physical, and psychological comorbidity, thus meaning, that they are oftentimes alienated from society. This results in making it harder for them to get assisted with health care [2, 47]. Geriatrics are more severely affected by the virus due to these comorbidities. Furthermore, numerous adults having diabetes, CKD, and hypertension are assigned angiotensin-converting enzyme (ACE) inhibitors, and angiotensin II receptor blockers as treatment. These medicaments cause the upregulation in ACE-2 receptors (receptors utilized by the virus to penetrate host cells), but these medicaments need further research especially in the roles that they play during this COVID-19 pandemic, as it has been speculated to increase the risk of infection. Data collected from the Centers for Disease Control and Prevention (CDC) [46] revealed that in the United States alone, geriatrics make up 17 percent of society, whereby 31 percent were infected by COVID-19, 45 percent of individuals were hospitalized, 53 percent were admitted into intensive care units, and 80 percent of fatalities were caused by infection. This indicates that older individuals are more likely to get infected by the virus as compared to the general public. COVID-19 has primarily been associated with Respiratory Distress Syndrome (breathing disorder that affects newborns), but gastrointestinal symptoms (heartburn, constipation, and bloating), and acute liver failure have also been reported. The process of liver injury is poorly perceived as a consequence of gut barrier, and microbiome alterations, viral

hepatitis, Systemic Inflammatory Response Syndrome, or SIRS (which is an inflammatory state affecting the whole body), intensive care treatment, or drug toxicity. Liver failure amongst individuals infected by COVID-19 is still not clearly understood, however research shows that it results in individuals infected by SARS and MERS [3, 5, 21, 46].

1.2 Objectives

1. Investigating the evolution of the COVID-19 pandemic, especially focusing on how much the inflow and outflow of migrants contributed to the effects on the South African population during the first wave from 20 July 2020 until 2 November 2020.
2. Developing a deterministic model that considers the effect of migrants into and out of the local South African population, asymptomatic carriers, and also effect of the environmental reservoir of the pathogen, the COVID-19 virus.
3. Formulating and solving an optimal control problem through efficiency analysis by introducing two control measures; non-pharmaceutical methods and vaccination control, into the COVID-19 model to see which control strategy works best to control and minimize the rate of infection of the coronavirus in the infectious class I and asymptomatic class A .
4. Improving skill in computer algorithms coding, and simulation in mathematical modelling. All code is done in Octave.
5. Interpretation of the obtained results via use of the developed model will hopefully give us a better understanding of the evolution of the COVID-19 pandemic during its first wave in South Africa and the effects it had on the population during this period.

1.3 Structuring of the project

In Chapter 1, we give some background on the history of some diseases, and discuss briefly on COVID-19. Chapter 2 looks more into SARS-CoV-2. It gives information on where and how it possibly originated, those who are more likely to get infected with the virus, research that was done on getting a vaccine in the works, and rules set out by governmental authorities that the public had to follow to avert the re-emergence of the virus. Chapter 3 gives a brief introduction to disease transmission in epidemiology by means of defining consequential concepts and properties. Chapter 4 introduces compartmental modelling of the COVID-19 population dynamics. Other concepts such as invariant region, positivity of solutions, disease-free equilibrium point, basic reproduction number, the existence of the endemic equilibrium point, and stability analysis are also discussed. Sensitivity analysis of the basic reproduction number R_0 , and numerical simulations are shown in Chapter 5. Here we look at the time period from 20 July 2020 until 2 November 2020 and we investigate how the South African population was affected by COVID-19 during the first wave. We provide results and discussion. In Chapter 6 we formulate and solve the optimal control problem by introducing two control measures into the COVID-19 model, also showing its impact via coding and simulations. In Chapter 7 we give some concluding remarks, including insightful and constructive ideas for future research.

Chapter 2

Literature review

In this chapter the following references are used: Fanelli and Piazza [1], Perez and Talebi [4], Kukla *et al.* [5], Al-Tawfiq and Rodriguez-Morales [6], Park and Thwaites and Openshaw [7], Gautam and Kaphle and Shrestha and Phuyal [9], Ford *et al.* [10], Shah and Modi and Sagar [11], Yao *et al.* [12], Strzelecki and Rizun [13], Padron-Regalado [14], Mcaleer [15], Vellingiri *et al.* [16], Ahmed and Quadeer and Mckay [17], Khan and Karatas and Rahman [18], Yaqinuddin and Kashir [19], Phelan and Katz and Gostin [20], Guan *et al.* [21], Huang *et al.* [23], Chen *et al.* [24], World Health Organisation [25] and [26], Shen *et al.* [27], James and Pitchford and Plank [28], Gopinath *et al.* [29], Kim *et al.* [30], Cowling *et al.* [31], and Hodcroft [32], Brauer [33], Maku-Vyambwera and Witbooi [35], Witbooi and Maku-Vyambwera [36], Worldometer [48], Broadbent and Combrink and Smart [70], Witbooi [77], World Health Organization [81], Moonasar *et al.* [90], Mukumbang and Ambe and Adebisi [91], Mwalili, Kimathi, Ojiambo, Gathungu and Mbogo [95], World Health Organisation [98], South African Government [99], South African News [100], Blumberg and Jassat and Mendelson and Cohen [101], South African Government [102], Statistics South Africa [103], and Migration Data Portal South Africa [104].

COVID-19 is considered to be chronologically the third most highly pathogenic coronavirus to emerge in the past 20 years after SARS and MERS. Its current outbreak

underlines just how crucial it is to find therapeutics to effectively lower the spread of cases as well as fatalities. Although research is currently being done to determine possible treatments to help control transmission, the WHO, CDC, and the US Food and Drug Administration (FDA) stated that no treatments have presently been found to effectively aid in the prevention of becoming infected. Human, and non-human beings such as geriatrics and persons that suffered from opioid use disorder (OUD) because of their comorbidities, and certain animals are more likely to get infected. From day one of this pandemic, researchers speculated that this virus would create numerous challenges in the daily lives of individuals, especially medical and governmental authorities as they are placed under pressure to try and effectively keep things under control. This current outbreak of COVID-19 underlines just how crucial it is to find therapeutics to target this virus so that the spread of cases, and the number of fatalities can be slowed down to reduce the pressure. Further research is being done to determine possible treatments that can be beneficial in controlling the spread of this disease. The development of vaccine candidates is already underway, as the method of drug repositioning (the investigation of existing drugs for therapeutic purposes) is being used. Several antiretroviral drugs previously developed, or used as treatments for SARS, MERS, malaria, and HIV are being considered for the treatment of COVID-19, and some of them are being used in clinical trials. Although there are no safe and reliable therapeutics for this current pandemic, knowledge was obtained from the vaccine development efforts during the SARS and MERS epidemics that could prove very useful [4, 10, 11, 12, 14, 16]. Evidence gathered from the clinical trials suggested that there is no safe and reliable vaccine to shield individuals against epidemics SARS and MERS. Since SARS disappeared in 2003, clinical trials are costly from the few trials on humans, and no safe and effective vaccines have yet resulted from this. Even though there have been reports on animal clinical trials for vaccines in several countries, there is a huge contrast between COVID-19 and epidemics SARS and MERS. The difference lies in that it is a pandemic instead of an epidemic, spread of infection, possible mutations, unknown rate of reinfections, and undetermined percentages of false positive and false negative diagnoses. At this early stage, not much

information exists regarding immune-reaction against the virus, which is a challenge in itself for the development of vaccines. Hence, additional clinical trials and research are sorely needed to substantiate the role, safety and effects of all the possible medicaments. Entire populations must abide by the rules implemented by their governments to assist in overcoming this pandemic [15, 17, 18, 19].

There has been a significant demand for inquiries made about this pandemic ever since it first broke out, which resulted in Google Trends blowing up. It was found that during the first few days this disease was referred to as SARS then general coronaviruses, whereas in other parts of the world it was referred to as coronaviruses. Epidemics such as the 2002 outbreak of SARS, and the 2012 outbreak of MERS are both incidents that caused concern, and piqued interest amongst people [13, 25, 26]. The Severe Acute Respiratory Syndrome coronavirus 2 otherwise known as SARS-CoV-2, or famously known as COVID-19 is a virus that mainly attacks the respiratory system of an individual, and depending on the person's health status and age, is proven to be fatal. This virus first came about in 2019 during December, and is believed to have originated from the 'wet market' in Wuhan, Hubei Province of China. COVID-19 is said to share a sequence identity of 88 percent, 79 percent, and 50 percent with coronaviruses bat-SLCoVZC45 and bat-SL-CoVZXC21 found in bats, and SARS and MERS, respectively. Compared to the 2002 outbreak of SARS that had a total number of 8422 cases, and claimed the lives of at least 916 people across 29 countries with an approximate number of deaths being 11 percent, the number of confirmed cases for COVID-19 has grown more rapidly, raising serious global health concerns. By 21/01/2020, viral cases were widespread across mainland China, and were soon spreading beyond its borders, and on 30/01/2020 it caused the WHO to announce the virus as a public health emergency of international concern after the uprising of infections in Wuhan. The organization then dubbed this virus as COVID-19, and on 11/03/2020 the virus was declared a pandemic [5, 7, 20, 21, 25]. Back in 2012, 27 countries reported cases of MERS, and in Saudi Arabia, there was an outbreak of MERS, that resulted in 2494 confirmed cases, and 858 deaths, where 38 deaths were reported in South Korea. Since

24/02/2020 the number of confirmed laboratory cases, and the number of deaths were recorded as 79331, and 2618, respectively; China having most of the confirmed cases at 77262 and 2595 deaths. Like COVID-19 and SARS, MERS was affiliated with thrombotic complications (complications in deep vein formation of blood clots), and hematologic manifestations (manifestations in systemic lupus erythematosus, or SLE with symptoms of leukopenia, lymphocytopenia, and anemia). Nevertheless, the lack of information on MERS is inaccessible compared to COVID-19, and SARS [7, 8, 22, 25, 26]. Several other coronaviruses exist that can be pathogenic (a term that first popped-up in the 1880s and means a germ that causes disease) to individuals with mild clinical traits, where the most common of traits are feeling feverish, having the coughs, and the feeling of breathlessness. COVID-19 is considered to be one of the most extreme pathogenic viruses, the third to be exact, to have surfaced in the past 20 years. Similar to COVID-19, coronas like SARS and MERS have originated from bats where they are then transmitted to individuals through respiratory droplets [7, 23, 24]. Besides individuals, animals such as primates, carnivores, and the herbivorous dromedary camel, or otherwise known as the Somali camel are most affected by the coronaviruses; SARS, COVID-19, and MERS, respectively [9]. Infected individuals are then known as ‘super-spreaders’. According to the WHO, a person coined a ‘super spreader’ is someone, or something (event) that is capable of transmitting an infection to a large group compared to one person, or thing. In the case of SARS, a super-spreading person/event occurs during the transmission phase where eight, or more individuals get into contact. A general definition is a person who gets a disease from exposure to a primary case (person with the disease, or person who first brings a disease into a group of people); this person is called a secondary case [27, 28]. Another definition of ‘super-spreader’ person/event is one in which the infected individual infects far more people than that of an average individual. This is estimated by the parameter R_0 which is the basic reproduction number. Recall, that R_0 is a parameter which controls the spread of diseases; if R_0 is strictly less than one, this results in a population with no infections, and if R_0 is strictly greater than one, this results in the possibility of the disease becoming endemic [6, 33, 35, 36]. A super-spreading event was recognized in Singapore during the

SARS outbreak where an infected individual, a flight attendant, infected more than 100 people. Separately in South Korea at a religious sect, the Shincheonji Church of Jesus, or simply Shincheonji, 37 persons were brought to light for contracting the virus. Another case was discovered during the MERS outbreak where one person infected 82 individuals during his course of illness. This index case (the first documented patient in a disease epidemic within a population that is noticed by the health authorities, and makes them aware that an outbreak might be emerging) in the Republic of Korea resulted in 27 secondary cases, where one of these cases infected 24 more tertiary cases, and a third patient was the cause of 73 tertiary cases. In the current COVID-19 pandemic, the third British man got infected with the disease while attending a conference in Singapore. After the conference, the man traveled to France where he stayed with a family at an Alpine ski resort. From the family that the man stayed with 5 people tested positive for having the virus [6, 29, 30, 31, 32]. Between 22/01/2020 and 15/03/2020 this virus outbreak caused a massive uproar amongst the Italian population, as Italy was more negatively affected than that of China and France; both countries having very high numbers of infections and deaths. Because of the rapid growth in numbers of positively tested cases, the Italian government ordered a national lockdown on 08/03/2020. An analysis was made about the virus outbreak in China, Italy and France, and it was discovered that simple mean-field models can be used to attain quantitative information regarding the spread, the height, and time of the peak of confirmed infected individuals due to the virus. Seeing that the number of confirmed cases of individuals who eventually get infected can be considered to be anywhere between 10 percent and 20 percent, the number of fatalities due to the virus in Italy is between 4 percent and 8 percent. These numbers for the most part seem to be lower in China with percentages being between 1 percent and 3 percent. Even so, to see a significant decrease in infection rates, epidemic peaks, and several fatalities, drastic measures need to be implemented and the entire populations need to abide by the rules of their governments [1].

Looking back to when the virus first broke out in South Africa and the effect its first phase

had on the population, the government aimed to place the country under lockdown, with the aim to control and decrease the spread of infections. The South African Ministry of Health in South Africa established its incident management team (on 30 January 2020) and modelled it on the WHO's Framework for a Public Health Emergency Operations Centre (PHEOC) [98]. South Africa recorded its first case of imported COVID-19 on 5 March 2020 (in the KwaZulu-Natal province), and on the same day former Minister of Health of South Africa (served from May 2019 until he resigned on 5 August 2021), Dr Zwelini Mkhize, made an announcement in Parliament (and following this, to the Nation) about the first case of COVID-19 in South Africa. On 15 March 2020 the national Cabinet established a National COVID-19 Command and Control Council (NCCC) for the purpose of government-wide decisions and for intergovernment coordination. The South African President Cyril Ramaphosa, also on 15 March 2020, regarding the COVID-19 disease declared it as a National State of Disaster. Right after the first case was reported, numerous infection cases followed from all over the country, and between the months of March to August, our country had the highest number of cases on the African continent [99]. A nation-wide (Level 5) lockdown (levels ranging from Level 1 to 5, the most relaxed to most forceful) was then announced by the President on 23 March 2020 to aid the spread of disease in South Africa [100]. This was done to make it possible for our health systems to prepare for the increasing inflow of COVID-19 cases [101]. As was mentioned, Level 5 was declared on 23 March 2020, however its process of implementation took place on 27 March 2020 (and onwards). During this complete lockdown the public was prohibited from leaving their homes. Instructions were given to only leave homes when absolutely necessary for essential purposes (following a permission list of essential activities). This caused a major shutting down of most economic activity in our country. The categories were separated by levels and transitioned (see below) from 5 to 4, 3, 2, and 1 (occurred on 27 March 2020, 01 May 2020, 01 June 2020, 17 August 2020, and 30 September 2020), respectively [90, 91]. Initially the Level 5 restrictions were placed on bars (limited to 50 percent capacity along with a four-hour nightly; midnight to four in the morning, curfew) and restaurants, tourism and travel, but from the implementation

(on 27 March 2020) the process went like this (for all in the country) [90, 102]:

- Drastic measures were put in place to curb (and avert) the spread (and deaths) of COVID-19 disease for Level 5.
- During Level 4 some economic activities resumed, however drastic preventative measures were set up in order to restrain transmission of the COVID-19 disease between members of the South African community.
- For Level 3 restrictions were placed on activities at social engagements and at the workplaces to aid in minimizing high transmission risks.
- During lockdown Level 2, social distancing measures and restrictions were put in place between those that are infectious and/or asymptomatic (affecting others with the COVID-19 virus) and those not infected (persons considered healthy) with the virus, and on leisure activities to prevent the resurgence of the disease.
- For Level 1, during this time South Africans were allowed to carry on with, not all, but most of their normal activities, on condition that they take protective measures and followed health regulations such as regular use of sanitizers, washing of hands, and the wearing of masks.

The rapid growth in infections was believed to have been caused by the community not taking isolation and quarantine guidelines (that were provided to them) seriously, and also not following rules of non-pharmaceutical interventions. In addition, a decision was made that only when the number of infections showed a significant decrease, the levels would be dropped too. So as the lockdown levels decreased (from 5 to 4) infections then increased again, and it was observed that during this time that migrant workers returning to work were a factor in the spread of COVID-19 disease and increase in infections (symptomatic/asymptomatic) [90]. Level 1 of the lockdown is known to be called the “new normal” and no doubt in continuing to exist in the very near future. The South African population in 2020 was estimated to be 59.62 million where females made up 51.1 percent of the total population, 9.1 percent or 5.4 million were of the older generation

(older than 60 years), and the younger generation (younger than 15 years) made up 28.6 percent or 17.1 million of the population. Back in 2020, 3.9 million migrants (70 percent from other African countries) called South Africa home [104] and nearly all gathered in the South African provinces of Gauteng (estimated immigrants to be 1.5 million in 2020) and the Western Cape (estimate of 470000). Three years before that, it was estimated that around 2 million foreign-born migrants between the age of fifteen and sixty-five were living in South Africa. This resulted in a huge increase of 1.9 million in the population between 2017 and 2020 [70, 103]. When word of the first COVID-19 case was first heard about in the country, the government immediately placed South Africa under level 5 of lockdown. As the number of infections increased, so did poverty, crime and hunger, it was felt more so during the strict lockdown in 2020, since not everyone was able to get access to food and daily essentials. This virus made the daily lives of individuals extremely challenging, especially those in the medical and governmental positions as they were put under a lot of pressure to effectively manage the problem. They did just that by making the decision to only allow for decreased lockdown levels when the number of infections lowered significantly. Doing this gave the health system ample time to make preparations in dealing with the pandemic, and the government was able to provide food parcels and other forms of assistance to those in need. The main thing to take from it all is that in places where regulations are set to control the spread of an infection, if those infected with a disease come into such places it can be the cause of increased infections in those populations. If preparations are not immediately set in place to deal with such situations, the result due to this can be quite damaging to all [70, 77, 90, 91, 95]. For our model we consider two interrelated population groups; migrants considered to be visiting the main, or local South African population for a short period, not permanently joining the local population, and the COVID-19 virus (SARS-CoV-2). We present a deterministic model, and we focus on the timeline of 105 days [48] from 20 July 2020 until 2 November 2020 [81] when the population experienced its first wave of COVID-19, and there was no vaccine available to the public yet. We want to investigate the evolution of the pandemic, especially how much the inflow and outflow of migrants contributed to the effects on the

population during this period.



UNIVERSITY *of the*
WESTERN CAPE

Chapter 3

Mathematical preliminaries



Central to this Chapter are the following references: Fanelli and Piazza [1], Brauer [33], Maku-Vyambwera and Witbooi [35], Hamer [41], Ross [42], Kermack and McKendrick [51], Ward [52], Etikan and Abubakar and Alkassim [53], Fajardo-Gutiérrez [54], Vetter and Jesser [55], Cesari [56], Wang and Song [57], Noordzij *et al.* [58], Chasnov [59], Allen [60], Britton [61], Wang and De Leenheer and Sontag [62], Muldowney [63], Chasnov [64], Sutton [65], Allen [66], Smith [67], Maku-Vyambwera [68], Hethcote [69], van den Driessche and Watmough [72], Emanuel [74], Lenhart and Workman [75], Lenhart and Yong [76], Witbooi [77], Tilahun and Demie and Eyob [78], and Khalil and Choi [96].

Our aim in this dissertation is to attain insight into the evolution of the COVID-19 pandemic during its first wave in South Africa through examining cases concerning past epidemics and endemics. We first give a brief introduction of disease transmission in epidemiology by means of defining consequential concepts and properties, which are useful in modelling.

3.1 Fundamental measures in epidemiology

Measures have an important role in epidemiology and can be sectioned into three classes: frequency, association, and potential impact. Describing the frequent occurrence of a disease, or some other incident in a community leads us to the measures of frequency. Incidence and prevalence fall within this class of measures. They both give information regarding the dynamics of a disease in a population. Prevalence is how many people in a population have that disease, or the extent to which the disease has spread. While the incidence of a disease gives detail regarding the risk of contracting the disease, so the new cases of a disease [58].

Below is an example of how to calculate prevalence and incidence.

Example 3.1.1. [58]

Let ' I ' denote the number of infectious individuals at the beginning of a specific year, ' N ' denote the total number of individuals within a population, and ' I_{new} ' denote the number of new infections occurring throughout the year. Then prevalence and incidence seen below

$$Prevalence = \frac{I}{N} \quad (3.1.1)$$

$$Incidence = \frac{I_{new}}{(N - I)} \quad (3.1.2)$$

are the rate at the start of the year and the yearly incidence rate, respectively [58].

In measures of association, incidence classes get compared with one another. Odds ratio, proportional mortality ratio, rate ratio, and relative risk (or risk rate) are all examples of measures of association. To compute the measure of association, one takes the risk difference (exposed individuals in population minus the unexposed individuals in population) divides it by the incidence of an exposed group of individuals, and convert the result to percentage by multiplying by a hundred. Observational epidemiological data analysis (case-control study, cohort study, and cross-sectional study) makes use of the measures

of association and the measures of frequency. Measures of association are called so since they measure the relation between exposure and outcome. Prevalence is calculated in a cross-sectional study, incidence is calculated in cohort studies, and odds ratio is computed in case-control study. Lastly, we look at measures of potential impact. This class is a mixture of the measures of association and the measures of frequency. Note that the research study you conduct determines which measure you will be using [53, 52, 54, 55].

3.2 General first-order differential equation

The general first-order differential equation for the function $z = z(\mathbf{y})$ is written as

$$\frac{dz}{d\mathbf{y}} = g(\mathbf{y}, z), \quad (3.2.1)$$

where $g(\mathbf{y}, z)$ represents any function having dependent variable 'z' and independent variable 'y'. If given the differential equation (3.2.1) with initial condition $z(\mathbf{y}_0) = z_0$, how would one go about finding the numerical solution? The numerical solution was determined by Chasnov [59] using the Euler method, and he also shows techniques to find solutions when the differential equation (3.2.1) is in special forms; linear first-order and separable.

3.3 Invariant set

Definition 3.3.1. [96]

1. A set P is an invariant set with respect to a system of ordinary differential equations (ODEs) $\dot{z} = g(z)$, if

$$z(0) \in P \implies z(t) \in P, \forall t \in \mathbb{R}.$$

2. A set P is a positively invariant set with respect to a system of ordinary differential equations (ODEs) $\dot{z} = g(z)$, if

$$z(0) \in P \implies z(t) \in P, \forall t \geq 0.$$

Since it is of great importance that solutions of a system are positive and bounded, we give the following Proposition 3.3.2 and Theorem 1 below, that will assist us in this regard with our own model, and proofs to both can also be found in [77]. With that being said, [77] makes use of the following system of ODEs, and introduce the feasible solution sets D_0 and D_1 , respectively,

The system of ODE for the model:

$$\begin{aligned} S'(t) &= K_0 - \mu S(t) - S(t)f(I(t)), \\ E'(t) &= K_1 + S(t)f(I(t)) - (\alpha_1 + \mu)E(t), \\ I'(t) &= K_2 + \alpha_1 E(t) - (\alpha_2 + \delta + \mu)I(t), \\ R'(t) &= K_3 - K_4 + \alpha_2 I(t) - \mu R(t). \end{aligned} \tag{3.3.1}$$

with initial conditions: $S(0) = x_1 > 0, E(0) = x_2 \geq B_1, I(0) = x_3 > B_2, R(0) = x_4 > 0$. Sets D_0 and D_1 are of the form

$$\begin{aligned} D_0 &= \{x \in \mathbb{R}^4 \mid x_1 > 0, x_2 > B_1, x_3 > B_2, x_4 > 0\}, \\ D_1 &= \left\{x \in \mathbb{R}^4 \mid x_1 > 0, x_2 > B_1, x_3 > B_2, x_4 > 0, x_1 + x_2 + x_3 + x_4 \leq \frac{K}{\mu}\right\}. \end{aligned}$$

Proposition 3.3.2. [77]

Let $N(t) = S(t) + E(t) + I(t) + R(t)$. Consider a number $t_1 \in (0, \infty)$. Suppose that $X(t)$ is a solution for the system (3.3.1) with $X(t) \in D_0, \forall t \in [0, t_1)$ and $N(0) < \frac{K}{\mu}$. Then $N(t) \leq \frac{K}{\mu}$ for all $t \in [0, t_1)$.

Proof. $\frac{d\left(N(t) - \frac{K}{\mu}\right)}{dt} = -\mu\left(N(t) - \frac{K}{\mu}\right) - \delta I \leq -\mu\left(N(t) - \frac{K}{\mu}\right)$. Therefore $N(0) < \frac{K}{\mu}$ implies that $N(t) < \frac{K}{\mu}, \forall t \leq t_1$. \square

Theorem 1. [77]

Suppose that for $t \geq 0$, $\mathbf{X}(t)$ is a solution of (3.3.1) with $\mathbf{X}(0) \in D_1$. Then $\mathbf{X}(t) \in D_1, \forall t > 0$.

Proof. The proof is done by contradiction. In the paper of Witbooi [77], he defines a function $L : [0, \infty) \rightarrow \mathbb{R}$ with the formula

$$L(t) = \ln \left(\frac{K}{\mu S(t)} \right) + \ln \left(\frac{K}{\mu J_1(t)} \right) + \ln \left(\frac{K}{\mu J_2(t)} \right) + \ln \left(\frac{K}{\mu R(t)} \right).$$

This function has four terms which are non-negative and the $\lim_{x \rightarrow 0} (\ln x) = +\infty$. This then means that

$$\lim_{t \rightarrow z_1^-} L(t) = \infty. \quad (3.3.2)$$

The point of contradiction to equation (3.3.2) is that

$$L'(t) = \frac{-S'(t)}{S(t)} - \frac{J_1'(t)}{J_1(t)} - \frac{J_2'(t)}{J_2(t)} - \frac{R'(t)}{R(t)} \leq M,$$

where $M = q \left(\mu + \frac{\beta K}{\mu} \right) + \alpha_1 + \mu + (\alpha_2 + \delta + \mu) + \mu$. Consequently

$$\lim_{t \rightarrow z_1^-} L(t) = \int_0^t L'(v) dv \leq M z_1.$$

This contradicts the statement in equation (3.3.2). □

Note: We also make use of the method used in [78] to find our positive invariant set.

3.4 Equilibrium solution

In the book of Allen [60] the author states that an equilibrium solution or a steady-state solution oftentimes is referred to their shortened terms equilibrium or steady-state. This applies to the two-dimensional first-order system,

$$\mathbf{x}_{t+1} = \mathbf{f}(\mathbf{x}_t, \mathbf{y}_t),$$

$$\mathbf{y}_{t+1} = \mathbf{g}(\mathbf{x}_t, \mathbf{y}_t),$$

an equilibrium solution is a solution $(\bar{\mathbf{x}}, \bar{\mathbf{y}})$ such that $\bar{\mathbf{x}} = \mathbf{f}(\bar{\mathbf{x}}, \bar{\mathbf{y}})$ and $\bar{\mathbf{y}} = \mathbf{g}(\bar{\mathbf{x}}, \bar{\mathbf{y}})$. An equilibrium solution for a higher-order difference equation $\mathbf{f}(\mathbf{x}_{t+k} \cdots, \mathbf{x}_{t+1}, \mathbf{x}_t) = \mathbf{0}$ is a solution $\bar{\mathbf{x}}$ satisfying $\mathbf{f}(\bar{\mathbf{x}}, \cdots, \bar{\mathbf{x}}, \bar{\mathbf{x}}) = \mathbf{0}$, and such a solution can be expressed in terms of the initial value \mathbf{x}_0 .

Take note of the following two definitions, $\mathbf{x}_t = \mathbf{f}(\mathbf{f}(\cdots \mathbf{f}(\mathbf{x}_0) \cdots)) = \mathbf{f}^t(\mathbf{x}_0)$, where the superscript t represents the number of time steps or iterations beginning from the initial value \mathbf{x}_0 .

Definition 3.4.1. [60]

1. For the first-order difference equation $\mathbf{x}_{t+1} = \mathbf{f}(\mathbf{x}_t)$, an equilibrium solution, or steady-state solution is a constant solution $\bar{\mathbf{x}}$ to the difference equation, that is, a solution $\bar{\mathbf{x}}$ satisfying $\bar{\mathbf{x}} = \mathbf{f}(\bar{\mathbf{x}})$.
2. For the first-order system $\mathbf{X}_{t+1} = \mathbf{F}(\mathbf{X}_t)$, an equilibrium solution, or a steady-state solution is a constant solution $\bar{\mathbf{X}}$ satisfying $\bar{\mathbf{X}} = \mathbf{F}(\bar{\mathbf{X}})$.
3. Solutions $\bar{\mathbf{x}}$ or $\bar{\mathbf{X}}$ are also called fixed points of the function \mathbf{f} or \mathbf{F} , respectively.

Definition 3.4.2. [60]

1. An equilibrium solution $\bar{\mathbf{x}}$ of $\mathbf{x}_{t+1} = \mathbf{f}(\mathbf{x}_t)$ is locally stable, if $\forall \epsilon > \mathbf{0}, \exists \delta > \mathbf{0}$, such that, if $|\mathbf{x}_0 - \bar{\mathbf{x}}| < \delta$, then $|\mathbf{x}_t - \bar{\mathbf{x}}| = |\mathbf{f}^t(\mathbf{x}_0) - \bar{\mathbf{x}}| < \epsilon, \forall t \geq \mathbf{0}$.
2. If $\bar{\mathbf{x}}$ is not stable it is said to be unstable.
3. The equilibrium solution $\bar{\mathbf{x}}$ is locally attracting, if $\exists \gamma > \mathbf{0}$, such that, $\forall |\mathbf{x}_0 - \bar{\mathbf{x}}| < \gamma, \lim_{t \rightarrow \infty} \mathbf{x}_t = \lim_{t \rightarrow \infty} \mathbf{f}^t(\mathbf{x}_0) = \bar{\mathbf{x}}$.
4. The equilibrium solution $\bar{\mathbf{x}}$ is locally asymptotically stable, if it is locally stable and locally attracting.

3.5 The Routh-Hurwitz criterion

Theorem 2 (The Routh-Hurwitz criterion). [60]

Given the polynomial,

$$P(\beta) = \beta^m + b_1\beta^{m-1} + b_2\beta^{m-2} + \dots + b_{m-1}\beta + b_m, \quad (3.5.1)$$

where the coefficients b_i are real constants, $i = 1, \dots, n$, define the m Hurwitz matrices using the coefficients b_i of the characteristic polynomial:

$$A_1 = (b_1),$$

$$A_2 = \begin{pmatrix} b_1 & 1 \\ b_3 & b_2 \end{pmatrix},$$

and

$$A_m = \begin{pmatrix} b_1 & 1 & \dots & 0 \\ b_3 & b_2 & \dots & 0 \\ \vdots & \vdots & \ddots & \vdots \\ 0 & 0 & \dots & b_m \end{pmatrix},$$

where $b_j = 0$, if $j > m$. All of the roots of the polynomial in (3.5.1) are negative, or have negative real part if and only if the determinants of all Hurwitz matrices are positive, that means, $\det(H_j) > 0$, for $j = 1, 2, \dots, m$. For further information regarding this Theorem 2 and its proof, readers can refer to Allen [60].

3.6 Linearization

Information in this section below can be seen in [61] and [72]. Let (C^*, D^*) be a steady state of the equations,

$$\dot{C} = g(C, D) \quad \dot{D} = h(C, D) \quad (3.6.1)$$

so that $\mathbf{g}(\mathbf{C}^*, \mathbf{D}^*) = \mathbf{h}(\mathbf{C}^*, \mathbf{D}^*) = \mathbf{0}$. Let $\mathbf{c} = (\mathbf{C} - \mathbf{C}^*)$ and $\mathbf{d} = (\mathbf{D} - \mathbf{D}^*)$. We obtain the approximated (linearized) equations below by assuming that we may neglect higher order terms, if ' \mathbf{c} ' and ' \mathbf{d} ' are sufficiently small.

$$\dot{\mathbf{c}} = \mathbf{g}_C(\mathbf{C}^*, \mathbf{D}^*)\mathbf{c} + \mathbf{g}_D(\mathbf{C}^*, \mathbf{D}^*)\mathbf{d}, \quad (3.6.2)$$

and

$$\dot{\mathbf{d}} = \mathbf{h}_C(\mathbf{C}^*, \mathbf{D}^*)\mathbf{c} + \mathbf{h}_D(\mathbf{C}^*, \mathbf{D}^*)\mathbf{d}, \quad (3.6.3)$$

or, defining the Jacobian matrix $\mathbf{J}(\mathbf{C}, \mathbf{D})$ in the usual way,

$$\dot{\mathbf{e}} = \mathbf{J}^*\mathbf{e}, \quad (3.6.4)$$

where ' \mathbf{e} ' is the column vector, $(\mathbf{c}, \mathbf{d})^T$ and a star (or, asterisk) denotes evaluation at the steady state. The behaviour of the system near the steady state $(\mathbf{C}^*, \mathbf{D}^*)$ depends on the eigenvalues of the matrix $\mathbf{J}^* = \mathbf{J}(\mathbf{C}^*, \mathbf{D}^*)$.

It can be shown that the assumption above is valid and that the nonlinear system behaves like the linear system near the steady state given that neither of the eigenvalues of \mathbf{J}^* has zero real part.

By defining $\beta = \text{tr}\mathbf{J}^*$, $\gamma = \det\mathbf{J}^*$ and $\delta = \text{disc}\mathbf{J}^*$, the eigenvalue equation is

$$\lambda^2 - \beta\lambda + \gamma = 0, \quad (3.6.5)$$

which assists in determining the character of the steady state by their signs.

Theorem 3 (Steady states and Eigenvalues). [61]

- a) If $\gamma < 0$, the (trivial) steady state of the second-order system in (3.6.4) is a saddle point. Both eigenvalues are real, one positive and one negative.
- b) If $\gamma > 0$, $\delta > 0$, and $\beta < 0$, it is a stable node. Both eigenvalues are real and negative.

- c) If $\gamma > 0$, $\delta > 0$, and $\beta > 0$, it is an unstable node. Both eigenvalues are real and positive.
- d) If $\gamma > 0$, $\delta < 0$, and $\beta < 0$, it is a stable focus. The eigenvalues are complex conjugates with negative real part.
- e) If $\gamma > 0$, $\delta < 0$, and $\beta > 0$, it is an unstable focus. The eigenvalues are complex conjugates with positive real part.
- f) If $\gamma > 0$, $\delta < 0$, and $\beta = 0$, it is a centre. The eigenvalues are complex conjugates and purely imaginary.

In the book of Britton [61], the proof follows from the formula for solutions of the quadratic equation in (3.6.5). See [61] for more information regarding this theorem.

Theorem 4 (Linearization Theorem). [61]

Suppose that the non-linear system

$$\dot{z} = Z(z), \quad (3.6.6)$$

has a simple fixed point at $z = 0$. Then in a neighbourhood of the origin, the phase portraits of the system and its linearization are qualitatively equivalent, provided that the linearized system is not at center.

Lemma 3.6.1. [72]

Suppose that z_0 is a disease-free equilibrium of a system,

$$\dot{z}_i = f_i(z) = F_i(z) - V_i(z); i = 1, \dots, n, \quad (3.6.7)$$

where,

$$V_i = V_i^- - V_i^+, \quad (3.6.8)$$

and the functions $f_i(z)$ satisfies the condition that, if $z \geq 0$, then

$$F_i, V_i^+, V_i^- \geq 0; i = 1, \dots, n. \quad (3.6.9)$$

With the condition that, if $F(z_0)$ is set to zero, then all eigenvalues of $Df(z_0)$ have negative real parts and the derivatives $DF(z_0)$ and $DV(z_0)$ are divided into

$$DF(z_0) = \begin{pmatrix} \mathbf{F} & \mathbf{0} \\ \mathbf{0} & \mathbf{0} \end{pmatrix} \quad DV(z_0) = \begin{pmatrix} \mathbf{V} & \mathbf{0} \\ \mathbf{J}_3 & \mathbf{J}_4 \end{pmatrix} \quad (3.6.10)$$

where \mathbf{F} and \mathbf{V} are the $\mathbf{m} \times \mathbf{m}$ matrices defined by

$$\mathbf{F} = \begin{pmatrix} \frac{\partial F_i}{\partial Z_j} \end{pmatrix} (z_0) \quad \mathbf{V} = \begin{pmatrix} \frac{\partial V_i}{\partial Z_j} \end{pmatrix} (z_0) \quad (3.6.11)$$

with $1 \leq i, j \leq m$.

Additionally, \mathbf{F} is a non-negative matrix \mathbf{V} is a non-singular \mathbf{M} -matrix and the eigenvalues coming from \mathbf{J}_4 have positive real parts.

For more on this lemma and its proof see [72].

3.7 The direct method of Lyapunov

It is common knowledge in stability theory that the direct method of Lyapunov is a key method used for differential equations (DEs). A Lyapunov function is a function with particular properties that is constructed to prove stability, or asymptotic stability of an equilibrium in a given region. The method can be applied to autonomous systems consisting of \mathbf{n} differential equations. This method is demonstrated for the following two-dimensional autonomous system

$$\frac{dy}{dt} = f(y, z) \quad \frac{dz}{dt} = g(y, z) \quad (3.7.1)$$

and the aim is to find a Lyapunov function having properties in relation to the system in (3.7.1). With the following definitions and theorem, we are under the assumption that the equilibrium of interest is at the origin. If not, a change of variable

$$\mathbf{u} = \mathbf{y} - \bar{\mathbf{y}} \quad \mathbf{v} = \mathbf{z} - \bar{\mathbf{z}} \quad (3.7.2)$$

translates the equilibrium to the origin [60].

Definition 3.7.1. [60]

Let \mathbf{B} be an open subset of \mathbb{R}^2 containing the origin. A real-valued $C^1(\mathbf{B})$ function V

$$V : \mathbf{B} \rightarrow \mathbb{R}, [(\mathbf{y}, z) \in \mathbf{B}, V(\mathbf{y}, z) \in \mathbb{R}],$$

is said to be positive definite on the set \mathbf{B} , if the following two conditions hold:

1. $V(\mathbf{0}, 0) = 0$.
2. $V(\mathbf{y}, z) > 0, \forall (\mathbf{y}, z) \in \mathbf{B}$ with $(\mathbf{y}, z) \neq (\mathbf{0}, 0)$.

The function V is said to be negative definite, if $-V$ is positive definite.

Below, we have an example that makes use of the above definition.

Example 3.7.2. [60]

Given the function

$$V(\mathbf{y}, z) = \mathbf{y}^2 + z^2, \tag{3.7.3}$$

check to see if $V(\mathbf{y}, z)$ is positive definite on set \mathbf{B} .

Solution: By use of the definition above see if the given function satisfies the first and second conditions.

1. $V(\mathbf{0}, 0) = (\mathbf{0})^2 + (\mathbf{0})^2 = 0$.

So, the first condition is satisfied.

2. Since $V(\mathbf{y}, z) > 0$, choose $(\mathbf{y}, z) \in \mathbf{B}$, $(\mathbf{y}, z) \neq (\mathbf{0}, 0)$.

Let $(1, 1) \in \mathbf{B}$. Then

$$V(1, 1) = (1)^2 + (1)^2 = 2 > 0.$$

Notice that $V(\mathbf{y}, z) > 0$. So, the second condition is satisfied as well.

Therefore the function $V(\mathbf{y}, \mathbf{z})$ is positive definite.

The reader can see [60] to try and check whether other functions $V(\mathbf{y}, \mathbf{z})$ are positive definite on set B .

Definition 3.7.3. [60] A positive definite function V in an open neighborhood of the origin is said to be a Lyapunov function for the autonomous differential system (3.7.1), if $\frac{dV(\mathbf{y}, \mathbf{z})}{dt} \leq 0, \forall (\mathbf{y}, \mathbf{z}) \in B - \{(0, 0)\}$. If $\frac{dV(\mathbf{y}, \mathbf{z})}{dt} < 0, \forall (\mathbf{y}, \mathbf{z}) \in B - \{(0, 0)\}$ the function V is called a strict Lyapunov function.

Theorem 5 (Lyapunov's Stability Theorem). [60]

Let $(0, 0)$ be an equilibrium of the autonomous system (3.7.1), and let V be a positive definite C^1 function in a neighborhood B of the origin.

- a) If $\frac{dV(\mathbf{y}, \mathbf{z})}{dt} \leq 0$, for $(\mathbf{y}, \mathbf{z}) \in B - \{(0, 0)\}$, then $(0, 0)$ is stable.
- b) If $\frac{dV(\mathbf{y}, \mathbf{z})}{dt} < 0$, for $(\mathbf{y}, \mathbf{z}) \in B - \{(0, 0)\}$, then $(0, 0)$ is asymptotically stable.
- c) If $\frac{dV(\mathbf{y}, \mathbf{z})}{dt} > 0$, for $(\mathbf{y}, \mathbf{z}) \in B - \{(0, 0)\}$, then $(0, 0)$ is unstable.

In the first condition the function V is a Lyapunov function and in the second condition the function V is a strict Lyapunov function.

Proof. The first and second conditions are proved.

First condition: Let $\epsilon > 0$ be sufficiently small so that the neighborhood of the origin consisting of the points $\|(\mathbf{y}, \mathbf{z})\| \leq \epsilon$ is contained in B ($\|\cdot\|$ denotes the Euclidean norm). Let p be the minimum value of V on the boundary of the neighbourhood $\|(\mathbf{y}, \mathbf{z})\| = \epsilon$. Since V is positive definite, and the set $\|(\mathbf{y}, \mathbf{z})\| = \epsilon$ is closed and bounded, it follows that $p > 0$. Now, choose a $\delta > 0$ with $0 < \delta \leq \epsilon$ such that, $V(\mathbf{y}, \mathbf{z}) < p$ for $\|(\mathbf{y}, \mathbf{z})\| \leq \delta$. Such a δ always exists because V is continuous with $V(0, 0) = 0$. If $\|(\mathbf{y}_0, \mathbf{z}_0)\| \leq \delta$, then the solution with initial conditions $(\mathbf{y}_0, \mathbf{z}_0)$ satisfies $\|(\mathbf{y}, \mathbf{z})\| \leq \epsilon$ for $t \geq 0$. Since $\frac{dV}{dt} \leq 0$ implies that $V(\mathbf{y}(t), \mathbf{z}(t)) \leq V(\mathbf{y}_0, \mathbf{z}_0) < p$ for $t \geq 0$. The origin is stable.

Second condition: The function $V(\mathbf{y}(t), z(t))$ decreases along solutions that lie in B . Thus as $t \rightarrow \infty$, $V(\mathbf{y}(t), z(t))$ approaches a limit. Suppose $V \rightarrow l > 0$. Then it follows from the uniform continuity of $\frac{dV(\mathbf{y}(t), z(t))}{dt}$ (solutions are bounded and functions \mathbf{f} and \mathbf{g} are C^1) that $\frac{dV(\mathbf{y}(t), z(t))}{dt} \rightarrow 0$ in an annular region excluding the origin. This is impossible since $\frac{-dV}{dt}$ is positive definite $\frac{dV}{dt} = 0$ only at the origin and $(\mathbf{y}(t), z(t))$ does not tend to the origin when $V \rightarrow l$. It follows that $V(\mathbf{y}(t), z(t))$ approaches 0, which implies $(\mathbf{y}(t), z(t))$ approaches $(0, 0)$. The origin is asymptotically stable. \square

Stability first needs to be verified by using Lyapunov's direct method since it will assist us in finding an appropriate Lyapunov function V . Below, is an example of this approach found in [60].

Example 3.7.4. Consider the logistic differential equation (DE)

$$\frac{dz}{dt} = rz \left(1 - \frac{z}{W} \right),$$

where $r, W > 0$. Notice that there are two equilibria $\bar{z} = 0, W$. From previous investigation, we know that W is globally asymptotically stable for positive initial conditions. Let $B = (0, \infty) = \mathbb{R}_+$ the positive z -axis. A strict Lyapunov function is given by

$$V(z) = (z - W)^2.$$

Since

$$\frac{dV(z)}{dt} = 2(z - W) \frac{dz}{dt} = 2(z - W)rz \left(1 - \frac{z}{W} \right) = -2rz \frac{(z - W)^2}{W},$$

the function V is a $C^1(B)$ function that is positive except at $z = W$ and $V(W) = 0$. Also, $\frac{-dV}{dt}$ is positive in B except at $z = W$ and $\frac{dV(W)}{dt} = 0$. Thus, according to the second condition of Lyapunov's Stability Theorem the equilibrium $z = W$ is asymptotically stable $\forall (\mathbf{y}, z) \in B - \{(0, 0)\}$.

3.8 The second additive compound matrix

Definition 3.8.1. [62] Let D be a matrix of order k . The second additive compound matrix $D^{[2]}$ is a matrix of order $\binom{k}{2}$, which is defined as follows:

$$D_{(i)(j)}^{[2]} = \begin{cases} D_{i_1 i_1} + D_{i_2 i_2}, & \text{if } (i) = (j); \\ (-1)^{r+s} D_{i_r j_s}, & \text{if exactly one entry, } i_r, \text{ of } (i) \text{ does not occur in } (j), \\ & \text{and, } j_s, \text{ does not occur in } (i), \text{ for some } r, s \in \{1, 2\}; \\ 0, & \text{if } (i) \text{ differs from } (j) \text{ in both entries.} \end{cases}$$

Here $(i) = (i_1, i_2)$ is the i^{th} member of the lexicographic order of integer pairs for which $1 \leq i_1 < i_2 \leq k$.

For more information regarding the definition of the second additive compound matrix, the reader may see [57, 62, 63].

We now show an example based on the second additive compound matrix.

Example 3.8.2. [57] If we are given a 3×3 matrix D where $D = (d_{ij})$, then its second additive compound matrix $D^{[2]}$ would then be

$$D^{[2]} = \begin{bmatrix} d_{11} + d_{22} & d_{23} & -d_{13} \\ d_{32} & d_{11} + d_{33} & d_{12} \\ -d_{31} & d_{21} & d_{22} + d_{33} \end{bmatrix}.$$

3.9 Compartmental modeling: spread of diseases

As previously mentioned, it should be noted that historical public health physicians such as Hamer [41], Ross [42], and Kermack and McKendrick [51], not mathematicians, made numerous advancements in epidemiology based on compartmental models and mathematical modelling of communicable diseases between the years of 1900 and 1935 [33]. The

spread of diseases in populations are best described by the use of compartmental models. A population being studied usually gets divided into classes, or compartments; \mathbf{S} , \mathbf{E} , \mathbf{I} , and \mathbf{R} . In all epidemiological models we must work under the assumption that the population being studied is well mixed as this gives each host a chance to become infected. Assumptions must also be made about the number of ways that new infections can arise, and hosts can move from compartment to compartment over time \mathbf{t} , that is, the size of the population in each class is written as a function of time and below we state these classes [35, 56].

- Let $\mathbf{S}(\mathbf{t})$ denote the hosts who are susceptible, in other words, those who are not yet infected with the disease at time \mathbf{t} .
- Let $\mathbf{E}(\mathbf{t})$ denote the hosts exposed (latent) to the disease at time \mathbf{t} .
- Let $\mathbf{I}(\mathbf{t})$ denote the hosts that are able to spread the disease through contact with susceptible hosts at time \mathbf{t} .
- Let $\mathbf{R}(\mathbf{t})$ denote the hosts removed due to reinfection being possible, or for spreading the disease again, or those that have recovered successfully at time \mathbf{t} .

There are many types of models and each of them uses a different approach when it comes to their construction in epidemiology. Essentially this implies that there will be cases where some classes have to be added or removed. One should also note that the number of compartments a model has depends on the supposition being made about the model [68].

3.9.1 Model terminology

To begin with, we briefly look at the three simplest mathematical models in epidemiology for the spread of an epidemic and endemic of a communicable disease. After that, we introduce our own Corona Model Equations. The three simplest models lay the groundwork for complicated models and it makes it easier for organizations such as the WHO, CDC, and the US FDA to estimate future spreads of diseases by means of developing

strategies allowing governments to implement drastic measures so that entire populations abide by their rules in order to see a decrease in epidemic peaks, infection rates, and several fatalities [1, 64].

The first simple model seen below, is the **SI** model. In this model you need to work under the assumption that the model itself is closed. Meaning that there is no inflow of new individuals via birth and by maturation, or by immigration into the population. In this model the hosts get divided into two classes: Susceptible and Infected. Disease transmission within this model takes place when a healthy susceptible host becomes infected through coming into contact with an infectious host. This leads to a decrease in the susceptible class and an increase in the infected class. Infected hosts will never have a chance at recovering, that is, they will forever be in the infected class. Death does not play a role when it comes to this model as the length of the disease outbreak is brief in comparison with the lifespan of average individuals. A disease such as HSV-1 or HSV-2 otherwise known as herpes caused by the virus Herpesviridae fit in this model since it spreads quickly and individuals infected by this disease never recover [64, 65, 66, 67, 69].

We diagram this **SI** model as follows,

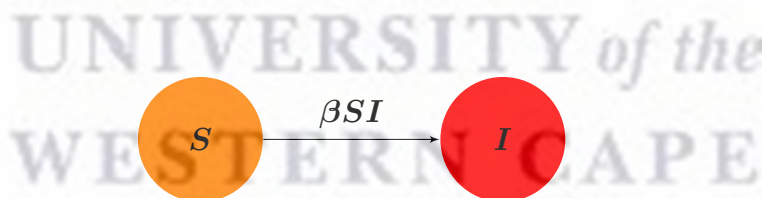


Figure 3.1: **The compartmental diagram for the SI model**

Note: It is always good to draw diagrams as they will help us with constructing more complex systems of differential equations.

The compartmental model below depicts the transmission between the classes **S** and **I** shown in (3.9.1).

$$\begin{aligned}
\frac{dS}{dt} &= -\beta SI, \\
\frac{dI}{dt} &= \beta SI, \\
N &= S + I.
\end{aligned}
\tag{3.9.1}$$

where N is the total population.

The first differential equation in (3.9.1) gives a description of how individuals move from the susceptible group to the infected group. In the second differential equation in (3.9.1), we see this increase in the infected group as susceptible hosts become sick. This shift is caused due to the number β which represents the rate at which the disease is transmitted when an infected host comes into contact with a susceptible host, the number βS represents contacts due to infection, and βSI represents the total number of contacts resulting in infection, increasing the infected class. Looking at the third equation in (3.9.1), we assume that the population being studied has constant size N , this means that birth rate and death rate are the same, so that $N = S + I$ [64, 68].

An interesting fact is that this model has a logistic solution. Using the second differential equation and by eliminating S we have,

$$\frac{dI}{dt} = \beta(N - I)I
\tag{3.9.2}$$

Rewriting this equation results in,

$$\frac{dI}{dt} = \beta NI \left(1 - \frac{I}{N}\right)
\tag{3.9.3}$$

which is a logistic equation having growth rate βN and carrying capacity N . Note that the entire host population will become infected as time goes on [64].

The second model seen below is the **SIS** model, and it is an extension of the **SI** model. Here, a host population being studied still gets divided into two classes: Susceptible and Infected. The only difference is that disease transmission within this model takes place when healthy susceptible hosts become infected through contact with infectious hosts, and

when these individuals recover from infection they move back to the susceptible class. In simple terms, the susceptible class first decreases while infected class increases. Then, the infected class decreases while the susceptible class increases. Hosts within this class have a chance at recovering, that is, they will not remain in the infected class forever. Diseases such as gonorrhoea, meningitis and streptococcal sore throat fit in this model. [64, 66, 69].

We represent this *SIS* model through the following diagram,

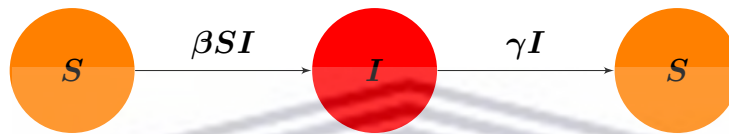


Figure 3.2: The compartmental diagram for the SIS model

The compartmental model below depicts the transmission between the classes *S* and *I* shown in (3.9.4).

$$\begin{aligned} \frac{dS}{dt} &= -\beta SI + \gamma I, \\ \frac{dI}{dt} &= \beta SI - \gamma I, \\ N &= S + I. \end{aligned} \tag{3.9.4}$$

where *N* is the total population.

Transmission in equation (3.9.4) proceeds in this manner, in the first differential equation of (3.9.4), individuals move from the susceptible group to the infected group, decreasing class *S*, causing an increase in population of class *I*. In the second differential equation of (3.9.4), we see the increased class *I* decrease in population as infected hosts can recover, moving back to class *S* where they become susceptible again, increasing this class. In the *SI* model there is only the number β . This number causes a shift representing the rate at which the disease is transmitted when an infected host comes into contact with a susceptible host. The number βS represents contacts due to infection and βSI represents the total number of contacts resulting in infection, increasing the infected class. In the

SIS model there is still the number β but added to this model is the number γ which represents the recovery rate of individuals from infection, and $\frac{1}{\gamma}$ represents the average length of time when no deaths occur due to infection. The third equation in (3.9.4) we are still under the assumption that the population being studied has constant size N , and means that birth rate and death rate are the same, so that $N = S + I$ [64, 68].

Just as in the *SI* model, the *SIS* model has a logistic solution. Using the second differential equation in (3.9.4) we eliminate S ,

$$\frac{dI}{dt} = \beta(N - I)I - \gamma I \quad (3.9.5)$$

Rewriting this equation results in,

$$\frac{dI}{dt} = \beta NI \left(1 - \frac{I}{N}\right) - \gamma I \quad (3.9.6)$$

which we can see is a logistic equation. The only difference now is that the growth rate is βN where N is found using the basic reproduction number R_0 of this model and the carrying capacity is N . Negative growth rate results in the disappearance of the disease, which is when the basic reproduction number R_0 is strictly less than zero. Having positive growth rate is when the basic reproduction number R_0 is strictly greater than zero, resulting in the disease becoming endemic. When the disease becomes endemic, the number of infected persons approaches the carrying capacity as time goes on [64].

Note: The reader can check [64] to see how R_0 of the *SIS* model is derived by method of integration.

We now move on to the final simple *SIR* model below. This model is famously known as the Kermack-McKendrick model. Here, a host population being studied gets divided into three classes: Susceptible, Infected, and Removed, at time t . Disease transmission within this model takes place when individuals become susceptible to disease. These individuals then get infected by the disease and afterwards they recover from the disease. Due to this transmission, we notice that the susceptible class first decreases while infected class increases. The infected class then decreases while the removed class increases. Therefore,

the individuals who are removed are not susceptible and also not infected anymore. Reasons for this can be because they are now immune to the disease due to recovery, they got vaccinated, isolated, or they simply just died from the disease. For transmission between classes I and R , infectives do not leave the I class with constant rate γ as in the SIS model, here they follow a direct path into the R class. Diseases that confer immunity and have been present in a population for more than 10 or 20 years fit within this model and are labeled as endemic. Due to the length of time this SIR model should contain births to increase the susceptible class and deaths in each of the other classes [64, 66, 69].

We diagram this SIR model as follows,

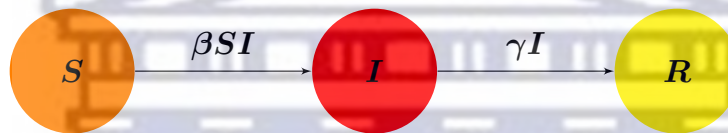


Figure 3.3: The compartmental diagram for the SIR model

The compartmental model below depicts the transmission between the classes S , I , and R shown in (3.9.7),

$$\begin{aligned}
 \frac{dS}{dt} &= -\beta SI, \\
 \frac{dI}{dt} &= \beta SI - \gamma I, \\
 \frac{dR}{dt} &= \gamma I,
 \end{aligned}
 \tag{3.9.7}$$

$$N = S + I + R.$$

where N is the total population.

The first differential equation in (3.9.7) shows how individuals move from the susceptible group to the infected group, decreasing class S . The second differential equation in (3.9.7) shows an increase in population of class I while also showing a decrease as these individuals are on their way to recovery, they directly move into R , increasing this class.

As in the *SIS* model, the basic *SIR* model's rates remain the same; the number β represents the rate at which the disease is transmitted when an infected host comes into contact with a susceptible host, the number βS represents contacts due to infection, and βSI represents the total number of contacts resulting in infection, increasing the infected class. The number γ represents the rate at which individuals recover from infection and $\frac{1}{\gamma}$ represents the average length of time when no deaths occur due to infection. We still assume that the population studied has a constant size N , so the birth rate and death rate are the same, so that $N = S + I + R$. Diseases caused by a virus fit within this model. There are also more complicated compartmental structures of this model such as *SEIR*, *SEIS*, and *SIRS*, where the first two models have an exposed period between being infected and becoming infective, and the third model describes short-term immunity on recovery from an infection [33, 64, 68].

3.9.2 The method of the next generation matrix operator

This method is used to find the basic reproduction number R_0 when a compartment model is given that has more than one infected class. Let us assume for example that we are given a model with n infected classes and m uninfected classes, and let \mathbf{x} be the vector in \mathbb{R}^n and \mathbf{y} be the vector in \mathbb{R}^m , both being subclasses in each of these compartments. \mathcal{G}_i will then be the vector of all new infection rates and \mathcal{V}_i will be the vector of all other rates except the new infection rates. This information then gives us the following compartmental model:

$$\begin{aligned}\frac{dx_i}{dt} &= \mathcal{G}_i(\mathbf{x}, \mathbf{y}) - \mathcal{V}_i(\mathbf{x}, \mathbf{y}); \quad i = 1, \dots, n, \\ \frac{dy_j}{dt} &= \mathcal{Q}_j(\mathbf{x}, \mathbf{y}); \quad j = 1, \dots, m.\end{aligned}$$

The basic reproduction number has calculations based on linearization of the ODE model about a disease-free equilibrium point. The following assumption ensures the existence of the equilibrium and well-posedness of the model:

- Assume $\mathcal{G}_i(\mathbf{0}, \mathbf{y}) = \mathbf{0}$ and $\mathcal{V}_i(\mathbf{0}, \mathbf{y}) = \mathbf{0}$, $\forall \mathbf{y} \geq \mathbf{0}$ and $i = 1, \dots, n$. All new infec-

tions are secondary infections arising from infected host and there is no immigration of individuals into the disease compartments.

- Assume $\mathcal{G}_i(\mathbf{0}, \mathbf{y}) \geq \mathbf{0}$, $\forall \mathbf{x}, \mathbf{y} > \mathbf{0}$ and $i = 1, \dots, n$. The function \mathbf{G} represents new infections and cannot be negative.
- Assume $\mathcal{V}_i(\mathbf{0}, \mathbf{y}) \leq \mathbf{0}$ whenever $x_i = 0$, $i = 1, \dots, n$. Each component \mathbf{V}_i represents a net outflow from compartment i and must be negative (inflow only) whenever the compartment is empty.
- Assume $\sum_{i=1}^n \mathbf{V}_i(\mathbf{x}, \mathbf{y}) \geq \mathbf{0}$, $\forall \mathbf{x}, \mathbf{y} > \mathbf{0}$. This sum represents the total outflow from all infected compartments. Terms in the model leading to increase in $\sum_{i=1}^n x_i$ are assumed to represent secondary infections and therefore belong in \mathbf{G} .
- Assume the disease-free system $\frac{d\mathbf{y}}{dt} = \mathbf{Q}(\mathbf{0}, \mathbf{y})$ has a unique equilibrium that is asymptotically stable. That is, all solutions with initial conditions of the form $(\mathbf{0}, \mathbf{y})$ approach a point $(\mathbf{0}, \mathbf{y}_0)$ as $t \rightarrow \infty$. This point is referred to as the disease free equilibrium.

Let us assume that \mathcal{G}_i and \mathcal{V}_i satisfies the conditions above, then the next generation matrix $\mathbf{G}\mathbf{V}^{-1}$ can be formed from matrices \mathbf{G} and \mathbf{V} having partial derivatives as entries. The reader can check [72] to see more information on the next generation matrix.

3.10 Pontryagin's maximum principle

This principle transforms the minimization, or the maximization of the objective functional \mathbf{J} joined with the state variable $\mathbf{z}(\mathbf{u})$ into pointwise minimizing, or maximizing of the Hamiltonian with respect to the control $\mathbf{v}(\mathbf{u})$. The Hamiltonian $\mathbf{H}(\mathbf{u}, \mathbf{z}(\mathbf{u}), \mathbf{v}(\mathbf{u}), \boldsymbol{\alpha}(\mathbf{u}))$ is a function of four variables, where time \mathbf{u} is the underlying variable. Variables \mathbf{z} , \mathbf{v} and $\boldsymbol{\alpha}$ are functions of \mathbf{u} and $\boldsymbol{\alpha}$ is called the adjoint variable [93, 75].

Theorem 6. [75] If $\mathbf{v}(\mathbf{u})$ and $\mathbf{z}(\mathbf{u})$ are optimal for problem (3.11.1), then there exists a piecewise differential adjoint variable $\boldsymbol{\alpha}(\mathbf{u})$, such that

$$\mathbf{H}(\mathbf{u}, \mathbf{z}^*(\mathbf{u}), \mathbf{v}(\mathbf{u}), \boldsymbol{\alpha}(\mathbf{u})) \leq \mathbf{H}(\mathbf{u}, \mathbf{z}^*(\mathbf{u}), \mathbf{v}^*(\mathbf{u}), \boldsymbol{\alpha}(\mathbf{u}))$$

for all controls $\mathbf{v}(\mathbf{u})$ at each time \mathbf{u} where the Hamiltonian \mathbf{H} is

$$\mathbf{H} = \mathbf{g}(\mathbf{u}, \mathbf{z}(\mathbf{u}), \mathbf{v}(\mathbf{u})) + \boldsymbol{\alpha}(\mathbf{u})\mathbf{h}(\mathbf{u}, \mathbf{z}(\mathbf{u}), \mathbf{v}(\mathbf{u}))$$

and

$$\frac{\boldsymbol{\alpha}(\mathbf{u})}{d\mathbf{u}} = -\frac{\partial \mathbf{H}(\mathbf{u}, \mathbf{z}^*(\mathbf{u}), \mathbf{v}^*(\mathbf{u}), \boldsymbol{\alpha}(\mathbf{u}))}{\partial \mathbf{z}}; \quad \boldsymbol{\alpha}(\mathbf{u}_g) = \mathbf{0}.$$

Necessary conditions: If $\mathbf{v}(\mathbf{u})$ and $\mathbf{z}(\mathbf{u})$ are optimal, then the following conditions hold:

$$\frac{\boldsymbol{\alpha}(\mathbf{u})}{d\mathbf{u}} = -\frac{\partial \mathbf{H}(\mathbf{u}, \mathbf{z}^*(\mathbf{u}), \mathbf{v}^*(\mathbf{u}), \boldsymbol{\alpha}(\mathbf{u}))}{\partial \mathbf{z}}; \quad \boldsymbol{\alpha}(\mathbf{u}_g) = \mathbf{0}.$$

and

$$\frac{\partial \mathbf{H}(\mathbf{u}, \mathbf{z}^*(\mathbf{u}), \mathbf{v}^*(\mathbf{u}), \boldsymbol{\alpha}(\mathbf{u}))}{\partial \mathbf{v}} = \mathbf{0}.$$

Sufficient conditions: If $\mathbf{v}(\mathbf{u})$, $\mathbf{z}(\mathbf{u})$ and $\boldsymbol{\alpha}(\mathbf{u}_g)$ satisfy the following conditions:

$$\frac{\boldsymbol{\alpha}(\mathbf{u})}{d\mathbf{u}} = -\frac{\partial \mathbf{H}(\mathbf{u}, \mathbf{z}^*(\mathbf{u}), \mathbf{v}^*(\mathbf{u}), \boldsymbol{\alpha}(\mathbf{u}))}{\partial \mathbf{z}}; \quad \boldsymbol{\alpha}(\mathbf{u}_g) = \mathbf{0},$$

and

$$\frac{\partial \mathbf{H}(\mathbf{u}, \mathbf{z}^*(\mathbf{u}), \mathbf{v}^*(\mathbf{u}), \boldsymbol{\alpha}(\mathbf{u}))}{\partial \mathbf{v}} = \mathbf{0},$$

then $\mathbf{v}(\mathbf{u})$ and $\mathbf{z}(\mathbf{u})$ are optimal.

3.11 Optimal control method

An optimal control is an optimization method for deriving control policies, and is an extension of the calculus of variations. It is important that a certain optimality criterion is achieved and this is done by finding a control law for a given system. Lev Pontryagin and his collaborators in the Soviet Union are credited for their work on optimal control theory as they were the ones to lay its foundation in the early years of the 1960s. This

method is very suitable in decision making regarding composite biological situations and has been a powerful mathematical technique derived from the calculus of variation. The behaviour of a dynamical system is described by the state variables (\mathbf{s}). A control problem includes a cost functional that is a function of state and control variables. The assumption is that there is a way to control the state variable \mathbf{z} , by acting upon it with a suitable control. Thus, the dynamics of the system (state \mathbf{z}) depends on the control \mathbf{v} . Given an objective functional $\mathbf{K}(\mathbf{v}(\mathbf{u}), \mathbf{z}(\mathbf{u}), \mathbf{u})$, the goal is to regulate control \mathbf{v} so as to maximize, or minimize \mathbf{K} . When the most desired goal is achieved with least cost this results in the optimal solution. The functional depends on the state variables and the control. The optimal control for specific model can be calculated in numerous ways. An example would be Pontryagin's Maximum Principle which allows the calculation of the optimal control for an ordinary differential equation model system with given constraints [56, 74, 75, 76]. Given a basic control problem of the form of an ODE, we use $\mathbf{v}(\mathbf{u})$ and $\mathbf{z}(\mathbf{u})$ for the control and state variables respectively. The result of the given differential equation will change as the control function changes. Note that the state variable $\mathbf{z}(\mathbf{u})$ satisfies a differential equation and depends on the control variable $\mathbf{v}(\mathbf{u})$:

$$\mathbf{z}'(\mathbf{u}) = \mathbf{h}(\mathbf{u}, \mathbf{z}(\mathbf{u}), \mathbf{v}(\mathbf{u})). \quad (3.11.1)$$

This method consists of finding the state variable $\mathbf{z}(\mathbf{u})$ and a piecewise continuous control $\mathbf{v}(\mathbf{u})$, so that the objective functional \mathbf{K} can be maximized,

$$\max_{\mathbf{v}} \int_{\mathbf{u}_0}^{\mathbf{u}_1} \mathbf{g}(\mathbf{u}, \mathbf{z}(\mathbf{u}), \mathbf{v}(\mathbf{u})) d\mathbf{u}$$

subject to $\mathbf{z}'(\mathbf{u}) = \mathbf{h}(\mathbf{u}, \mathbf{z}(\mathbf{u}), \mathbf{v}(\mathbf{u}))$ and $\mathbf{z}(\mathbf{u}_0) = \mathbf{z}_0$ and $\mathbf{z}(\mathbf{u}_1)$ is unrestricted. The following characteristics are important when dealing with an optimal control problem:

- Controllability: Used to steer a system from one position to another.
- Observability: Used to assist with deducing a system's information from control input and observe output.
- Stabilization: Used in implementing controls to force stability.

For more information regarding optimal control method, the reader may see [56, 75, 76].

3.12 Sensitivity analysis

Through sensitivity analysis one sees the significance of each parameter in a model and the effect, or the relationship they have on the basic reproduction number R_0 . With this analysis you want to calculate the sensitivity indices of the basic reproduction number R_0 . By doing so you can determine if an infectious disease will spread in the population. Since errors usually occur in the pre-assumed values and data collection, this analysis is then used in determining the robustness of model predictions to parameter values. Another thing that this analysis is good for, is that when a parameter changes, it also allows for the measurement of relevant changes in a state variable. The method of normalized forward sensitivity index of a variable is commonly used when doing this analysis. This method is the ratio of relative change in the variable to the relative change in the parameter. When the given variable is a differentiable function of the parameter, the sensitivity may also be defined using partial derivatives [83].

Definition 3.12.1. [83] *The normalized-forward sensitivity index is calculated using the normalized sensitivity index of the variable R_0 , which is differentiable on the parameter m :*

$$C_m^{R_0} = \frac{\partial R_0}{\partial m} \times \frac{m}{R_0},$$

where R_0 is the variable to be analyzed and m is the parameter.

Chapter 4

A model of COVID-19 population dynamics

In this chapter we often refer to the following references: Vecchio *et al.* [2], Park and Thwaites and Openshaw [7], Gautam *et al.* [9], Huang *et al.* [23], Chen *et al.* [24], Shen *et al.* [27], James and Pitchford and Plank [28], Maku-Vyambwera and Witbooi [35], Volkow [47], Cesari [56], Osei [71], van den Driessche and Watmough [72], Witbooi [77], Tilahun and Demie and Eyob [78], Maku-Vyambwera and Witbooi [79], and Nyabadza *et al.* [80].

In this chapter we look at the invariant region, positivity of solutions, disease-free equilibrium point, basic reproduction number, existence of endemic equilibrium points, and stability analysis around our model (4.1.2).

4.1 Mathematical model

We now explain the process of compartmental modeling by introducing our corona model system of ODEs. We also bring in other concepts of compartmental modeling. As we mentioned, spread of diseases in populations are best described by use of comparten-

tal models. When studying a population, one usually has to divide it into classes, or compartments; \mathbf{S} , \mathbf{E} , \mathbf{I} , and \mathbf{R} . It is also important when dealing with epidemiological models to work under the assumption that the population being studied is well mixed as this gives each host a chance to become infected. Assumptions must also be made about the number of ways that new infections can arise and how hosts move from compartment to compartment over time \mathbf{t} , that is, the size of the population in each class is written as a function of time [35, 56].

For our model let us consider two interrelated population groups. On the one side we have the host population of migrants considered to be visiting the main, or local South African population for a short period, not permanently joining the local population. On the other side we have the pathogens, or the COVID-19 virus (SARS-CoV-2). The host population being studied gets divided into five groups; susceptible $\mathbf{S}(\mathbf{t})$, symptomatic infectious $\mathbf{I}(\mathbf{t})$; those showing clinical symptoms of the COVID-19 disease, asymptomatic infectious $\mathbf{A}(\mathbf{t})$; those showing no visible clinical symptoms of the COVID-19 disease but still being infected, removed $\mathbf{R}(\mathbf{t})$, and the density of the virus in the environmental reservoir denoted as $\mathbf{P}(\mathbf{t})$. The sum of each compartment is represented as a function of time \mathbf{t} and results in the total population number $\mathbf{N}(\mathbf{t})$ that is to be considered as constant, which is also a function of time \mathbf{t} , mathematically denoted as the equation below,

$$\mathbf{N}(\mathbf{t}) = \mathbf{S}(\mathbf{t}) + \mathbf{I}(\mathbf{t}) + \mathbf{A}(\mathbf{t}) + \mathbf{R}(\mathbf{t}) + \mathbf{P}(\mathbf{t}). \quad (4.1.1)$$

As we stated previously COVID-19 is a virus that mainly attacks the respiratory system of an individual, and depending on the person's age and health status is proven to be fatal. Researchers have found that this virus causes more fatalities, and is especially bad for geriatrics with comorbidities (the presence of one, or more additional conditions co-occurring with a primary condition) where the most common comorbidities are diabetes, chronic kidney disease, respiratory disease, hypertension, cardiac disease, renal disease, malignancy, and pregnancy. Apart from geriatrics, individuals that have previously suffered from opioid use disorder are also more likely to be infected by the virus as they have increased physical, and psychological comorbidity, thus meaning that they are oftentimes

alienated from society. This results in making it harder for them to get assisted with health care can be seen in [2, 47]. Besides humans, animals such as primates, carnivores, and the herbivorous dromedary camel, or otherwise known as the Somali camel, are also affected by the coronaviruses; SARS, COVID-19, and MERS, respectively [9]. According to the WHO, a person coined a ‘super spreader’ is someone, or something (event) that is capable of transmitting an infection to a large group compared to one person, or thing. In the case of SARS, a super-spreading person/event occurs during the transmission phase where eight, or more individuals get into contact. A general definition is a person who gets a disease from exposure to a primary case (person with the disease, or person who first brings a disease into a group of people); this person is called a secondary case [27, 28]. Several other coronaviruses exist that can be pathogenic (a term that first popped-up in the 1880s and means a germ that causes disease) to individuals with mild clinical traits where the most common of traits are feeling feverish, having the coughs, and the feeling of breathlessness. This virus is considered to be one of the most extreme pathogenic viruses, the third to be exact, to have surfaced in the past 20 years. Similar to COVID-19, coronas like SARS and MERS have originated from bats where they are then transmitted to individuals through respiratory droplets [7, 23, 24].

Let us now consider our **SIARP** model for disease transmission of COVID-19, which is given by the system of ODEs in (4.1.2). Within this model transmission of the disease takes place when susceptible individuals **S**, migrants visiting the local population of South Africa for a short period of time **t** become infected with the disease due to contact with infectious persons. These individuals then move out of being susceptible and move on to either becoming symptomatically infected **I**, or they become asymptotically infected **A** by the disease. This process then causes a decrease in the susceptible compartment and an increase in classes **I**, and **A**. The symptomatic, and asymptomatic infectious individuals then increase the density of the pathogens in the environmental reservoir **P** by sneezing, or coughing. The pathogens **P** then survive in the environment for a few days and exposed susceptible hosts come into contact with the infected environment causing

them to become infectious with the disease. From here the exposed infectious hosts can become asymptomatic A to the disease thus decreasing the class I and increasing class A , they can also infect others. After a short stay the surviving migrants will depart from the population as recovered individuals, increasing class R and decreasing class A .

Below in Figure 4.1 is an illustration of the **SIARP** model. It shows two interrelated population groups; the host population (migrants) and the pathogens (COVID-19 virus) in the environmental reservoir, and the transmission of migrants from each compartment. The compartmental model can be seen in equation (4.1.2). Descriptions of the parameters used for the model are shown in Table 5.1 of Chapter 5.

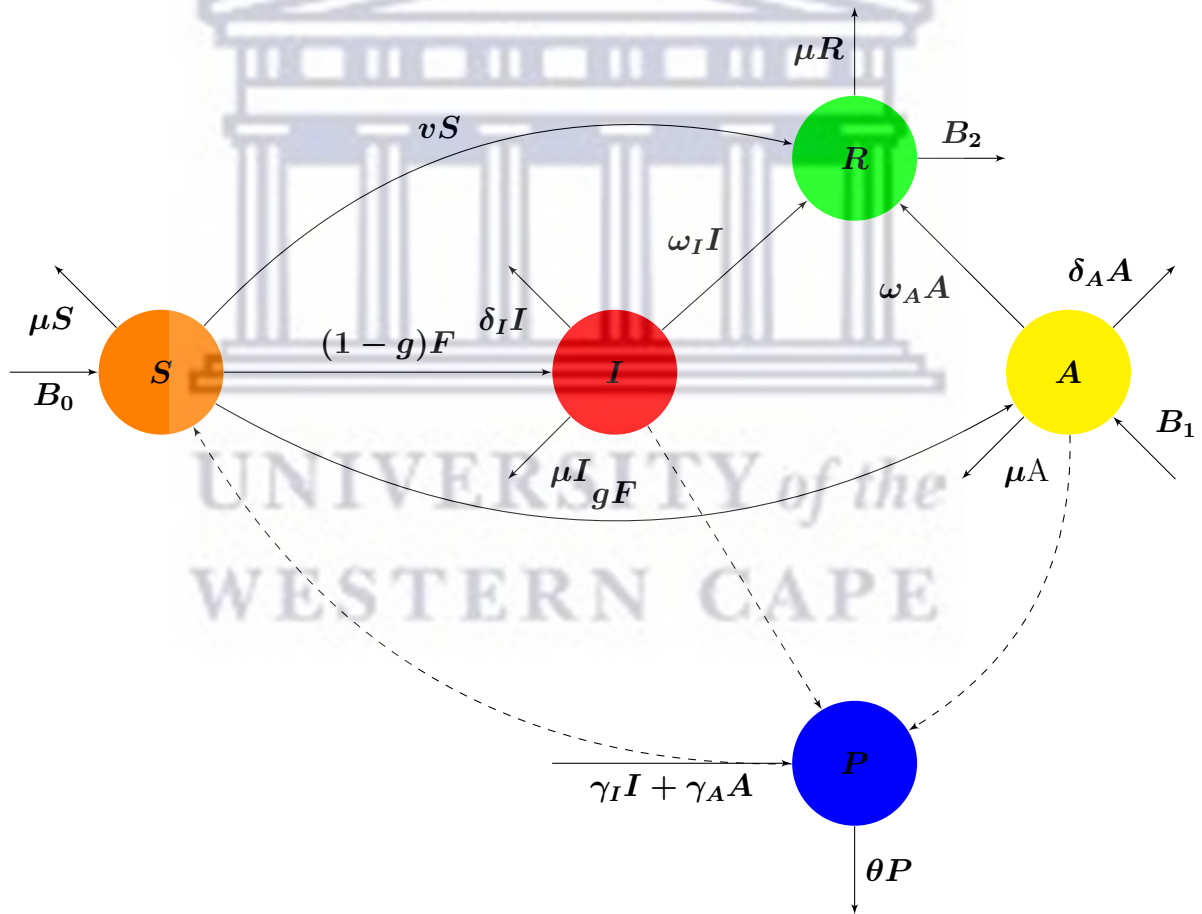


Figure 4.1: The flow diagram for the **SIARP** model

The compartmental model (4.1.2) below depicts the transmission between the classes S ,

I , A , R , and P shown in Figure 4.1 above.

$$\begin{aligned}
\frac{dS}{dt} &= B_0 - F - \mu_0 S, \\
\frac{dI}{dt} &= (1 - g)F - \mu_1 I, \\
\frac{dA}{dt} &= B_1 + gF - \mu_2 A, \\
\frac{dR}{dt} &= vS + \omega_I I + \omega_A A - \mu R - B_2, \\
\frac{dP}{dt} &= \gamma_I I + \gamma_A A - \theta P, \\
N &= S + I + A + R + P,
\end{aligned} \tag{4.1.2}$$

where $F = \frac{\alpha SP}{1 + CP} + \beta S(I + A)$, $\mu_0 = (\mu + v)$, $\mu_1 = (\mu + \delta_I + \omega_I)$, $\mu_2 = (\mu + \delta_A + \omega_A)$, and N is the total population. The deterministic model describes the transmission dynamics of COVID-19 disease in the South African population by $N(t)$ and is divided into five different compartments: those susceptible to the disease $S(t)$, the symptomatically infected persons $I(t)$, those that are asymptotically infected with the disease $A(t)$, those removed from the population $R(t)$, and the density of the virus in the environmental reservoir denoted as $P(t)$. The first equation in (4.1.2) shows a constant inflow of susceptibles at rate B_0 . It is the recruitment parameter into the susceptible class S . α is the transmission rate from S to I (due to contact with environmental reservoir P). C is the proportion of interaction with infectious environment P . β is the transmission rate from S to I (due to contact with I and/or A). The susceptible class decreases by rates of new infections, or those leaving the susceptible compartment βSI and βSA (also called incidences of the disease). The number of infected individuals moving from the asymptomatic compartment per unit time is at time t . The rate of vaccination is shown as v and is taken as 0 , since no vaccine was available at that time. In the second equation we see parameters g , δ_I , and ω_I . They are the proportion of symptomatic infectious persons, the death rate due to COVID-19, and rate at which persons in compartment S recover from the disease, respectively. Lastly, in the third,

fourth and fifth equations in (4.1.2), parameters B_i for $i = 1, 2$ describes respectively, the influx rate of asymptotically infected migrants into South Africa, and the departing rate of surviving migrants as they recover from COVID-19. There is also the death rate due to COVID-19 for the asymptomatic infectious persons δ_A , the recovery rate from the COVID-19 disease for this asymptomatic group ω_A , the rate γ_I at which the virus spreads in the environmental reservoir P by I , and γ_A being the rate at which virus spreads in environmental reservoir P by A . The rate of susceptible, symptomatic infected (showing clinical symptoms), asymptomatic infected (showing no clinical symptoms), removed individuals, and the pathogens from each of the five compartments through natural death (and disease induced death) are represented by μS , μI , μA , μR , and θP , respectively. The individuals move from the susceptible group to the infected group, decreasing class S , since the number of susceptible individuals decreases during the outbreak as hosts become infected. In the second and third equations in (4.1.2), there is an increase in population of symptomatic infectious class I , and there is a decrease as some of these individuals can become asymptomatic infectious, moving into class A at a rate of B_1 , increasing this class. Equation four of (4.1.2) shows that there are symptomatic and asymptomatic individuals that move to class R at rates $\omega_I I$ and $\omega_A A$ due to recovery from the coronavirus, and susceptibles recover due to being vaccinated at a rate of vS . This causes class R to increase, but it then decreases since migrants depart from local population as they recover from virus at rate B_2 . Lastly, in equation five of (4.1.2) we see an increase in the environmental reservoir P due to susceptibles being exposed to infection from symptomatic and asymptomatic infectious individuals. In all of the compartments natural death for host population takes place at rate μ , and for pathogen mortality at rate θ .

4.2 Boundedness and positivity of solutions

It is important that solutions of our system (4.1.2) are positive and bounded. We show this through making use of methods used by [77, 78] to find our positive invariant set and then we proceed with making use of proposition and theorem seen in [77].

Let us write the total population $N(t)$ as,

$$N(t) = S(t) + I(t) + A(t) + R(t) \quad (4.2.1)$$

excluding the pathogens $P(t)$ from the compartments of the human population. We also introduce two sets H_0 and H_1 ,

$$H_0 = \mathbb{R}_{++}^5,$$

$$H_1 = \left\{ x \in \mathbb{R}_{++}^5 \mid x_1 + x_2 + x_3 + x_4 + x_5 \leq \frac{B}{\mu} \right\}.$$

We are now going to study the positivity and boundedness of solutions of our system. From equation (4.2.1) take the derivative of $N(t)$ on both sides w.r.t. t which leaves us with,

$$\frac{dN}{dt} = \frac{dS}{dt} + \frac{dI}{dt} + \frac{dA}{dt} + \frac{dR}{dt}. \quad (4.2.2)$$

Substituting in the equations of (4.1.2) we have,

$$\frac{dN}{dt} = (B_0 + B_1 - B_2) - (S + I + A + R)\mu - \delta_I I - \delta_A A. \quad (4.2.3)$$

In the case of having zero infections i.e. $I, A = 0$, or zero deaths due to COVID-19, the above equation becomes the inequality,

$$\frac{dN}{dt} \leq (B - N\mu), \quad (4.2.4)$$

where $(B_0 + B_1 - B_2) = B$ and $N = (S + I + A + R)$. Integration yields that,

$$N \leq \frac{B}{\mu}. \quad (4.2.5)$$

So, $0 \leq N \leq \frac{B}{\mu}$ which means that H_1 is a positive invariant set for system (4.1.2).

We now state and give proofs using the following proposition and theorems from [77] and [79].

Proposition 4.2.1. [77] Consider a number $t_1 \in (0, \infty)$. Suppose that $\mathbf{X}(t) = (S(t), I(t), A(t), R(t), P(t))$ is a solution for the system (4.1.2) with $\mathbf{X}(t) \in H_0$ for all $t \in [0, t_1)$ and $N(0) < \frac{B}{\mu}$. Then $N(t) \leq \frac{B}{\mu}, \forall t \in [0, t_1)$.

Proof.

$\frac{d\left(N(t) - \frac{B}{\mu}\right)}{dt} = -\mu\left(N(t) - \frac{B}{\mu}\right) - \delta I \leq -\mu\left(N(t) - \frac{B}{\mu}\right)$. Therefore $N(0) < \frac{B}{\mu}$ implies that $N(t) < \frac{B}{\mu}, \forall t \leq t_1$. \square

Theorem 7. [77] Suppose that for $t \geq 0$, $\mathbf{X}(t) = (S(t), I(t), A(t), R(t), P(t))$ is a solution of (4.1.2) with $\mathbf{X}(0) \in H_1$. Then $\mathbf{X}(t) \in H_1, \forall t > 0$.

Proof.

Suppose that we have non-empty set $\Phi := \{t > 0 : \mathbf{X}(t) \notin H_0\}$. Then Φ has an infimum ϕ_1 , and ϕ_1 is the smallest time-value for which $\mathbf{X}(t)$ exits the set H_0 . Also, $\phi_1 > 0$ since $\mathbf{X}(t)$ is continuous. Now let us define a function $M : [0, \infty) \rightarrow \mathbb{R}$ as follows,

$$M(t) = \ln\left(\frac{B}{\mu S(t)}\right) + \ln\left(\frac{B}{\mu I(t)}\right) + \ln\left(\frac{B}{\mu A(t)}\right) + \ln\left(\frac{B}{\mu R(t)}\right) + (P(t) - \ln(P(t))).$$

Note that each of the terms are non-negative for any $0 \leq t < \phi_1$. Our next step is to take the derivative of function $M(t)$ on both sides w.r.t. t resulting in,

$$\dot{M} = \left[\frac{-S'(t)}{S(t)}\right] + \left[\frac{-I'(t)}{I(t)}\right] + \left[\frac{-A'(t)}{A(t)}\right] + \left[\frac{-R'(t)}{R(t)}\right] + \left[\left(1 - \frac{1}{P(t)}\right) P'(t)\right]. \quad (4.2.6)$$

By appropriately substituting our system of equations (4.1.2) yields,

$$\begin{aligned} \dot{M} = & \frac{-B_0}{S} + \frac{F}{S} + \mu_0 - \frac{1}{I} + \frac{gF}{I} + \mu_1 - \frac{B_1}{A} - \frac{gF}{A} + \mu_2 - \frac{vS}{R} - \frac{\omega_I I}{R} - \frac{\omega_A A}{R} \\ & + \mu + \frac{B_2}{R} + \gamma_I I + \gamma_A A - \theta P - \frac{\gamma_I I}{P} - \frac{\gamma_A A}{P} + \theta. \end{aligned} \quad (4.2.7)$$

By eliminating the negative terms we obtain the inequality,

$$\dot{M} \leq T_1, \quad (4.2.8)$$

where

$$T_1 = \frac{F}{S} + \frac{gF}{I} + \frac{B_2}{R} + \gamma_I I + \gamma_A A + \mu_0 + \mu_1 + \mu_2 + \mu + \theta. \quad (4.2.9)$$

Integrating (4.2.8) from 0 to ϕ_1 gives,

$$\dot{M}(t) = M(0) + \int_0^{\phi_1} \dot{M}(s) ds \leq M(0) + M_1 t \leq M(0) + M_1 \phi_1. \quad (4.2.10)$$

Taking note that $\lim_{x \rightarrow \infty} (\ln x) = \infty$ and $\lim_{x \rightarrow 0^+} (x - \ln(x)) = \infty$, we can come to the conclusion that

$$\lim_{t \rightarrow \phi_1^-} M(t) = \infty. \quad (4.2.11)$$

However, we notice in (4.2.10) how M is bounded above. This is the contradiction. \square

4.3 Equilibria and the basic reproduction number of our *SIARP* Model

Compartmental models in epidemiology have two equilibria; the disease-free equilibrium point and the endemic equilibrium point [71]. For our *SIARP* model (4.1.2) the basic reproduction number is denoted by R_0 and is obtained through first finding the disease-free equilibrium point.

Finding the partial derivatives inside matrices \mathbf{G} and \mathbf{V} and evaluating them at the disease-free equilibrium point gives us \mathbf{G} and \mathbf{V} as,

$$\mathbf{G} = \begin{bmatrix} (1-g)\beta S^0 & (1-g)\beta S^0 & (1-g)\alpha S^0 \\ g\beta S^0 & g\beta S^0 & g\alpha S^0 \\ 0 & 0 & 0 \end{bmatrix},$$

and

$$\mathbf{V} = \begin{bmatrix} (\mu + \delta_I + \omega_I) & 0 & 0 \\ 0 & (\mu + \delta_A + \omega_A) & 0 \\ -\gamma_I & -\gamma_A & \theta \end{bmatrix}.$$

Our next step is to find the next generation matrix denoted by \mathbf{GV}^{-1} for our model. But before we do so, let us briefly give information regarding this operator.

4.3.1 The next generation matrix operator

In order for us to calculate the matrix \mathbf{GV}^{-1} , we first need to find the inverse matrix \mathbf{V}^{-1} .

$$\mathbf{V}^{-1} = \begin{bmatrix} \frac{1}{(\mu + \delta_I + \omega_I)} & 0 & 0 \\ 0 & \frac{1}{(\mu + \delta_A + \omega_A)} & 0 \\ \frac{\gamma_I}{\theta(\mu + \delta_I + \omega_I)} & \frac{\gamma_A}{\theta(\mu + \delta_A + \omega_A)} & \frac{1}{\theta} \end{bmatrix}.$$

From above, we can now find \mathbf{GV}^{-1} . Then \mathbf{GV}^{-1} is as below,

$$\mathbf{GV}^{-1} = \begin{bmatrix} \left(\frac{(1-g)\beta S^0}{(\mu + \delta_I + \omega_I)} + \frac{\gamma_I(1-g)\alpha S^0}{\theta(\mu + \delta_I + \omega_I)} \right) & \left(\frac{(1-g)\beta S^0}{(\mu + \delta_A + \omega_A)} + \frac{\gamma_A(1-g)\alpha S^0}{\theta(\mu + \delta_A + \omega_A)} \right) & \left(\frac{(1-g)\alpha S^0}{\theta} \right) \\ \left(\frac{g\beta S^0}{(\mu + \delta_I + \omega_I)} + \frac{g\alpha S^0 \gamma_I}{\theta(\mu + \delta_I + \omega_I)} \right) & \left(\frac{g\beta S^0}{(\mu + \delta_A + \omega_A)} + \frac{g\alpha S^0 \gamma_A}{\theta(\mu + \delta_A + \omega_A)} \right) & \left(\frac{g\alpha S^0}{\theta} \right) \\ 0 & 0 & 0 \end{bmatrix}.$$

Keeping in mind that $\mu_1 = (\mu + \delta_I + \omega_I)$ and $\mu_2 = (\mu + \delta_A + \omega_A)$, we therefore have the above matrix as

$$\mathbf{GV}^{-1} = \begin{bmatrix} \left(\frac{(1-g)\beta S^0}{\mu_1} + \frac{\gamma_I(1-g)\alpha S^0}{\theta\mu_1} \right) & \left(\frac{(1-g)\beta S^0}{\mu_2} + \frac{\gamma_A(1-g)\alpha S^0}{\theta\mu_2} \right) & \left(\frac{(1-g)\alpha S^0}{\theta} \right) \\ \left(\frac{g\beta S^0}{\mu_1} + \frac{g\alpha S^0 \gamma_I}{\theta\mu_1} \right) & \left(\frac{g\beta S^0}{\mu_2} + \frac{g\alpha S^0 \gamma_A}{\theta\mu_2} \right) & \left(\frac{g\alpha S^0}{\theta} \right) \\ 0 & 0 & 0 \end{bmatrix}.$$

We now find the spectral radius of \mathbf{GV}^{-1} by finding the characteristic equation and its eigenvalues. The maximum positive eigenvalue will then be our basic reproduction number, \mathbf{R}_0 .

Finding the $\det(\mathbf{GV}^{-1} - \lambda\mathbf{I}) = 0$, gives us

$$\begin{aligned} 0 &= -\lambda^3 + \left[\left(\frac{(1-g)\beta S^0}{\mu_1} + \frac{\gamma_I(1-g)\alpha S^0}{\theta\mu_1} \right) + \left(\frac{g\beta S^0}{\mu_2} + \frac{g\alpha S^0\gamma_A}{\theta\mu_2} \right) \right] \lambda^2, \\ 0 &= \lambda^2 \left[-\lambda + \left[\left(\frac{(1-g)\beta S^0}{\mu_1} + \frac{\gamma_I(1-g)\alpha S^0}{\theta\mu_1} \right) + \left(\frac{g\beta S^0}{\mu_2} + \frac{g\alpha S^0\gamma_A}{\theta\mu_2} \right) \right] \right]. \end{aligned}$$

So, the roots are $\lambda_1^2 = 0$ and λ_2 , where

$$\lambda_2 = \left(\frac{(1-g)\beta S^0}{\mu_1} + \frac{\gamma_I(1-g)\alpha S^0}{\theta\mu_1} \right) + \left(\frac{g\beta S^0}{\mu_2} + \frac{g\alpha S^0\gamma_A}{\theta\mu_2} \right). \quad (4.3.1)$$

By simplifying the above expression (4.3.1) and by the substitution of S^0 , the basic reproduction number is therefore

$$\mathbf{R}_0 = \frac{B_0 \left[(1-g)\mu_2(\beta\theta + \alpha\gamma_I) + g\mu_1(\beta\theta + \alpha\gamma_A) \right]}{\theta\mu_0\mu_1\mu_2}.$$

4.4 Existence of the endemic equilibrium

This section tells us more about the existence of the endemic equilibrium and how we ended up with a polynomial $\mathbf{G}(\mathbf{I}^*)$ seen in the equation (4.4.11) when the rate of influx of migrants who are asymptotically infected, \mathbf{B}_1 not equal to zero and when \mathbf{B}_1 is zero, $\mathbf{G}(\mathbf{I}^*)$ becomes a cubic equation in \mathbf{I}^* . We now set the left hand side already to zero for computing the coordinates of the endemic equilibrium \mathbf{E}^* .

$$\begin{aligned}
0 &= B_0 - F - \mu_0 S, \\
0 &= (1 - g)F - \mu_1 I, \\
0 &= B_1 + gF - \mu_2 A, \\
0 &= vS + \omega_I I + \omega_A A - \mu R - B_2, \\
0 &= \gamma_I I + \gamma_A A - \theta P, \\
N &= S + I + A + R + P,
\end{aligned} \tag{4.4.1}$$

where $F = \frac{\alpha SP}{1 + CP} + \beta S(I + A)$.

From the first equation of (4.4.1) we have,

$$F = B_0 - \mu_0 S^*,$$

and from the second equation of (4.4.1) we have,

$$F = \frac{\mu_1 I^*}{(1 - g)}.$$

The latter two equations enable us to express S^* as,

$$S^* = \frac{\left[B_0 - \frac{\mu_1 I^*}{(1 - g)} \right]}{\mu_0}. \tag{4.4.2}$$

The third and fifth equations yield A^* as,

$$A^* = \frac{[B_1 + g_0 \mu_1 I^*]}{\mu_2}, \tag{4.4.3}$$

with $g_0 = \frac{g}{(1 - g)}$, and

$$P^* = \frac{[\gamma_I I^* + \gamma_A A^*]}{\theta}. \tag{4.4.4}$$

Starting with the two expressions for F , we obtain the identity:

$$\frac{\mu_1 I^*}{(1 - g)} = S^* \left[\frac{\alpha P^*}{1 + CP^*} + \beta(I^* + A^*) \right], \tag{4.4.5}$$

which can be written as,

$$\frac{\mu_2^2 \theta \mu_1 I^* (1 + CP^*)}{(1 - g)} = \mu_2^2 \theta S^* [\alpha P^* + \beta (I^* + A^*) (1 + CP^*)]. \quad (4.4.6)$$

The left hand side is therefore

$$LHS = Q_1 I^{*2} + Q_2 I^*, \quad (4.4.7)$$

where

$$Q_1 = \frac{\mu_2^2 \mu_1 \gamma_I C}{(1 - g)} + \frac{\mu_2 \mu_1^2 \gamma_A g_0 C}{(1 - g)},$$

$$Q_2 = \frac{\mu_2^2 \theta \mu_1}{(1 - g)} + \frac{\mu_2 \mu_1 \gamma_A B_1 C}{(1 - g)}.$$

By letting $\frac{\mu_1}{(1 - g)} = \phi$, it becomes

$$Q_1 = \mu_2^2 \phi \gamma_I C + \mu_2 \mu_1 \phi \gamma_A g_0 C,$$

$$Q_2 = \mu_2^2 \theta \phi + \mu_2 \phi \gamma_A B_1 C. \quad (4.4.8)$$

For the right hand side, it becomes

$$RHS = S^* [Q_3 I^{*2} + Q_4 I^* + Q_5]. \quad (4.4.9)$$

where

$$Q_3 = \mu_2^2 \beta \gamma_I C + \mu_2 \mu_1 \beta \gamma_A g_0 C + \mu_2 \mu_1 \gamma_I \beta g_0 C + \beta g_0^2 \mu_1^2 \gamma_A C,$$

$$Q_4 = \mu_2^2 \alpha \gamma_I + \mu_2 \alpha \gamma_A g_0 \mu_1 + \mu_2^2 \theta \beta + \mu_2 \theta \beta g_0 \mu_1 + \mu_2 \gamma_A \beta B_1 C$$

$$+ \mu_2 \gamma_I \beta B_1 C + 2\beta B_1 \gamma_A g_0 \mu_1 C,$$

$$Q_5 = \mu_2 \alpha \gamma_A B_1 + \mu_2 \theta \beta B_1 + \beta B_1^2 \gamma_A C.$$

So, substituting S^* in the equation of (4.4.9) and multiplying out and simplifying the answer yields

$$\begin{aligned}
RHS &= S^*[Q_3I^{*2} + Q_4I^* + Q_5], \\
&= \frac{\left[B_0 - \frac{\mu_1 I^*}{(1-g)}\right]}{\mu_0} [Q_3I^{*2} + Q_4I^* + Q_5], \\
&= \frac{1}{\mu_0} \left[B_0Q_3I^{*2} + B_0Q_4I^* + B_0Q_5 - \frac{\mu_1 Q_3 I^{*3}}{(1-g)} - \frac{\mu_1 Q_4 I^{*2}}{(1-g)} - \frac{\mu_1 Q_5 I^*}{(1-g)} \right].
\end{aligned}$$

By letting $\frac{\mu_1}{(1-g)} = \phi$, the right hand side of the equation is therefore

$$RHS = -\frac{Q_3\phi I^{*3}}{\mu_0} + \frac{(B_0Q_3 - Q_4\phi)I^{*2}}{\mu_0} + \frac{(B_0Q_4 - Q_5\phi)I^*}{\mu_0} + \frac{B_0Q_5}{\mu_0}. \quad (4.4.10)$$

Subtracting the left hand side and right hand side equations gives the polynomial $G(I^*)$. The final answer of the polynomial $G(I^*)$ therefore then has the form we see in the last equation of (4.4.11) below. Take note that $G(I^*)$ is a cubic equation in I^* .

$$\begin{aligned}
G(I^*) &= LHS - RHS, \\
G(I^*) &= \frac{Q_3\phi I^{*3}}{\mu_0} + \left[\mu_2^2\phi\gamma_I C + \mu_2\mu_1\phi\gamma_A g_0 C - \frac{(B_0Q_3 - Q_4\phi)}{\mu_0} \right] I^{*2} \\
&\quad + \left[\mu_2^2\theta\phi + \mu_2\phi\gamma_A B_1 C - \frac{(B_0Q_4 - Q_5\phi)}{\mu_0} \right] I^* - \frac{B_0Q_5}{\mu_0}.
\end{aligned} \quad (4.4.11)$$

Looking at our own model, we state the following two theorems. They show that our system has a unique endemic equilibrium point X^* for cases when the influx rate of asymptotically infected migrants is positive ($B_1 > 0$) seen in (4.4.12), and for $R_0 > 0$ when the influx rate is zero ($B_1 = 0$) seen in (4.4.14).

Theorem 8. *If $B_1 > 0$, then the system (4.1.2) has a unique endemic equilibrium point*

X^* , with coordinates

$$\begin{aligned}
S^* &= \frac{(1-g)B_0 - (\mu + \delta_I + \omega_I)I^*}{(1-g)}, \\
A^* &= \frac{(1-g)B_1 - g(\mu + \delta_I + \omega_I)I^*}{(1-g)(\mu + \delta_A + \omega_A)}, \\
R^* &= \frac{[(1-g)(\mu + \delta_A + \omega_A)\omega_I + \omega_A g(\mu + \delta_I + \omega_I) - (\mu + \delta_A + \omega_A)v(\mu + \delta_I + \omega_I)]I^*}{\mu(1-g)(\mu + \delta_A + \omega_A)} \\
&\quad + \frac{(\mu + \delta_A + \omega_A)v(1-g)B_0 + \omega_A(1-g)B_0 - (1-g)(\mu + \delta_A + \omega_A)B_2}{\mu(1-g)(\mu + \delta_A + \omega_A)}, \\
P^* &= \frac{\gamma_A(1-g)B_1 + [(1-g)(\mu + \delta_A + \omega_A)\gamma_I - g(\mu + \delta_I + \omega_I)\gamma_A]I^*}{\theta(1-g)(\mu + \delta_A + \omega_A)},
\end{aligned} \tag{4.4.12}$$

where I^* is the unique positive root of the polynomial $G(I^*)$ of the equation (4.4.11).

Proof.

We recall that $G(I^*) = a_3 I^{*3} + a_2 I^{*2} + a_1 I^* + a_0$ with

$$\begin{aligned}
a_3 &= \frac{Q_3 \phi}{\mu_0}, \\
a_2 &= \left[\mu_2^2 \phi \gamma_I C + \mu_2 \mu_1 \phi \gamma_A g_0 C - \frac{(B_0 Q_3 - Q_4 \phi)}{\mu_0} \right], \\
a_1 &= \left[\mu_2^2 \theta \phi + \mu_2 \phi \gamma_A B_1 C - \frac{(B_0 Q_4 - Q_5 \phi)}{\mu_0} \right], \text{ and} \\
a_0 &= \frac{B_0 Q_5}{\mu_0}.
\end{aligned}$$

We note that $a_3 > 0$ and $a_0 < 0$. Thus, by Descartes's rule of signs, in order to prove that $G(I^*)$ has a unique positive root, it suffices to prove that either $a_2 > 0$ or $a_1 < 0$. Now let us suppose that to the contrary we have

$$a_2 \leq 0 \quad \text{and} \quad a_1 \geq 0.$$

Since $Q_3 > 0$ and $Q_4 > 0$, we must have

$$\mu_0(Q_3 a_1 - Q_4 a_2) \geq 0.$$

We calculate that

$$\begin{aligned}
& \mu_0(Q_3a_1 - Q_4a_2) \\
= & \mu_0Q_3 \left[\mu_2^2\theta\phi + \mu_2\phi\gamma_A B_1C - \frac{(B_0Q_4 - Q_5\phi)}{\mu_0} \right] \\
& - \mu_0Q_4 \left[\mu_2^2\phi\gamma_I C + \mu_1\mu_2\phi\gamma_A g_0C - \frac{(B_0Q_3 - Q_4\phi)}{\mu_0} \right] \\
= & \mu_0Q_3 \left[\mu_2^2\theta\phi + \mu_2\phi\gamma_A B_1C \right] + \phi Q_3 Q_5 \\
& - \mu_0Q_4 \left[\mu_2^2\phi\gamma_I C + \mu_1\mu_2\phi\gamma_A g_0C \right] - \phi Q_4^2 \\
= & Q_3 \left[\mu_0\mu_2^2\theta\phi + \mu_0\mu_2\phi\gamma_A B_1C + \phi Q_5 \right] \\
& - Q_4 \left[\mu_0\mu_2^2\phi\gamma_I C + \mu_0\mu_1\mu_2\phi\gamma_A g_0C + \phi Q_4 \right] \\
= & \left[\mu_2^2\beta\gamma_I C + \mu_2\mu_1\beta\gamma_A g_0C + \mu_2\mu_1\gamma_I\beta g_0C + \beta g_0^2\mu_1^2\gamma_A C \right] \\
& \times \left[\mu_0\mu_2^2\theta\phi + \mu_0\mu_2\phi\gamma_A B_1C + \phi(\mu_2\alpha\gamma_A B_1 + \mu_2\theta\beta B_1 + \beta B_1^2\gamma_A C) \right] \\
& - \left[\mu_2^2\alpha\gamma_I + \mu_2\alpha\gamma_A g_0\mu_1 + \mu_2^2\theta\beta + \mu_2\theta\beta g_0\mu_1 \right. \\
& \left. + \beta B_1C(\mu_2\gamma_A + \mu_2\gamma_I + 2\gamma_A g_0\mu_1) \right] \\
& \times \left[\mu_0\mu_2^2\phi\gamma_I C + \mu_0\mu_1\mu_2\phi\gamma_A g_0C + \phi Q_4 \right] \\
= & \left[\mu_2^2\beta\gamma_I C + \mu_2\mu_1\beta\gamma_A g_0C + \mu_2\mu_1\gamma_I\beta g_0C + \beta g_0^2\mu_1^2\gamma_A C \right] \\
& \times \left[\mu_0\mu_2^2\theta\phi + \mu_0\mu_2\phi\gamma_A B_1C + \phi(\mu_2\alpha\gamma_A B_1 + \mu_2\theta\beta B_1 + \beta B_1^2\gamma_A C) \right] \\
& - \left[\mu_2^2\alpha\gamma_I + \mu_2\alpha\gamma_A g_0\mu_1 + \mu_2^2\theta\beta + \mu_2\theta\beta g_0\mu_1 \right. \\
& \left. + \beta B_1C(\mu_2\gamma_A + \mu_2\gamma_I + 2\gamma_A g_0\mu_1) \right] \\
& \times \left[\mu_0\mu_2^2\phi\gamma_I C + \mu_0\mu_1\mu_2\phi\gamma_A g_0C \right] \\
& - \phi \left[\mu_2^2\alpha\gamma_I + \mu_2\alpha\gamma_A g_0\mu_1 + \mu_2^2\theta\beta + \mu_2\theta\beta g_0\mu_1 \right. \\
& \left. + \beta B_1C(\mu_2\gamma_A + \mu_2\gamma_I + 2\gamma_A g_0\mu_1) \right]^2
\end{aligned}$$

When we expand the latter expression, we obtain a number of terms, twenty of which are positive. A routine exercise, which we omit, reveals that all of these positive terms cancel away, and we can conclude that

$$Q_3 a_1 - Q_4 a_2 < 0$$

which is a contradiction. Therefore, the assumption that we can have $a_1 \geq 0$ and $a_2 \leq 0$ is false. Therefore, by Descartes' rule of signs, the polynomial G has exactly one positive root, which is the value I^* of a unique endemic equilibrium point. \square

For the case when $B_1 = 0$, we have the following:

$$Q_1 = \mu_2^2 \phi \gamma_I C + \mu_2 \mu_1 \phi \gamma_A g_0 C,$$

$$Q_2 = \mu_2^2 \theta \phi,$$

$$Q_3 = \mu_2^2 \beta \gamma_I C + \mu_2 \mu_1 \beta \gamma_A g_0 C + \mu_2 \mu_1 \gamma_I \beta g_0 C + \beta g_0^2 \mu_1^2 \gamma_A C,$$

$$Q_4 = \mu_2^2 \alpha \gamma_I + \mu_2 \alpha \gamma_A g_0 \mu_1 + \mu_2^2 \theta \beta + \mu_2 \theta \beta g_0 \mu_1,$$

$$Q_5 = 0.$$

After making some substitutions, multiplying out, subtracting terms, and then simplifying, we notice that when $B_1 = 0$, the polynomial $G(I^*)$ can be replaced by a quadratic equation in I^* . It has the form shown below in (4.4.13).

$$G_0(I^*) = LHS - RHS,$$

$$G_0(I^*) = \frac{Q_3 \phi I^{*2}}{\mu_0} + \left[\mu_2^2 \phi \gamma_I C + \mu_2 \mu_1 \phi \gamma_A g_0 C - \frac{(B_0 Q_3 - Q_4 \phi)}{\mu_0} \right] I^* + \left[\mu_2^2 \theta \phi - \frac{B_0 Q_4}{\mu_0} \right]. \quad (4.4.13)$$

Theorem 9. *If $B_1 = 0$ and $R_0 > 1$, then the system (4.1.2) has a unique endemic*

equilibrium point \mathbf{X}^* , with coordinates

$$\begin{aligned}
S^* &= \frac{(1-g)B_0 - (\mu + \delta_I + \omega_I)I^*}{(1-g)}, \\
A^* &= -\frac{g(\mu + \delta_I + \omega_I)I^*}{(1-g)(\mu + \delta_A + \omega_A)}, \\
R^* &= \frac{[(1-g)(\mu + \delta_A + \omega_A)\omega_I + \omega_A g(\mu + \delta_I + \omega_I) - (\mu + \delta_A + \omega_A)v(\mu + \delta_I + \omega_I)]I^*}{\mu(1-g)(\mu + \delta_A + \omega_A)} \\
&\quad + \frac{(\mu + \delta_A + \omega_A)v(1-g)B_0 + \omega_A(1-g)B_0 - (1-g)(\mu + \delta_A + \omega_A)B_2}{\mu(1-g)(\mu + \delta_A + \omega_A)}, \\
P^* &= \frac{[(1-g)(\mu + \delta_A + \omega_A)\gamma_I - g(\mu + \delta_I + \omega_I)\gamma_A]I^*}{\theta(1-g)(\mu + \delta_A + \omega_A)},
\end{aligned} \tag{4.4.14}$$

where I^* is the unique positive root of the polynomial $\mathbf{G}_0(I^*)$ of the equation (4.4.13).

Proof.

Recall that $\mathbf{G}_0(I^*) = a_3 I^{*2} + a_2 I^* + a_1$ with

$$\begin{aligned}
a_3 &= \frac{Q_3 \phi}{\mu_0}, \\
a_2 &= \mu_2^2 \phi \gamma_I C + \mu_2 \mu_1 \phi \gamma_A g_0 C - \frac{(B_0 Q_3 - Q_4 \phi)}{\mu_0}, \\
a_1 &= \mu_2^2 \theta \phi - \frac{B_0 Q_4}{\mu_0}.
\end{aligned}$$

Note that $a_3 > 0$. We need to prove that $\mathbf{G}_0(I^*)$ has a unique positive root. By Descartes' rule of signs, all we need to do is show that $a_1 < 0$. We calculate, noting that $\phi = \frac{\mu_1}{(1-g)}$, and after some simplification, we obtain:

$$a_1 = \frac{\mu_2^2 \mu_1 \theta}{(1-g)} [1 - R_0] < 0,$$

since $R_0 > 1$. □

4.5 Global stability of the disease-free equilibrium

For investigating global stability of the disease-free equilibrium, we must assume that there is no inflow of infecteds. Also, we introduce invariant R_{glo} of the model (4.1.2),

$$R_{glo} = \max \left\{ \frac{(\theta\beta + \alpha\gamma_I) S^0}{\mu_1\theta}, \frac{(\theta\beta + \alpha\gamma_A) S^0}{\mu_2\theta} \right\}. \quad (4.5.1)$$

The work of van den Driessche and Watmough [72] ensures the local stability of the disease-free equilibrium that we calculated previously. Methods of the theorem [72] can be found in [80].

Theorem 10. [80] *The disease-free equilibrium of system (2.1) is locally asymptotically stable whenever $R_0 < 1$ and unstable otherwise.*

The number R_0 can be expressed as,

$$R_0 = b \left\{ R_{I_1} + \frac{\sigma R_{I_2}}{\sigma + \mu} + \frac{\rho\sigma(1-q)R_A}{(\sigma + \mu)(\delta + \mu)} \right\},$$

where $R_{I_1} = \frac{\beta c}{\mu + \sigma}$, $R_{I_2} = \frac{\eta_1 \beta c}{\rho + \mu}$ and $R_A = \frac{\eta_2 \beta c}{\delta + \mu}$, and they represent the contribution of the asymptomatic, symptomatic and AIDS individuals to the overall model reproduction number R_0 respectively. The proportion of asymptomatic individuals who become symptomatic and individuals who develop to full-blown AIDS are given by $\frac{\sigma}{\sigma + \mu}$ and $\left(\frac{\rho}{\mu + \rho}\right) \left(\frac{\sigma}{\mu + \sigma}\right)$ respectively.

We continue now with stating the theorem of global stability of the disease-free equilibrium of our model and then prove it.

Theorem 11. *The disease-free equilibrium of the COVID-19 model (4.1.2) is globally asymptotically stable if $R_{glo} < 1$.*

Proof. This will be investigated using the Lyapunov method [94]. Since by assumption $R_{glo} < 1$, the following inequalities then hold

$$\begin{aligned} (\theta\beta + \alpha\gamma_I) S^0 - \mu_1\theta &< 0, \\ (\theta\beta + \alpha\gamma_A) S^0 - \mu_2\theta &< 0. \end{aligned} \quad (4.5.2)$$

Then there exists $z_0 > 0$ such that,

$$\begin{aligned} [\theta\beta + (\alpha + z_0)\gamma_I] S^0 - \mu_1\theta &< 0, \\ [\theta\beta + (\alpha + z_0)\gamma_A] S^0 - \mu_2\theta &< 0. \end{aligned} \quad (4.5.3)$$

We introduce the number z as below,

$$z = \frac{(\alpha + z_0) S^0}{\theta}. \quad (4.5.4)$$

Now we define the function $V = V(S(t), I(t), A(t), P(t))$ as follows,

$$V = S - S^0 + S^0 \ln\left(\frac{S^0}{S}\right) + I + A + zP. \quad (4.5.5)$$

Then V is positive-definite w.r.t. the disease-free equilibrium. We calculate the derivative of $V(t)$:

$$\begin{aligned} \dot{V} &= S' \left(1 - \frac{S^0}{S}\right) + I' + A' + zP' \\ &= [B_0 - F - \mu_0 S] \left(1 - \frac{S^0}{S}\right) + [(1-g)F - \mu_1 I] \\ &\quad + [gF - \mu_2 A] + z[\gamma_I I + \gamma_A A - \theta P] \\ &= [\mu_0 S^0 - \mu_0 S - F] \left(1 - \frac{S^0}{S}\right) + [(1-g)F - \mu_1 I] \\ &\quad + [gF - \mu_2 A] + z[\gamma_I I + \gamma_A A - \theta P]. \end{aligned} \quad (4.5.6)$$

After multiplying out the brackets and canceling out a few terms, we are left with the following

$$\dot{V} \leq -\frac{\mu_0 (S^0 - S)^2}{S} + [z\gamma_I - \mu_1] I + [z\gamma_A - \mu_2] A - z\theta P + \frac{FS^0}{S}. \quad (4.5.7)$$

Using the fact that $F = \frac{\alpha SP}{1 + CP} + \beta S(I + A)$ and substituting F into the equation

of \dot{V} in (4.5.7) yields

$$\begin{aligned}
\dot{V} &= -\frac{\mu_0 (S^0 - S)^2}{S} + z\gamma_I I - \mu_1 I + z\gamma_A A - \mu_2 A - z\theta P \\
&\quad + \left[\frac{\alpha S P}{1 + CP} + \beta S(I + A) \right] \frac{S^0}{S}, \\
&= -\frac{\mu_0 (S^0 - S)^2}{S} + z\gamma_I I - \mu_1 I + z\gamma_A A - \mu_2 A - z\theta P \\
&\quad + \frac{\alpha S^0 P}{1 + CP} + \beta S^0 I + \beta S^0 A, \\
&= -\frac{\mu_0 (S^0 - S)^2}{S} + [z\gamma_I - \mu_1 + \beta S^0] I + [z\gamma_A - \mu_2 + \beta S^0] A \\
&\quad + \left[\frac{\alpha S^0 P}{1 + CP} - z\theta P \right].
\end{aligned} \tag{4.5.8}$$

Note that,

$$\frac{\alpha S^0 P}{1 + CP} \leq \alpha S^0 P.$$

Therefore,

$$\dot{V} \leq -\frac{\mu_0 (S^0 - S)^2}{S} + Q_1 I + Q_2 A + Q_3 P, \tag{4.5.9}$$

where $Q_1 = [z\gamma_I - \mu_1 + \beta S^0]$, $Q_2 = [z\gamma_A - \mu_2 + \beta S^0]$ and $Q_3 = [\alpha S^0 - z\theta]$.

From (4.5.3) and substitution of (4.5.4) into Q_1 , Q_2 and Q_3 results in:

$$Q_1 = \beta S^0 - \mu_1 + \frac{(\alpha + z_0) \gamma_I S^0}{\theta} < 0,$$

$$Q_2 = \beta S^0 - \mu_2 + \frac{(\alpha + z_0) \gamma_A S^0}{\theta} < 0,$$

$$Q_3 = -z_0 S^0 < 0.$$

Therefore $\dot{V} \leq 0$.

Furthermore, since $R_{glo} < 1$, from the last expression in (4.5.8), it can be seen that

$$\dot{V}(X) = 0 \iff X = (S^0, 0, 0, 0).$$

Therefore, $\dot{\mathbf{V}}(t)$ is negative-definite at the disease-free equilibrium. So, $\mathbf{V}(t)$ is a Lyapunov function proving that the disease-free equilibrium is globally asymptotically stable. \square



UNIVERSITY *of the*
WESTERN CAPE

Chapter 5

South African population during its first wave of COVID-19

The following references are made use of in this chapter: Worldometer [48], Witbooi *et al.* [73], Witbooi [77], World Health Organization [81], Son [82], Rangkuti *et al.* [83], Jassat *et al.* [84], National Institute for Communicable Diseases [85], Stiegler and Bouchard [86], Greyling and Rossouw and Adhikari [87], Businessstech [88], October *et al.* [89], and Moonasar and Pillay and Leonard *et al.* [90].

This chapter focuses on sensitivity analysis of the basic reproduction number R_0 and numerical simulations of system (4.1.2). We looked into the South African population during its first wave of COVID-19 and obtained results such as values of R_0 and graphs showing the observed daily new cases and active cases averaged over 7-days based on the timeline from World Health Organization [81] for 20 July 2020 until 2 November 2020. Euler's method was used to find approximate solutions to the model (4.1.2) via coding in Octave. The Octave code used for this section appears in the appendix section of thesis.

5.1 Sensitivity analysis of R_0

In this section sensitivity analysis of the basic reproduction number R_0 is performed. The results obtained in this section will tell us the significance of each parameter in our model and the effect each has on R_0 ; which of them increases, or decreases R_0 . This will then give us a better understanding of the transmission dynamics and the spread of the COVID-19 disease, and in turn will allow for measures to be made in controlling the spread of disease amongst the South African population. There are different methods one can use to perform sensitivity analysis. One of these methods, the fixed point estimation is used in Son [82]. We, however, will be making use of the normalized-forward sensitivity index method 3.12.1 defined previously in the section of the same name under the mathematical preliminaries chapter of this thesis. The reader can also check [83] for further information on the normalized-forward sensitivity index method.

Since we want to see how each of the sixteen parameters in Table 5.1 influences R_0 , we need to follow the process of finding the normalized-forward sensitivity index, which is quite simple. One needs to find the partial derivative of R_0 over the partial derivative of the parameter you are working with. That final answer, in its simplest form, you then multiply by the parameter of interest divided by the worked out calculation of R_0 . The definition 3.12.1 from [83] sums it up quite well, and we recall it below. Note that for $C^{R_0}_m$ to be high, $\frac{\partial R_0}{\partial m}$ must be higher. For R_0 to be sensitive to a parameter, the index must be higher.

The normalized-forward sensitivity index is calculated using the normalized sensitivity index of the variable R_0 , which is differentiable on the parameter m :

$$C^{R_0}_m = \frac{\partial R_0}{\partial m} \times \frac{m}{R_0},$$

where R_0 is the variable to be analyzed and m is the parameter.

The sensitivity index of each parameter is derived from R_0 using the definition stated above. Table 5.1 shows the parameters we are going to be making use of in deriving the sensitivity of R_0 , excluding parameters P_0 , n , and n_1 .

Table 5.1: Parameters with values and their descriptions

Parameter	Description	Values (<i>day</i> ⁻¹)	Source
B_0	Constant inflow rate of susceptibles	$P_0\mu \approx 2500$	[48]
B_1	Influx rate of asymptotically infected migrants	200	Nominal
B_2	Departing rate of surviving migrants as they recover from COVID-19	$\omega_A B_1 \mu \approx 0.00253$	
μ	Mortality rate	$(65 \times 365)^{-1} \approx 4.2150 \times 10^{-5}$	[77]
P_0	South African population in 2020	59308690	[48]
α	Transmission rate from S to I , due to contact with environmental reservoir P	$0.3\beta \approx 4.0466 \times 10^{-10}$	
C	Proportion of interaction with infectious environment P	0.02	Estimated
g	Proportion of symptomatic infectious persons	0.1	Estimated
β	Transmission rate from S to I , due to contact with I and/or A	$(0.08)(P_0)^{-1} \approx 1.3489 \times 10^{-9}$	Estimated
v	Rate of vaccination	0	
n, n_1	Timeline from 20 July 2020 until 2 November 2020	$n = 14$ and $n_1 = 7(n + 1)$	[81]
γ_I	Rate at which virus spreads in environmental reservoir P by I	0.05	Estimated
γ_A	Rate at which virus spreads in environmental reservoir P by A	0.005	Estimated
δ_I	Death rate due to COVID-19	0.0002	[73]
δ_A	Death rate due to COVID-19	0.0001	[73]
ω_I	Rate at which persons in S recover	0.15	[73]
ω_A	Rate at which persons in A recover	$2\omega_I = 0.3$	[73]
θ	Death rate of pathogens in the environmental reservoir P	1/4	Estimated

Recall the basic reproduction number R_0 having the form

$$R_0 = \frac{B_0 \left[(1 - g)\mu_2(\beta\theta + \alpha\gamma_I) + g\mu_1(\beta\theta + \alpha\gamma_A) \right]}{\theta\mu_0\mu_1\mu_2},$$

where $\mu_0 = (\mu + v)$, $\mu_1 = (\mu + \delta_I + \omega_I)$, and $\mu_2 = (\mu + \delta_A + \omega_A)$. Working from the definition of the normalized-forward sensitivity index of R_0 , our calculations of sensitivity indices yields

$$\frac{\partial R_0}{\partial B_0} \times \frac{B_0}{R_0} = +1, \quad \frac{\partial R_0}{\partial B_1} \times \frac{B_1}{R_0} = 0, \quad \frac{\partial R_0}{\partial B_2} \times \frac{B_2}{R_0} = 0, \quad \text{and} \quad \frac{\partial R_0}{\partial C} \times \frac{C}{R_0} = 0.$$

We also have equations of sensitivity indices as below

$$\begin{aligned} \frac{\partial R_0}{\partial \alpha} \times \frac{\alpha}{R_0} &= \frac{\alpha \left[(1-g) \left[\mu + \gamma_I (\delta_I + \delta_A) + g \gamma_A (\mu + \delta_I) \right] \right]}{(1-g)\mu_2(\beta\theta + \alpha\gamma_I) + g\mu_1(\beta\theta + \alpha\gamma_A)}, \\ \frac{\partial R_0}{\partial g} \times \frac{g}{R_0} &= \frac{g \left[\beta\theta(\mu_1 - \mu_2) - (\gamma_I\mu_1 - \gamma_A\mu_2) \right]}{(1-g)\mu_2(\beta\theta + \alpha\gamma_I) + g\mu_1(\beta\theta + \alpha\gamma_A)}, \\ \frac{\partial R_0}{\partial \beta} \times \frac{\beta}{R_0} &= \frac{\beta\theta \left[(1-g)\mu_2 + g\mu_1 \right]}{(1-g)\mu_2(\beta\theta + \alpha\gamma_I) + g\mu_1(\beta\theta + \alpha\gamma_A)}, \\ \frac{\partial R_0}{\partial v} \times \frac{v}{R_0} &= - \frac{v \left[\mu_2(1-g)(\beta\theta + \alpha\gamma_I) \left[\mu\mu_1 + \mu_2(\delta_I + \omega_I) \right] \right]}{\mu_0 \left[(1-g)\mu_2^2\mu_1(\beta\theta + \alpha\gamma_I) + g\mu_1^2\mu_2(\beta\theta + \alpha\gamma_A) \right]} \\ &\quad - \frac{v \left[\mu_1 g (\beta\theta + \alpha\gamma_A) \left[\mu\mu_1 + \mu_2(\delta_I + \omega_I) \right] \right]}{\mu_0 \left[(1-g)\mu_2^2\mu_1(\beta\theta + \alpha\gamma_I) + g\mu_1^2\mu_2(\beta\theta + \alpha\gamma_A) \right]}, \\ \frac{\partial R_0}{\partial \gamma_I} \times \frac{\gamma_I}{R_0} &= \frac{\alpha\mu_2\gamma_I(1-g)}{(1-g)\mu_2(\beta\theta + \alpha\gamma_I) + g\mu_1(\beta\theta + \alpha\gamma_A)}, \\ \frac{\partial R_0}{\partial \gamma_A} \times \frac{\gamma_A}{R_0} &= \frac{g\alpha\mu_1\gamma_A}{(1-g)\mu_2(\beta\theta + \alpha\gamma_I) + g\mu_1(\beta\theta + \alpha\gamma_A)}, \\ \frac{\partial R_0}{\partial \delta_I} \times \frac{\delta_I}{R_0} &= - \frac{\delta_I \left[\mu_1\mu g(\beta\theta + \alpha\gamma_A) + \mu_2(1-g)(\beta\theta + \alpha\gamma_I)(2\mu + \delta_A + \omega_A) \right]}{(1-g)\mu_2^2\mu_1(\beta\theta + \alpha\gamma_I) + g\mu_1^2\mu_2(\beta\theta + \alpha\gamma_A)}, \\ \frac{\partial R_0}{\partial \delta_A} \times \frac{\delta_A}{R_0} &= - \frac{\delta_A \left[\mu_1 g (\beta\theta + \alpha\gamma_A) (\delta_I + \omega_I) - \mu_2 \mu (1-g) (\beta\theta + \alpha\gamma_I) \right]}{(1-g)\mu_2^2\mu_1(\beta\theta + \alpha\gamma_I) + g\mu_1^2\mu_2(\beta\theta + \alpha\gamma_A)}, \\ \frac{\partial R_0}{\partial \omega_I} \times \frac{\omega_I}{R_0} &= - \frac{\omega_I \left[\mu_1\mu g(\beta\theta + \alpha\gamma_A) + \mu_2(1-g)(\beta\theta + \alpha\gamma_I)(2\mu + \delta_A + \omega_A) \right]}{(1-g)\mu_2^2\mu_1(\beta\theta + \alpha\gamma_I) + g\mu_1^2\mu_2(\beta\theta + \alpha\gamma_A)}, \\ \frac{\partial R_0}{\partial \omega_A} \times \frac{\omega_A}{R_0} &= \frac{\omega_A \left[\mu_2\mu(1-g)(\beta\theta + \alpha\gamma_I) - \mu_1 g (\beta\theta + \alpha\gamma_A) (\delta_I + \omega_I) \right]}{(1-g)\mu_2^2\mu_1(\beta\theta + \alpha\gamma_I) + g\mu_1^2\mu_2(\beta\theta + \alpha\gamma_A)}, \\ \frac{\partial R_0}{\partial \theta} \times \frac{\theta}{R_0} &= \frac{\mu_2(1-g) \left[\beta\theta\mu_1\mu_2 - (\beta\theta + \alpha\gamma_I) \left[\mu\mu_1 + \mu_2(\delta_I + \omega_I) \right] \right]}{(1-g)\mu_2^2\mu_1(\beta\theta + \alpha\gamma_I) + g\mu_1^2\mu_2(\beta\theta + \alpha\gamma_A)} \\ &\quad + \frac{\mu_1 g \left[\beta\theta\mu_1\mu_2 - (\beta\theta + \alpha\gamma_A) \left[\mu\mu_1 + \mu_2(\delta_I + \omega_I) \right] \right]}{(1-g)\mu_2^2\mu_1(\beta\theta + \alpha\gamma_I) + g\mu_1^2\mu_2(\beta\theta + \alpha\gamma_A)}. \end{aligned}$$

Lastly, we have that the sensitivity index equation $\frac{\partial R_0}{\partial \mu} \times \frac{\mu}{R_0}$ is equal to

$$\frac{\mu \left[\mu_2(1-g)(\beta\theta + \alpha\gamma_I) \left[\mu_0\mu_1 - [\mu(3\mu + 2v) + (\delta_I + \omega_I)] [2(2\mu + v) + (\delta_A + \omega_A)] \right] \right]}{\mu_0 \left[(1-g)\mu_2^2\mu_1(\beta\theta + \alpha\gamma_I) + g\mu_1^2\mu_2(\beta\theta + \alpha\gamma_A) \right]} + \frac{\mu \left[\mu_1g(\beta\theta + \alpha\gamma_A) \left[\mu_0\mu_2 - [\mu(3\mu + 2v) + (\delta_I + \omega_I)] [2(2\mu + v) + (\delta_A + \omega_A)] \right] \right]}{\mu_0 \left[(1-g)\mu_2^2\mu_1(\beta\theta + \alpha\gamma_I) + g\mu_1^2\mu_2(\beta\theta + \alpha\gamma_A) \right]}.$$

The sensitivity indices of R_0 from equations above we see in Table 5.2.

Table 5.2: Sensitivity indices of R_0

Parameter	Description	Sensitivity index
B_0	Constant inflow rate of susceptibles	+1
β	Transmission rate from S to I , due to contact with I and/or A	+0.9459
α	Transmission rate from S to I , due to contact with environmental reservoir P	+0.053910
γ_I	Rate at which virus spreads in environmental reservoir P by I	+0.053766
γ_A	Rate at which virus spreads in environmental reservoir P by A	+0.00029904
C	Proportion of interaction with infectious environment P	0
v	Rate of vaccination	0
δ_I	Death rate due to COVID-19	-0.00000062875
δ_A	Death rate due to COVID-19	-0.000016612
ω_I	Rate at which persons in S recover	-0.00036817
ω_A	Rate at which persons in A recover	-0.049835
θ	Death rate of pathogens in the environmental reservoir P	-0.053925
μ	Mortality rate	-1.0000
g	Proportion of symptomatic infectious persons	-5913600

In Table 5.2 we see parameters having positive and negative sensitivity indices. The parameters with a positive sensitivity index are B_0 , α , C , v , β , γ_I , and γ_A . Those

with a negative sensitivity index are μ , g , δ_I , δ_A , ω_I , ω_A , and θ . The positive sign gives an indication that there is a direct relationship between the parameter and R_0 . It also indicates that increases in the basic reproductive number is significant. Negative sensitivity indexes gives an indication that, that parameter which increases the basic reproductive number has negative significance, or is not that significant on R_0 . The most sensitive parameter is B_0 the constant inflow of susceptible persons. Others are the transmission rate β from S -class to I -class via contact with symptomatic and/or asymptomatic persons, the transmission rate α from S -class to I -class via contact with environment of the pathogens P , and γ_I the rate at which the virus spreads in P by I . Then we also have γ_A , C , and v . The least sensitive parameter is g the proportion of symptomatic infectious persons. Looking at the sensitivity index of R_0 with respect to B_0 the rate of constant inflow of susceptibles, we see it is $+1$. The 1 means that a unit increase in B_0 results in a unit increase in R_0 , and this increase in R_0 is very significant. In other words, increasing (or decreasing) B_0 by 10 percent results in R_0 then increasing (or decreasing) by 10 percent. Similarly, if we look at the mortality rate μ , decreasing (or increasing) this parameter by 10 percent causes R_0 to increase (or decrease) by 10 percent. We can also check the index for recovery rate of those in the asymptomatic class -0.049835 . Its interpretation is that if ω_A gets increased by 10 percent, the basic reproduction number will decrease by 0.49835 percent, or 0.5 percent.

5.2 Numerical simulations

In this section we examine and showcase the transmission dynamics of the COVID-19 disease based on our compartmental model (4.1.2) through numerical simulations. We focus on the timeline from 20 July 2020 until 2 November 2020 [81], that is, during the 105 days when the South African population [48] was experiencing its first wave of COVID-19, taking note that during this time, there was no vaccine available to the public yet. The simulations are performed by taking parameters from Table 5.1 and using data from Worldometer South Africa [48].

5.2.1 The country under lockdown and behaviour of South Africans

On Thursday 5 March 2020, the National Institute for Communicable Diseases of South Africa reported the first ever case of positive polymerase chain reaction test result for SARS-CoV-2 infection, a 38-year-old male that returned to the country from a trip to Italy with his wife. After that incident an increase of infections was reported to grow steadily in the country until the number of infections reached a weekly result of 10 488 on 13 July 2020, this being the peak of the first wave, and having confirmed weekly cases reported as 86 695 infections. Thereafter, the second wave was then reported to peak on 4 January 2021 with a weekly increase of infections being 31 309 and weekly confirmed cases of infection being 125 287, see in [81, 84, 85].

With infections increasing so rapidly, the government aimed to place the country under lockdown, the aim being to control and decrease the spread of the virus. Furthermore, a decision was made that only when the number of infections showed a significant decrease, the levels would too, giving the health system ample time to make preparations to deal with the pandemic. Levels of lockdown ranged from level 1 to level 5, the most relaxed to most forceful. Level 5 was declared on 23 March 2020 and its process of implementation took place on 27 March 2020 onwards. During this period lockdown was at its most stringent stage in order to restrain the spread of infection and to avert death rates from increasing. By end of March, the weekly confirmed cases decreased from 947 to 398 [81]. The government eased lockdown restrictions to level 4 on 01 May 2020 however, excessive preventative initiatives were still forced on the public so as to restrict transmission between communities; South Africans were permitted to only leave their homes when they had to get essential goods and needed to seek medical attention. Shops, restaurants and non-essential businesses were to remain closed until a suitable time was given for them to open again, while only essential establishments were permitted to remain open. Level

3 was then implemented on 01 June 2020, limiting the interaction at social gatherings and workplaces to reduce high risk disease transmission. On the evening of Saturday 15 August 2020, the President of South Africa, President Cyril Ramaphosa, addressed the nation where he disclosed the country's level of advancement in its combat with the virus, and because of SA's good fight and positive results showing the improvement in the spread of COVID-19, lockdown restrictions were then lowered further to level 2 on midnight Monday 17 August 2020. Rules on restrictive measures to attend gatherings were still in place, but slowly eased as the public still had to abide by social distancing and health regulations to avert the re-emergence of the virus. South Africa reached level 1 of lockdown on 30 September 2020, and during this time South Africans were allowed to carry on with, not all, but most of their normal activities, on condition that they take protective measures and followed health regulations such as wearing masks, keeping distance from each other, and regularly washed their hands, or made use of sanitizers, when going out in public [86, 87, 88, 89, 90].

5.2.2 Graphical representation of new and active cases

The following graphs show the behaviour of the deterministic model (4.1.2) and how it fits with the data [81]. We estimate solutions to the model equations (4.1.2) using Euler's method via coding in Octave. The initial conditions used are the following: $\mathbf{S}(0) = 59012147$, $\mathbf{I}(0) = 171000$, $\mathbf{A}(0) = 17000$, $\mathbf{R}(0) = \mathbf{0}$, and $\mathbf{P}(0) = 2000$. Throughout this process we are under the assumption that no one has recovered from the virus yet. Figure 5.1 to Figure 5.4 below illustrates the behaviour of the infectious South African population and how the numbers change through the process of the first wave as time increases from 0 to 105 days. Figure 5.1 and Figure 5.3 show the new cases and active cases of our model. Figure 5.2 and Figure 5.4 show the new and active cases when the model is modified to fit the data [81] more accurately. In Figure 5.1 and Figure 5.2 we notice that the model under-valuates the observed data. Our suspicion is (in line with

[73]) that a significant drop in the daily new cases has the effect that susceptibles become less wary, with behavioural change that is detrimental to the fight against COVID-19. We account for this effect by introducing the following factor, at the appropriate time ($t=16$ days), and we run the simulations over 105 days. The parameter β is replaced by $\beta[1 + ((t - 16)/105)^{0.5}]$. The normal red curves represent the daily new cases according to our model when β is taken at the fixed value $\frac{0.08}{P_0}$. We see that the number of cases are steadily decreasing from $t=0$ up until 105 days. But for the modified model, when the curve fits the observed data very well over the first few weeks, observed daily new cases stay around 2000 until 105 days. This tells us that when lockdown levels were lowered, the public did not take health regulations and protective measures seriously, in the end causing the re-emergence of the virus, or the second wave. For active cases in the normal model, we see that the number of cases rapidly drop until it stays at zero by 105 days, and by the modified model, the active cases drop as well, but around 105 days the cases stay at approximately just below 10000 or so. The graphs we obtained look similar to those in the paper of Witbooi *et al.* [73], however their graphs are a result of a different model.



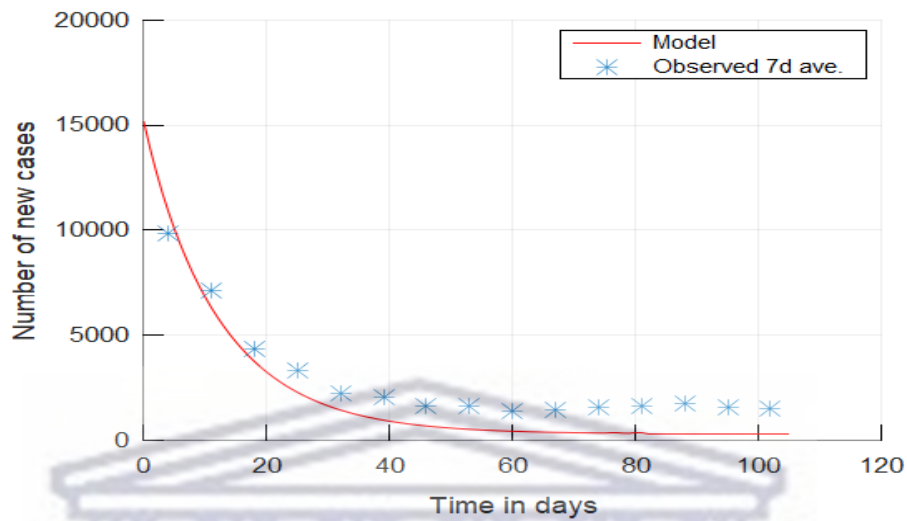


Figure 5.1: Daily new cases averaged over seven days during first wave, 105 days, in 2020 parameters as in Table 5.1, $R_0 = 0.5348$.

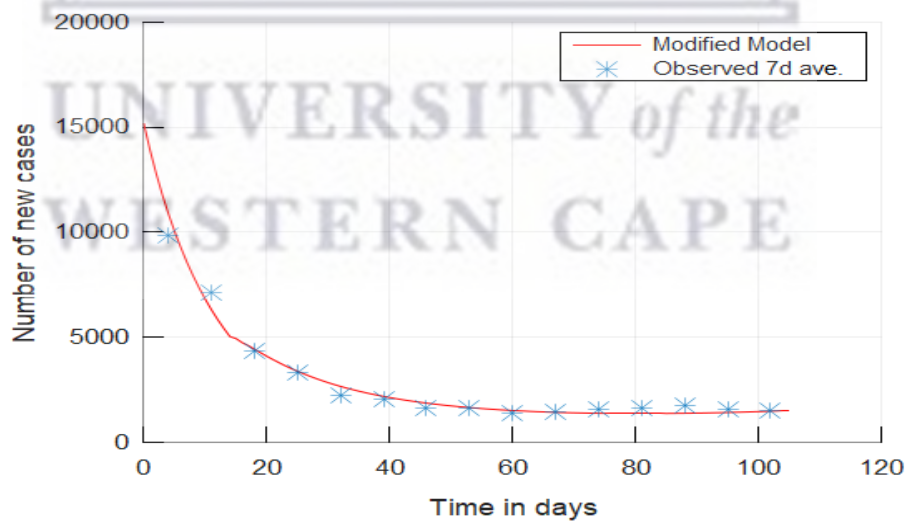


Figure 5.2: Daily new cases averaged over seven days during the first wave, 105 days in 2020, for the modified model.

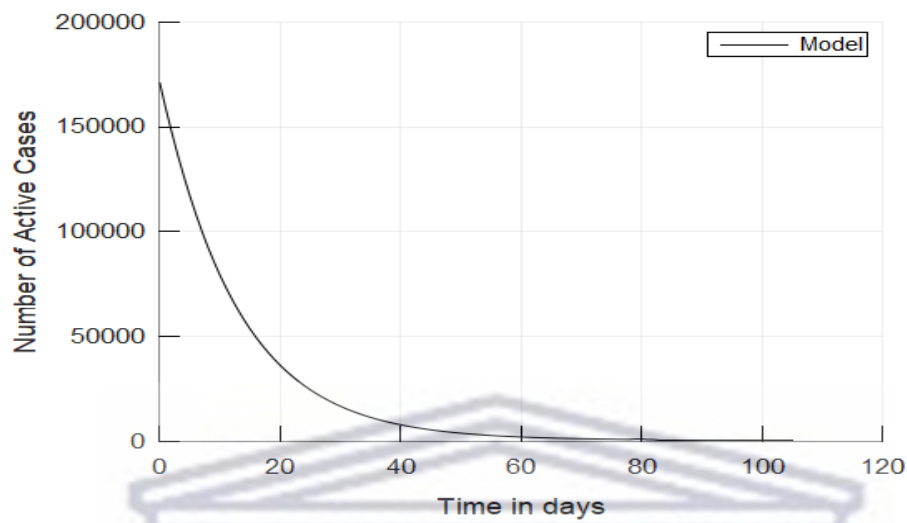


Figure 5.3: Model output of active cases averaged over seven days during the first wave, 105 days in 2020, with parameters as in Table 5.1.

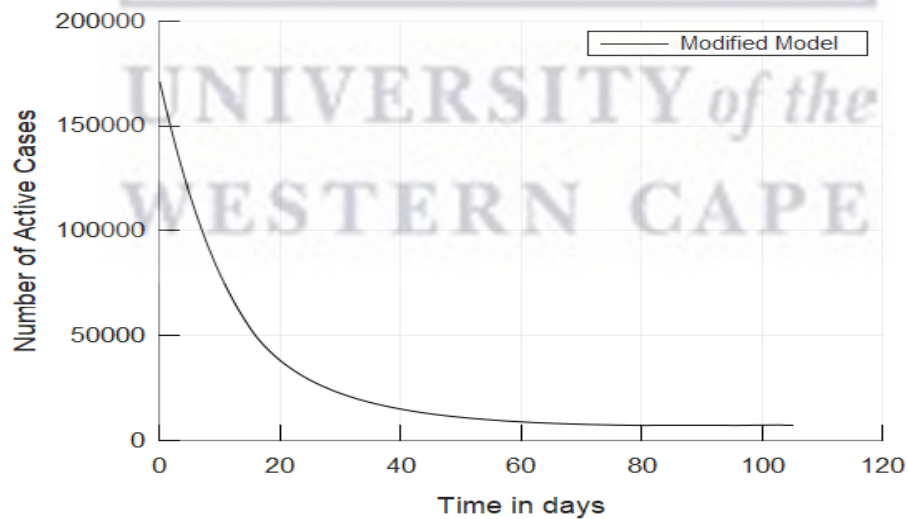


Figure 5.4: Model output of active cases averaged over seven days during the first wave, 105 days in 2020, for the modified model.

Chapter 6

Optimal control

This chapter makes use of the following references: Lenhart and Workman [75], Shen *et al.* [92], and Pontryagin, Boltyanskii *et al.* [93].

In this chapter, we formulate and solve the optimal control problem by introducing the control measures into the COVID-19 model in (4.1.2). We want to do this by incorporating non-pharmaceutical methods and vaccination control in our system. Through the process of efficiency analysis, we basically want to see which control strategy works best to control and minimize the rate of infection of the coronavirus in the infectious class I and asymptomatic class A in a population where the number of resources available are finite. We use Pontryagin's Maximum Principle [75, 92, 93] to define the optimal levels of the two controls.

6.1 The optimal control problem

Optimal control theory is applied to our COVID-19 model in (4.1.2) by presenting two controls u_1 and u_2 . The first control variable u_1 is defined to be the non-pharmaceutical intervention which includes the following:

- Social distancing between those that are infectious and/or asymptomatic (affecting

others with the COVID-19 virus) and those not infected (persons considered healthy) with the virus.

- Regular use of sanitizers, washing of hands, and the wearing of masks.
- A person having to avoid places where large gatherings take place, and restrictions imposed on traveling to places where the number of cases are very high.

The second control variable \mathbf{u}_2 is defined as the vaccination control. This variable gives us an indication of all possible vaccinated individuals in a population and how it affects the spread of the virus, hopefully causing a decrease in the number of infections. A significant decrease of infectious individuals will give us an indication that being vaccinated can be a right call to make when it comes to decreasing the rate of infection and the risk of spread.

Our intent while revising the optimal control problem is to minimize the objective functional in (6.1.1) below over a compact interval $[0, T]$:

$$J(\mathbf{u}_1(t), \mathbf{u}_2(t)) = \int_0^T (\omega_1 u_1^2(t) + \omega_2 u_2^2(t) + \omega_3 I(t) + \omega_4 A(t)) dt. \quad (6.1.1)$$

The constants ω_i for $i = 1, 2, 3, 4$ are called balancing or weight constants and T is the final time. Note that $\omega_1, \omega_2, \omega_3$, and ω_4 are positive constants. We consider a quadratic cost on the controls \mathbf{u}_1 and \mathbf{u}_2 and apply it because the controls' cost of intervention is nonlinear. This means that no linear relationship exists amongst the cost of intervention, its effects, and the persons infected with the virus. The controls taken in squared form ensures convexity of the optimal control problem. The controls \mathbf{u}_1 and \mathbf{u}_2 are Lebesgue integrable and bounded. For more information see the book of Lenhart and Workman [75].

For the purpose of optimal control our model is modified as follows

$$\begin{aligned}
\frac{dS}{dt} &= B_0 - \frac{\alpha SP}{1 + CP} - \beta S(1 - u_1(t))(I + A) - (\mu + vu_2(t))S, \\
\frac{dI}{dt} &= \frac{\alpha SP}{1 + CP} + \beta S(1 - u_1(t))(I + A) - g \left[\frac{\alpha SP}{1 + CP} + \beta S(I + A) \right] - \mu_1 I, \\
\frac{dA}{dt} &= B_1 + g \left[\frac{\alpha SP}{1 + CP} + \beta S(I + A) \right] - \mu_2 A, \\
\frac{dR}{dt} &= vu_2(t)S + \omega_I I + \omega_A A - \mu R - B_2, \\
\frac{dP}{dt} &= \gamma_I I + \gamma_A A - \theta P, \\
N &= S + I + A + R + P,
\end{aligned} \tag{6.1.2}$$

where $\mu_1 = (\mu + \delta_I + \omega_I)$, $\mu_2 = (\mu + \delta_A + \omega_A)$, and N is the total population. The initial conditions are non-negative,

$$S(0) \geq 0, I(0) \geq 0, A(0) \geq 0, R(0) \geq 0, P(0) \geq 0, \tag{6.1.3}$$

and the terminal conditions

$$S(T), I(T), A(T), R(T), P(T) \tag{6.1.4}$$

are free, while the control variables are assumed to be bounded,

$$u_1, u_2 \in [0, 1]. \tag{6.1.5}$$

Our main goal is to have an optimal control u_1 being associated with non-pharmaceutical intervention and another optimal control u_2 representing vaccine control, such that

$$J(u_1^*, u_2^*) = \min_{\Lambda} \{J(u_1, u_2)\},$$

where the control sets are defined as

$$\Lambda = \left\{ (u_1, u_2) : [0, T] \rightarrow [0, 1], (u_1(t), u_2(t)) \text{ is Lebesgue measurable} \right\}. \tag{6.1.6}$$

6.1.1 Constructing the Hamiltonian H for pointwise minimization

The Hamiltonian H is a function of the inside integral of the objective functional in (6.1.1) together with the adjoint variables $\dot{\lambda}_i$ for $i = 1, \dots, 5$ associated with state variables S , I , A , R and P , and the optimal controls u_i for $i = 1, 2$.

Knowing this fact, the Hamiltonian H is then written as

$$\begin{aligned}
 H &= H(S(t), I(t), A(t), R(t), P(t), \lambda(t), u_1(t), u_2(t)) \\
 &= \omega_1 u_1^2(t) + \omega_2 u_2^2(t) + \omega_3 I(t) + \omega_4 A(t) \\
 &\quad + \lambda_1 \left[B_0 - \frac{\alpha SP}{1 + CP} - \beta S(1 - u_1(t))(I + A) - (\mu + v u_2(t))S \right] \\
 &\quad + \lambda_2 \left[\frac{\alpha SP}{1 + CP} + \beta S(1 - u_1(t))(I + A) - g \frac{\alpha SP}{1 + CP} + \beta S(I + A) - \mu_1 I \right] \\
 &\quad + \lambda_3 \left[B_1 + g \frac{\alpha SP}{1 + CP} + \beta S(I + A) - \mu_2 A \right] \\
 &\quad + \lambda_4 \left[v u_2(t)S + \omega_I I + \omega_A A - \mu R - B_2 \right] \\
 &\quad + \lambda_5 \left[\gamma_I I + \gamma_A A - \theta P \right].
 \end{aligned} \tag{6.1.7}$$

The partial derivatives of H are taken with respect to each state variable to a system of the adjoint equations. This similar process but with respect to the controls u_1 and u_2 gives the optimal control equations.

Theorem 12. *Let S^* , I^* , A^* , R^* , P^* , and u_1^* and u_2^* be optimal solutions for the optimal control problem (6.1.1), (6.1.3), (6.1.4), and (6.1.5). Then the costate variables satisfy the following differential equations:*

$$\left\{ \begin{array}{l}
\dot{\lambda}_1^*(t) = \left[\frac{\alpha P^*(t)}{1 + CP^*(t)} + \beta(1 - u_1^*(t))(I^*(t) + A^*(t)) \right] (\lambda_1 - \lambda_2)^*(t) + \mu_1 \lambda_1^*(t) \\
\quad + g \left[\frac{\alpha P^*(t)}{1 + CP^*(t)} + \beta(I^*(t) + A^*(t)) \right] (\lambda_2 - \lambda_3)^*(t) + v u_2^*(t) (\lambda_1 - \lambda_4)^*(t), \\
\dot{\lambda}_2^*(t) = -\omega_3 + \beta S^*(t)(1 - u_1^*(t))(\lambda_1 - \lambda_2)^*(t) + g\beta S^*(t)(\lambda_2 - \lambda_3)^*(t) \\
\quad + \mu_1 \lambda_2^*(t) - \omega_I \lambda_4^*(t) - \gamma_I \lambda_5^*(t), \\
\dot{\lambda}_3^*(t) = -\omega_4 + \beta S^*(t)(1 - u_1^*(t))(\lambda_1 - \lambda_2)^*(t) + g\beta S^*(t)(\lambda_2 - \lambda_3)^*(t) \\
\quad + \mu_2 \lambda_3^*(t) - \omega_A \lambda_4^*(t) - \gamma_A \lambda_5^*(t), \\
\dot{\lambda}_4^*(t) = \mu \lambda_4^*(t), \\
\dot{\lambda}_5^*(t) = \frac{\alpha S^*(t)(\lambda_1 - \lambda_2)^*(t)}{(1 + CP^*(t))^2} + \frac{g\alpha S^*(t)(\lambda_2 - \lambda_3)^*(t)}{(1 + CP^*(t))^2} - \theta \lambda_5^*(t)
\end{array} \right. \tag{6.1.8}$$

with transversality conditions

$$\lambda_i(T) = 0, \quad i = 1, \dots, 5.$$

Furthermore, the controls take the form of

$$\begin{aligned}
u_1^* &= \min \left\{ \max \left\{ 0, \frac{\beta S^*(t)(I^*(t) + A^*(t))(\lambda_2 - \lambda_1)^*(t)}{2\omega_1} \right\}, 1 \right\} \\
u_2^* &= \min \left\{ \max \left\{ 0, \frac{v S^*(t)(\lambda_1 - \lambda_4)^*(t)}{2\omega_2} \right\}, 1 \right\}.
\end{aligned} \tag{6.1.9}$$

Proof. For this proof we make use of Pontryagin's Maximum Principle in [93] and more of this can be seen in [75]. The partial derivatives of the Hamiltonian \mathbf{H} with respect to the state variables \mathbf{S}^* , \mathbf{I}^* , \mathbf{A}^* , \mathbf{R}^* , \mathbf{P}^* are computed. This results in the costate variables $\lambda_i(T)$, $i = 1, \dots, 5$. Since $\mathbf{S}^*(T)$, $\mathbf{I}^*(T)$, $\mathbf{A}^*(T)$, $\mathbf{R}^*(T)$, and $\mathbf{P}^*(T)$ are free, the following terminal conditions hold:

$$\dot{\lambda}_i^*(T) = 0, \quad i = 1, \dots, 5.$$

We start by examining

$$\dot{\lambda}_4^*(T) = -\frac{\partial H}{\partial R} = \mu\lambda_4^*(t).$$

By integration on both sides, we get

$$\lambda_4^* = Ne^{\mu t},$$

for some constant t . The terminal condition $\dot{\lambda}_4^*(T) = 0$ forces N to disappear. Therefore λ_4^* is equal to zero. We now calculate the following:

$$\dot{\lambda}_1^*(t) = -\frac{\partial H}{\partial S}, \quad \dot{\lambda}_2^*(t) = -\frac{\partial H}{\partial I}, \quad \dot{\lambda}_3^*(t) = -\frac{\partial H}{\partial A}, \quad \dot{\lambda}_5^*(t) = -\frac{\partial H}{\partial P},$$

and obtain the equations stated in equation (6.1.8). The function \mathbf{u}^* must optimize H .

Choosing \mathbf{u}_1 and \mathbf{u}_2 we have,

$$\frac{\partial H}{\partial \mathbf{u}_1} = 2\omega_1\mathbf{u}_1 + \beta S^*(I^* + A^*)[\lambda_1 - \lambda_2]$$

and

$$\frac{\partial H}{\partial \mathbf{u}_2} = 2\omega_2\mathbf{u}_2 + vS^*[\lambda_4 - \lambda_1].$$

The values of \mathbf{u}_1 and \mathbf{u}_2 must be optimal. Applying optimality conditions where we let $\frac{\partial H}{\partial \mathbf{u}_1} = 0$ and $\frac{\partial H}{\partial \mathbf{u}_2} = 0$,

$$2\omega_1\mathbf{u}_1 + \beta S^*(I^* + A^*)[\lambda_1 - \lambda_2] = 0,$$

which gives

$$\mathbf{u}_1 = \frac{\beta S^*(t)(I^*(t) + A^*(t))(\lambda_2 - \lambda_1)^*(t)}{2\omega_1}.$$

Similarly, we have

$$2\omega_2\mathbf{u}_2 + vS^*[\lambda_4 - \lambda_1] = 0,$$

resulting in

$$\mathbf{u}_2 = \frac{vS^*(t)(\lambda_1 - \lambda_4)^*(t)}{2\omega_2}.$$

Now if for some values \mathbf{u}_1 and \mathbf{u}_2 in $[0, 1]$, then they are optimal. If for every \mathbf{u}_1 and \mathbf{u}_2 in $[0, 1]$, the controls are then as in equation (6.1.9) that have costate equations mentioned in Theorem 12. \square

6.2 Numerical results and discussion

In this section, we graphically present the results obtained from the previous section 6.1 where we solved our optimality system; optimal control problem (6.1.2) along with its adjoint equations (6.1.8) and its characterization equation of optimal controls (6.1.9). We make use of the Forward-Backward fourth-order Runge-Kutta method. The forward sweep solves the system of the optimal control problem. The backward sweep and the transversality conditions assist in solving the system of adjoint equations. It does this by making use of the current iteration of state equations. The controls \mathbf{u}_1 and \mathbf{u}_2 keeps on getting updated by use of a convex combination of the previous controls' iteration and receives new values from the characterization equation (6.1.9). The iteration comes to a stop when the values of unknowns from previous iteration are too close to that of the present. More information on this can be seen in Silva and Torres [97] and their references. The Forward-Backward fourth-order Runge-Kutta method was done in Octave and the code can be found at the back by appendix. For our optimal control problem, we focus on the time unit of \mathbf{T} being 105 days. Looking at our objective functional (6.1.1) the weight constants ω_i for $i = 1, 2, 3, 4$ are 0.08, 0.000967, 0.0528, and 0.0421, respectively. As for our state variables, they have initial values being $\mathbf{S}(1) = (0.995)\mathbf{P}_0$, $\mathbf{I}(1) = 171000$, $\mathbf{A}(1) = 17000$, $\mathbf{R}(1) = 0$, and $\mathbf{P}(1) = 2000$. Here $\mathbf{P}_0 = 59308690$ is the South African population in 2020 as seen on Worldometer [48]. Since we are looking at the first wave of COVID-19 and working from the timeline 20 July 2020 to 2 November 2020 as seen on World Health Organization [81], we assumed that the initial value of recovery from the virus to be zero; no recovered individuals. Also, during the first wave there was no vaccine available in South Africa. From the figures below, we see the changes occurring in the populations of each class over the period from $\mathbf{T} = 0$ to $\mathbf{T} = 105$ days. During \mathbf{T} of 0 to 105, Figure 6.1 and Figure 6.2 shows an increase in the susceptible and symptomatic infectious population. We also see that for the first 16 days in Figure 6.3 the asymptomatic infectious population increases rapidly, and from day 17 until 105 it remains constant. This is due to persons of the \mathbf{S} -class coming into contact with

those of the *I*-class and *A*-class. This increase can also be seen in Figure 6.5 between days 0 and 21 days, after that it also remains at constant until the end of *T*. It being caused by the symptomatic persons assumed to be more infectious than those that fall under the asymptomatic class. Because of this COVID-19 gets spread via contact as persons commute, foodstuffs being touched, a lot of people gathering in the households, workplaces, and schools. This then leads to a rise in the environmental reservoir of the pathogen as more positive cases get confirmed. Moving on to our figures of control strategies, we notice that both are successful in decreasing the number of infections and by the end of time *T* the disease seems to be eliminated. From Figure 6.6 we see that the control strategy of non-pharmaceutical intervention only starts working from day 80 onwards and steadily decreases until day 105. Comparing that to Figure 6.7, the vaccination control works from around day 35 as it lowers the spread of the virus amongst the population, keeping it constant up until day 81. From there we see a very small surge in infections around day 82, and a rapid drop in the graph as the infections die down. In Figure 6.8 we see the combination of both control strategies. One can see how they noticeably have an influence on the spread of COVID-19 disease during the timeframe *T* of 0 to 105 days. The graphs show that non-pharmaceutical intervention and vaccination are important in controlling the spread of the virus. We note however that getting the vaccine is more effective.

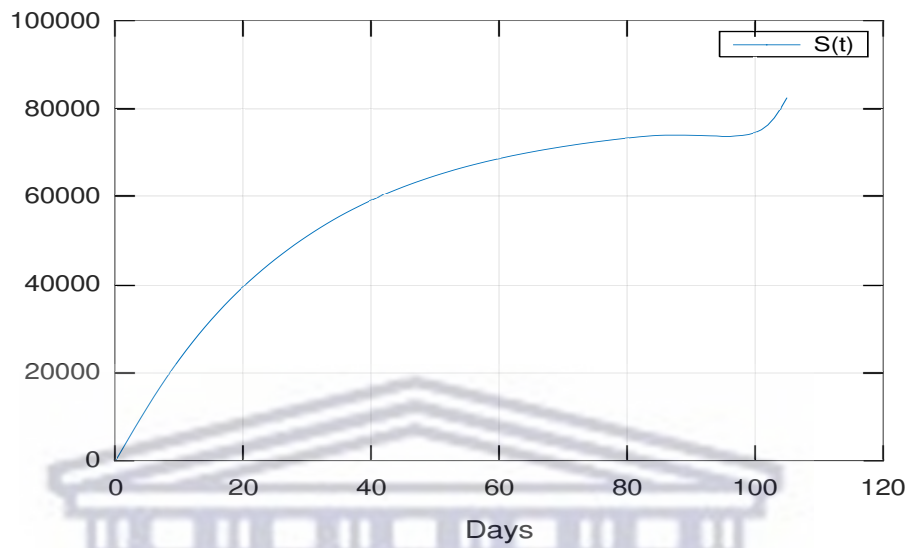


Figure 6.1: Susceptible population under optimal control strategies

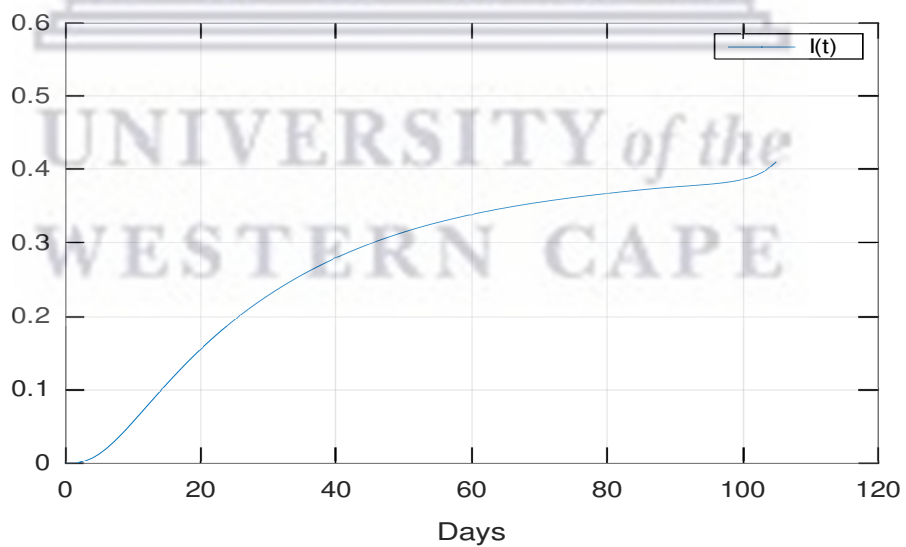


Figure 6.2: Symptomatic infectious population under optimal control strategies.

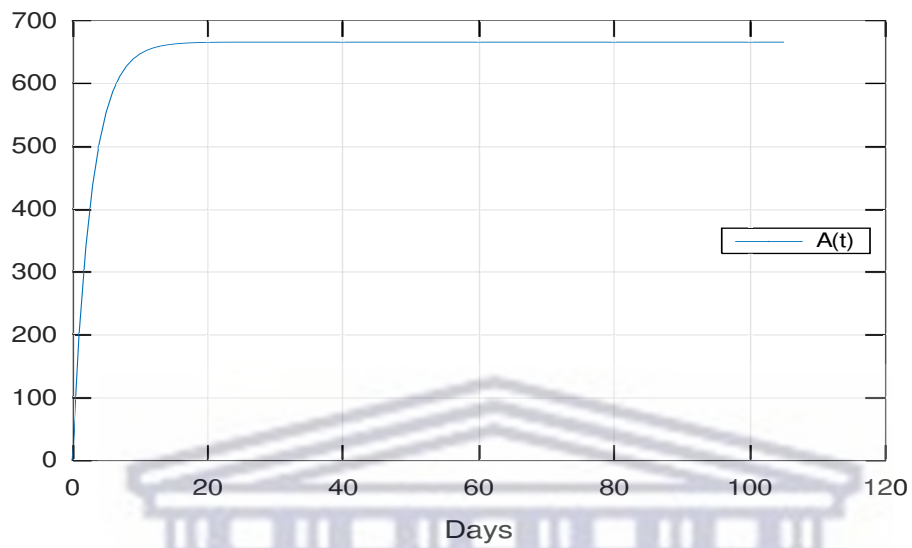


Figure 6.3: Asymptomatic infectious population under optimal control strategies.

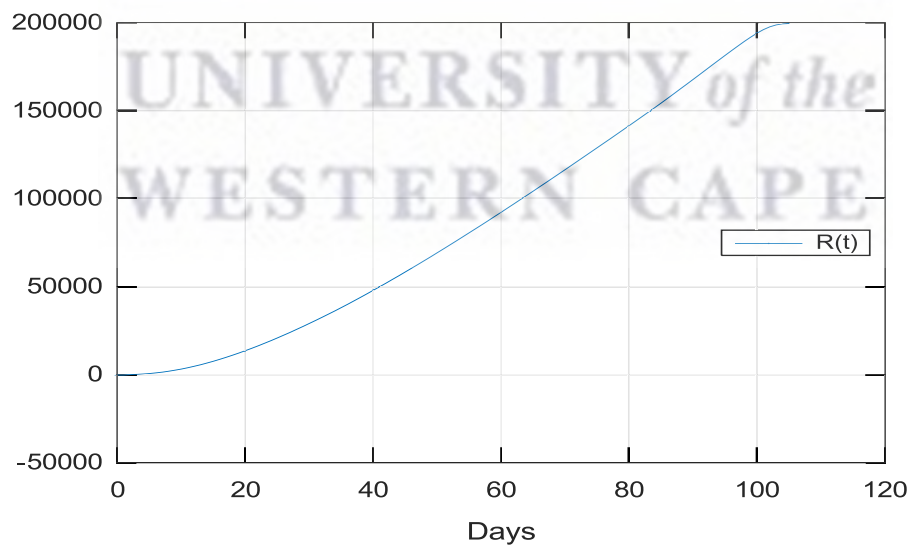


Figure 6.4: Recovered population under optimal control strategies.

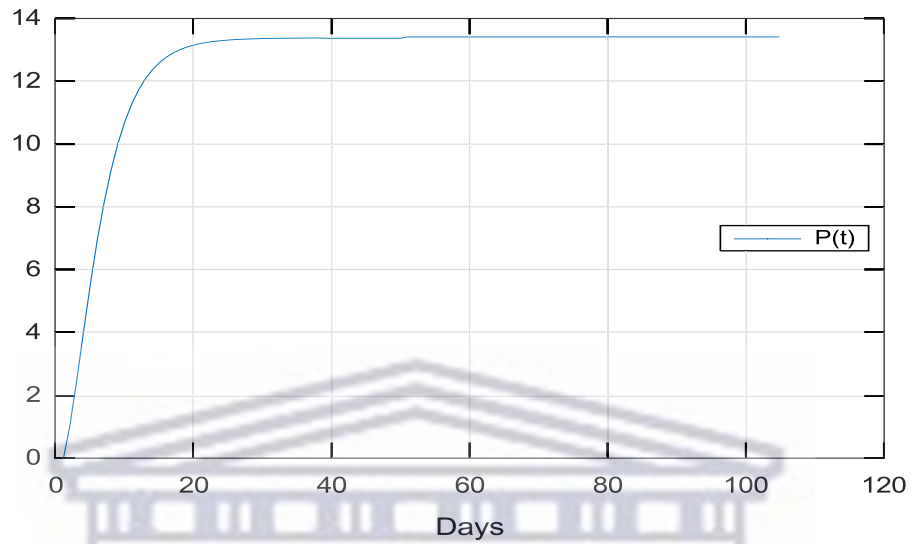


Figure 6.5: Pathogen population under optimal control strategies.

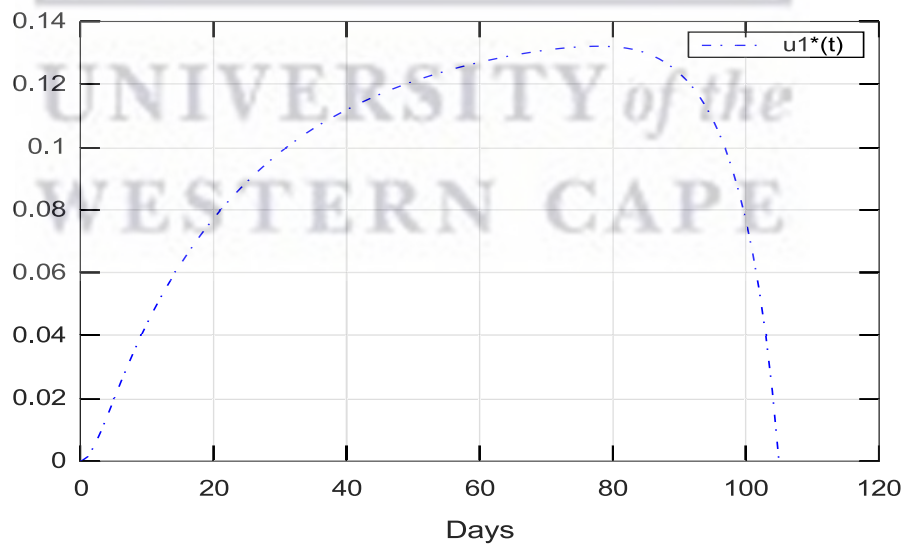


Figure 6.6: Non-pharmaceutical intervention.

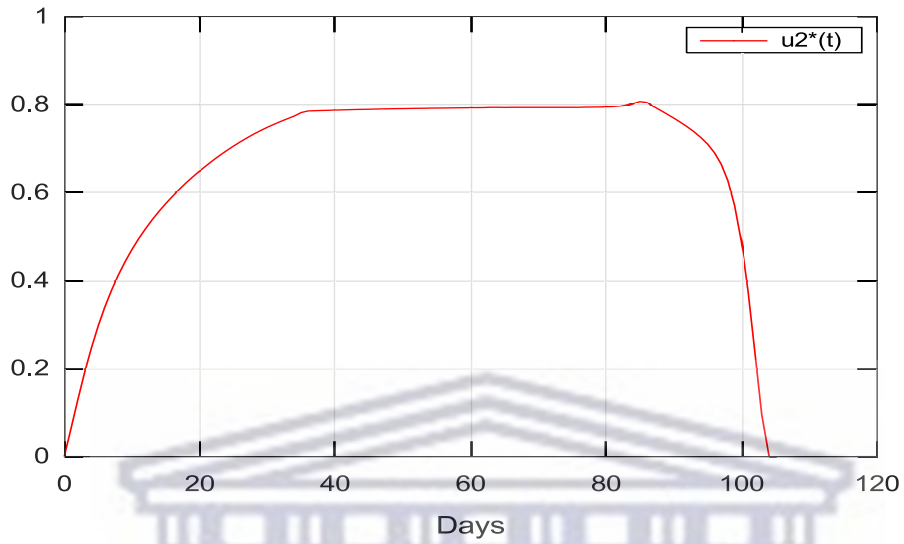


Figure 6.7: Vaccination control.

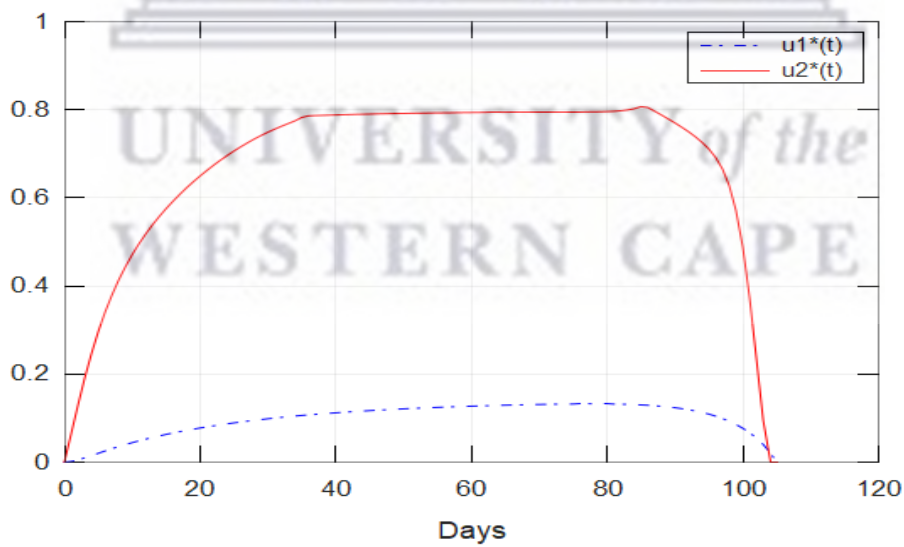
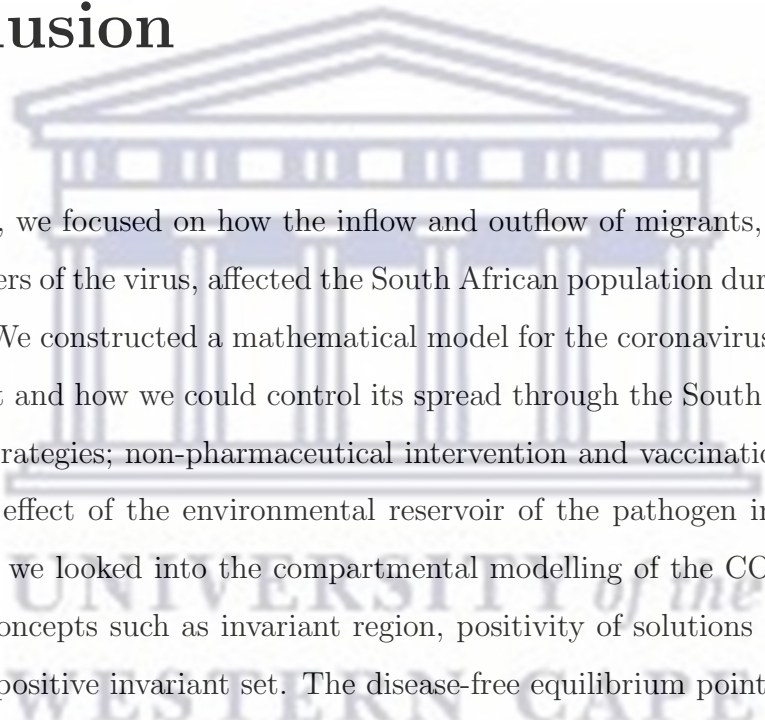


Figure 6.8: Combination of non-pharmaceutical intervention u_1^* and vaccination control u_2^* .

Chapter 7

Conclusion



In this thesis, we focused on how the inflow and outflow of migrants, mainly the asymptomatic carriers of the virus, affected the South African population during the first wave of COVID-19. We constructed a mathematical model for the coronavirus wanting to see the workings of it and how we could control its spread through the South African population via control strategies; non-pharmaceutical intervention and vaccination control. We also included the effect of the environmental reservoir of the pathogen in our investigation. In Chapter 4 we looked into the compartmental modelling of the COVID-19 population dynamics. Concepts such as invariant region, positivity of solutions showed us that our model has a positive invariant set. The disease-free equilibrium point that we calculated helped us in finding the basic reproduction number of our model. For the existence of the endemic equilibrium point, we had to modify our model a bit in order to get a polynomial with less complex coefficients. We ended up with a cubic equation in \mathbf{I}^* where we stated and proved two theorems to show that our system has a unique endemic equilibrium point \mathbf{X}^* for cases when the influx rate of asymptotically infected migrants is positive ($\mathbf{B}_1 > \mathbf{0}$), and for when the influx rate is zero ($\mathbf{B}_1 = \mathbf{0}$). We also proved via the Lyapunov method that the disease-free equilibrium of the COVID-19 model is globally asymptotically stable. In Chapter 5 we looked into sensitivity analysis of the basic reproduction number \mathbf{R}_0 for our COVID-19 model, and used the model to show how it

fits real data reported from Worldometer [48] and the World Health Organization [81] during the first wave in South Africa between 20 July 2020 to 2 November 2020. These results gave us an indication of which parameters are most significant in affecting R_0 . We found that those with a positive sensitivity index such as B_0 , α , C , v , β , γ_I , and γ_A are directly proportional to the basic reproduction number. Those with a negative sensitivity index such as μ , g , δ_I , δ_A , ω_I , ω_A , and θ are indirectly proportional. The importance of the threshold quantity R_0 was validated through our investigation. We know that if $R_0 < 1$ the disease vanishes from the population, and if $R_0 > 1$ the disease is able to become endemic. From the numerical simulations we observed the daily new cases and active cases averaged over seven days during the first wave, and our R_0 yielded **0.5348**. Lastly, in Chapter 6 we formulated and solved the optimal control problem by introducing the control measures into the COVID-19 model. We did this by incorporating non-pharmaceutical methods and vaccination control in our system. Through the process of efficiency analysis we saw which control strategy works best to control and minimize the rate of infection of the coronavirus in the infectious class I and asymptomatic class A in a population where the number of resources available are finite. We also defined the optimal levels of the two controls using Pontryagin's Maximum Principle. The results from the calculations we presented graphically, and from that found that the control in the form of vaccination is more efficient in reducing the spread of the virus compared to the control of non-pharmaceutical intervention. Our future research can embark in to stochastic models in order to accommodate such effects of environmental perturbations into the model.

Bibliography

- [1] Fanelli, D., & Piazza, F. (2020). Analysis and forecast of COVID-19 spreading in China, Italy and France. *Chaos, solitons, and fractals*, 134, 109761. <https://doi.org/10.1016/j.chaos.2020.109761>.
- [2] Vecchio, S., Ramella, R., Drago, A., Carraro, D., Littlewood, R., & Somaini, L. (2020). COVID19 pandemic and people with opioid use disorder: innovation to reduce risk. *Psychiatry research*, 289, 113047. <https://doi.org/10.1016/j.psychres.2020.113047>.
- [3] Shahid, Z., Kalayanamitra, R., McClafferty, B., Kepko, D., Ramgobin, D., Patel, R., Aggarwal, C. S., Vunnam, R., Sahu, N., Bhatt, D., Jones, K., Golamari, R., & Jain, R. (2020). COVID-19 and Older Adults: What We Know. *Journal of the American Geriatrics Society*, 68(5), 926–929. <https://doi.org/10.1111/jgs.16472>.
- [4] Perez Perez, G. I., & Talebi Bezmin Abadi, A. (2020). Ongoing Challenges Faced in the Global Control of COVID-19 Pandemic. *Archives of medical research*, 51(6), 574–576. <https://doi.org/10.1016/j.arcmed.2020.04.016>.
- [5] Kukla, M., Skonieczna-Żydecka, K., Kotfis, K., Maciejewska, D., Łoniewski, I., Lara, L. F., Pazgan-Simon, M., Stachowska, E., Kaczmarczyk, M., Koulaouzidis, A., & Marlicz, W. (2020). COVID-19, MERS and SARS with Concomitant Liver Injury-Systematic Review of the Existing Literature. *Journal of clinical medicine*, 9(5), 1420. <https://doi.org/10.3390/jcm9051420>.
- [6] Al-Tawfiq, J. A., & Rodriguez-Morales, A. J. (2020). Super-spreading events and con-

- tribution to transmission of MERS, SARS, and SARS-CoV-2 (COVID-19). *The Journal of hospital infection*, 105(2), 111–112. <https://doi.org/10.1016/j.jhin.2020.04.002>.
- [7] Park, M., Thwaites, R., & Openshaw, P. (2020). COVID-19: Lessons from SARS and MERS. *European Journal of Immunology*, 50(3), 308–311. <https://doi.org/10.1002/eji.202070035>.
- [8] Giannis, D., Ziogas, I. A., & Gianni, P. (2020). Coagulation disorders in coronavirus infected patients: COVID-19, SARS-CoV-1, MERS-CoV and lessons from the past. *Journal of clinical virology : the official publication of the Pan American Society for Clinical Virology*, 127, 104362. <https://doi.org/10.1016/j.jcv.2020.104362>.
- [9] Gautam, A., Kaphle, K., Shrestha, B., & Phuyal, S. (2020). Susceptibility to SARS, MERS, and COVID-19 from animal health perspective. *Open veterinary journal*, 10(2), 164–177. <https://doi.org/10.4314/ovj.v10i2.6>.
- [10] Ford, N., Vitoria, M., Rangaraj, A., Norris, S. L., Calmy, A., & Doherty, M. (2020). Systematic review of the efficacy and safety of antiretroviral drugs against SARS, MERS or COVID-19: initial assessment. *Journal of the International AIDS Society*, 23(4), e25489. <https://doi.org/10.1002/jia2.25489>.
- [11] Shah, B., Modi, P., & Sagar, S. R. (2020). In silico studies on therapeutic agents for COVID-19: Drug repurposing approach. *Life sciences*, 252, 117652. <https://doi.org/10.1016/j.lfs.2020.117652>.
- [12] Yao, T. T., Qian, J. D., Zhu, W. Y., Wang, Y., & Wang, G. Q. (2020). A systematic review of lopinavir therapy for SARS coronavirus and MERS coronavirus-A possible reference for coronavirus disease-19 treatment option. *Journal of medical virology*, 92(6), 556–563. <https://doi.org/10.1002/jmv.25729>.
- [13] Strzelecki, A., & Rizun, M. (2020). Infodemiological Study Using Google Trends on Coronavirus Epidemic in Wuhan, China. *International Jour-*

- nal of Online and Biomedical Engineering (iJOE)*, 16(04), pp. 139–146.
<https://doi.org/10.3991/ijoe.v16i04.13531>.
- [14] Padron-Regalado E. (2020). Vaccines for SARS-CoV-2: Lessons from Other Coronavirus Strains. *Infectious diseases and therapy*, 9(2), 255–274.
<https://doi.org/10.1007/s40121-020-00300-x>.
- [15] McAleer M. (2020). Prevention Is Better Than the Cure: Risk Management of COVID-19. *Journal of Risk and Financial Management*, 13(3):46.
<https://doi.org/10.3390/jrfm13030046>.
- [16] Vellingiri, B., Jayaramayya, K., Iyer, M., Narayanasamy, A., Govindasamy, V., Giridharan, B., Ganesan, S., Venugopal, A., Venkatesan, D., Ganesan, H., Rajagopalan, K., Rahman, P. K. S. M., Cho, S. G., Kumar, N. S., & Subramaniam, M. D. (2020). COVID-19: A promising cure for the global panic. *The Science of the total environment*, 725, 138277. <https://doi.org/10.1016/j.scitotenv.2020.138277>.
- [17] Ahmed, S. F., Quadeer, A. A., & McKay, M. R. (2020). Preliminary Identification of Potential Vaccine Targets for the COVID-19 Coronavirus (SARS-CoV-2) Based on SARS-CoV Immunological Studies. *Viruses*, 12(3), 254.
<https://doi.org/10.3390/v12030254>.
- [18] Khan, Z., Karataş, Y., & Rahman, H. (2020). Anti COVID-19 Drugs: Need for More Clinical Evidence and Global Action. *Adv Ther* 37, 2575–2579.
<https://doi.org/10.1007/s12325-020-01351-9>.
- [19] Yaqinuddin, A., & Kashir, J. (2020). Innate immunity in COVID-19 patients mediated by NKG2A receptors, and potential treatment using Monalizumab, Cholroquine, and antiviral agents. *Medical hypotheses*, 140, 109777. Advance online publication.
<https://doi.org/10.1016/j.mehy.2020.109777>.
- [20] Phelan, A. L., Katz, R., & Gostin, L. O. (2020). The Novel Coronavirus Originating in Wuhan, China: Challenges for Global Health Governance. *JAMA*, 323(8), 709–710.

<https://doi.org/10.1001/jama.2020.1097>.

- [21] Guan, W. J., Ni, Z. Y., Hu, Y., Liang, W. H., Ou, C. Q., He, J. X., Liu, L., Shan, H., Lei, C. L., Hui, D. S. C., Du, B., Li, L. J., Zeng, G., Yuen, K. Y., Chen, R. C., Tang, C. L., Wang, T., Chen, P. Y., Xiang, J., Li, S. Y., ... China Medical Treatment Expert Group for Covid-19 (2020). Clinical Characteristics of Coronavirus Disease 2019 in China. *The New England journal of medicine*, 382(18), 1708–1720. <https://doi.org/10.1056/NEJMoa2002032>.
- [22] World Health Organization. (2020). Coronavirus disease 2019 (COVID-19): Situation Report, 35. World Health Organization. Available from: <https://apps.who.int/iris/handle/10665/331221>.
- [23] Huang, C., Wang, Y., Li, X., Ren, L., Zhao, J., Hu, Y., Zhang, L., Fan, G., Xu, J., Gu, X., Cheng, Z., Yu, T., Xia, J., Wei, Y., Wu, W., Xie, X., Yin, W., Li, H., Liu, M., Xiao, Y., ... Cao, B. (2020). Clinical features of patients infected with 2019 novel coronavirus in Wuhan, China. *Lancet (London, England)*, 395(10223), 497–506. [https://doi.org/10.1016/S0140-6736\(20\)30183-5](https://doi.org/10.1016/S0140-6736(20)30183-5).
- [24] Chen, N., Zhou, M., Dong, X., Qu, J., Gong, F., Han, Y., Qiu, Y., Wang, J., Liu, Y., Wei, Y., Xia, J., Yu, T., Zhang, X., & Zhang, L. (2020). Epidemiological and clinical characteristics of 99 cases of 2019 novel coronavirus pneumonia in Wuhan, China: a descriptive study. *Lancet (London, England)*, 395(10223), 507–513. [https://doi.org/10.1016/S0140-6736\(20\)30211-7](https://doi.org/10.1016/S0140-6736(20)30211-7).
- [25] World Health Organization. (2003). Consensus document on the epidemiology of severe acute respiratory syndrome (SARS). World Health Organization. Available from: <https://apps.who.int/iris/handle/10665/70863>.
- [26] World Health Organization. (2020). Middle East respiratory syndrome coronavirus (MERS-CoV). Available from: <https://www.who.int/emergencies/mers-cov/en/>.
- [27] Shen, Z., Ning, F., Zhou, W., He, X., Lin, C., Chin, D. P., Zhu, Z., & Schuchat,

- A. (2004). Superspreading SARS events, Beijing, 2003. *Emerging infectious diseases*, 10(2), 256–260. <https://doi.org/10.3201/eid1002.030732>.
- [28] James, A., Pitchford, J. W., & Plank, M. J. (2007). An event-based model of superspreading in epidemics. *Proceedings. Biological sciences*, 274(1610), 741–747. <https://doi.org/10.1098/rspb.2006.0219>.
- [29] Gopinath, S., Lichtman, J. S., Bouley, D. M., Elias, J. E., & Monack, D. M. (2014). Role of disease-associated tolerance in infectious superspreaders. *Proceedings of the National Academy of Sciences of the United States of America*, 111(44), 15780–15785. <https://doi.org/10.1073/pnas.1409968111>.
- [30] Kim, Y., Lee, S., Chu, C., Choe, S., Hong, S., & Shin, Y. (2016). The Characteristics of Middle Eastern Respiratory Syndrome Coronavirus Transmission Dynamics in South Korea. *Osong public health and research perspectives*, 7(1), 49–55. <https://doi.org/10.1016/j.phrp.2016.01.001>.
- [31] Cowling, B. J., Park, M., Fang, V. J., Wu, P., Leung, G. M., & Wu, J. T. (2015). Preliminary epidemiological assessment of MERS-CoV outbreak in South Korea, May to June 2015. *Euro surveillance : bulletin Europeen sur les maladies transmissibles = European communicable disease bulletin*, 20(25), 7–13. <https://doi.org/10.2807/1560-7917.es2015.20.25.21163>.
- [32] Hodcroft E. B. (2020). Preliminary case report on the SARS-CoV-2 cluster in the UK, France, and Spain. *Swiss medical weekly*, 150, w20212. <https://doi.org/10.4414/smw.2020.20212>.
- [33] Brauer F. (2008). Compartmental Models in Epidemiology. *Mathematical Epidemiology*, 1945, 19–79. https://doi.org/10.1007/978-3-540-78911-6_2.
- [34] Böttiger, M., and Norrby, E. (1983). The epidemiology of virus diseases. *Textbook of Medical Virology*, 202–211. <https://doi.org/10.1016/B978-0-407-00253-1.50026-8>.

- [35] Maku-Vyambwera, S. Witbooi, P. (2018). A stochastic TB model for a crowded environment. *Journal of Applied Mathematics*, 1–8. <https://doi.org/10.1155/2018/3420528>.
- [36] Witbooi, P., & Vyambwera, S. M. (2017). A model of population dynamics of TB in a prison system and application to South Africa. *BMC research notes*, 10(1), 643. <https://doi.org/10.1186/s13104-017-2968-z>.
- [37] McNeill W. H. (1998). *Plagues and peoples*. Anchor Books/Doubleday.
- [38] Ellner, S., Gallant, A. R., Theiler, J., & Mollison, D. (1995). Epidemic Models: Their Structure and Relation to Data. In: Mollison D., editor. *Epidemic Models: Their Structure and Relation to Data*. Cambridge: Cambridge University Press. pp. 229–247.
- [39] Matthew Glomski, & Edward Ohanian. (2012). Eradicating a Disease: Lessons from Mathematical Epidemiology. *The College Mathematics Journal*, 43(2), 123–132. <https://doi.org/10.4169/college.math.j.43.2.123>.
- [40] Dietz, K. (1988). The first epidemic model: a historical note on PD En'ko. *Australian Journal of Statistics*, 30(1), 56-65.
- [41] Hamer, W. H. (1906). *Epidemic disease in England: the evidence of variability and of persistency of type*. Bedford Press.
- [42] Ross R. Howard L. O. & Gorgas W. C. (1911). *The prevention of malaria (2e éd)*. John Murray.
- [43] M'Kendrick, A. (1925). Applications of Mathematics to Medical Problems. *Proceedings of the Edinburgh Mathematical Society*, 44, 98-130. <https://doi:10.1017/S0013091500034428>.
- [44] Bailey, N. T. (1975). *The mathematical theory of infectious diseases and its applications*. Charles Griffin & Company Ltd, 5a Crendon Street, High Wycombe, Bucks HP13 6LE..

- [45] Guan, W. J., Liang, W. H., Zhao, Y., Liang, H. R., Chen, Z. S., Li, Y. M., Liu, X. Q., Chen, R. C., Tang, C. L., Wang, T., Ou, C. Q., Li, L., Chen, P. Y., Sang, L., Wang, W., Li, J. F., Li, C. C., Ou, L. M., Cheng, B., Xiong, S., . . . China Medical Treatment Expert Group for COVID-19 (2020). Comorbidity and its impact on 1590 patients with COVID-19 in China: a nationwide analysis. *The European respiratory journal*, 55(5), 2000547. <https://doi.org/10.1183/13993003.00547-2020>.
- [46] CDC COVID-19 Response Team (2020). Severe Outcomes Among Patients with Coronavirus Disease 2019 (COVID-19) - United States, February 12-March 16, 2020. *MMWR. Morbidity and mortality weekly report*, 69(12), 343–346. <https://doi.org/10.15585/mmwr.mm6912e2>.
- [47] Volkow N. D. (2020). Collision of the COVID-19 and Addiction Epidemics. *Annals of internal medicine*, 173(1), 61–62. <https://doi.org/10.7326/M20-1212>.
- [48] Worldometer, South African population in 2020. <https://www.worldometers.info/world-population/south-africa-population/> (Accessed on 01 September 2022).
- [49] Bernoulli D. (1766). Essai d’une nouvelle analyse de la mortalite causee par la petite verole. *Mem. Math. Phys. Acad. Roy. Sci., Paris*. 1 (Reprinted in: L.P. Bouckaert, B.L. van der Waerden (Eds.), Die Werke von Daniel Bernoulli, Bd. 2 Analysis und Wahrscheinlichkeitsrechnung, Birkhäuser, Basel, 1982, p. 235. English translation entitled ‘An attempt at a new analysis of the mortality caused by smallpox and of the advantages of inoculation to prevent it’ in: L. Bradley, Smallpox Inoculation: An Eighteenth Century Mathematical Controversy, Adult Education Department, Nottingham, 1971, p. 21. Reprinted in: S. Haberman, T.A. Sibbett (Eds.) History of Actuarial Science, vol. VIII, Multiple Decrement and Multiple State Models, William Pickering, London, 1995, p. 1.).
- [50] En’ko P. D. (1989). On the course of epidemics of some infectious diseases. *International journal of epidemiology*, 18(4), 749–755. <https://doi.org/10.1093/ije/18.4.749>.

- [51] Kermack, W. O., & McKendrick, A. G. (1927). A contribution to the mathematical theory of epidemics. *Proceedings of the royal society of london. Series A, Containing papers of a mathematical and physical character*, 115(772), 700-721.
- [52] Ward M. M. (2013). Estimating disease prevalence and incidence using administrative data: some assembly required. *The Journal of rheumatology*, 40(8), 1241–1243. <https://doi.org/10.3899/jrheum.130675>.
- [53] Etikan, I., Abubakar, S., Alkassim, R. (2017). Frequency measures of epidemiological studies. *Biom Biostat Int J*. 5(1):20-23. <https://doi.org/10.15406/bbij.2017.05.00124>.
- [54] Fajardo-Gutiérrez, Arturo. (2017). Measurement in epidemiology: prevalence, incidence, risk, impact measures. *Revista alergia México*, 64(1), 109-120. <https://doi.org/10.29262/ram.v64i1.252>.
- [55] Vetter, T. R., & Jesser, C. A. (2017). Fundamental Epidemiology Terminology and Measures: It Really Is All in the Name. *Anesthesia and analgesia*, 125(6), 2146–2151. <https://doi.org/10.1213/ANE.0000000000002554>.
- [56] Cesari, L. (1983). Optimization-Theory and Applications. Problems with Ordinary Differential Equations. *Applications and Mathematics. Vol. 17*, Springer-Verlag, New York, Heidelberg-Berlin.
- [57] Wang, X., Song, X.Y. (2007). Global stability and periodic solution of a model for HIV infection of CD4+Tcells. *Applied Mathematics and Computation*, 189, 1331-1340.
- [58] Noordzij, M., Dekker, F. W., Zoccali, C., & Jager, K. J. (2010). Measures of disease frequency: prevalence and incidence. *Nephron. Clinical practice*, 115(1), c17–c20. <https://doi.org/10.1159/000286345>.
- [59] Chasnov, J. R. (2009–2016). *Introduction to Differential Equations*. Lecture notes for MATH 2351/2352. The Hong Kong University of Science and Technology, Department of Mathematics, Clear Water Bay, Kowloon, Hong Kong.
- [60] Allen L. J. S. (2007). *An introduction to mathematical biology*. Pearson/Prentice Hall.

- [61] Britton, N. F., & Britton, N. F. (2003). *Essential mathematical biology* (Vol. 453). London: Springer. <https://doi.org/10.1007/978-1-4471-0049-2>.
- [62] Wang, L., Leenheer, P. D., & Sontag, E. D. (2010). Conditions for Global Stability of Monotone Tridiagonal Systems with Negative Feedback. *Systems & control letters*, 59(2), 130–138. <https://doi.org/10.1016/j.sysconle.2009.12.008>.
- [63] MULDOWNNEY, J. S. (1990). COMPOUND MATRICES AND ORDINARY DIFFERENTIAL EQUATIONS. *The Rocky Mountain Journal of Mathematics*, 20(4), 857–872. <http://www.jstor.org/stable/44237627>.
- [64] Chasnov, J. R. (2009–2016). *Mathematical Biology*. Lecture notes for MATH 4333. The Hong Kong University of Science and Technology, Department of Mathematics, Clear Water Bay, Kowloon, Hong Kong.
- [65] Sutton, K. M. (2014) "Discretizing the SI Epidemic Model," *Rose-Hulman Undergraduate Mathematics Journal*: Vol. 15: Iss. 1, Article 12. Available at: <https://scholar.rose-hulman.edu/rhumj/vol15/iss1/12>.
- [66] Allen L. J. (1994). Some discrete-time SI, SIR, and SIS epidemic models. *Mathematical biosciences*, 124(1), 83–105. [https://doi.org/10.1016/0025-5564\(94\)90025-6](https://doi.org/10.1016/0025-5564(94)90025-6).
- [67] Smith, R. J. (2008). *Modelling disease ecology with mathematics*. Springfield: American Institute of Mathematical Sciences.
- [68] Maku-Vyambwera, S. (2020). *Mathematical modeling of TB disease dynamics in a crowded population*. [PhD Thesis, Department of Mathematics and Applied Mathematics, University of the Western Cape]. Philosophiae Doctor - PhD (Mathematics). <http://hdl.handle.net/11394/7357>.
- [69] Hethcote, H.W. (1989). Three Basic Epidemiological Models. In: Levin, S.A., Hallam, T.G., Gross, L.J. (eds) *Applied Mathematical Ecology*. Biomathematics, vol 18. Springer, Berlin, Heidelberg. https://doi.org/10.1007/978-3-642-61317-3_5.

- [70] Broadbent, A., Combrink, H., & Smart, B. (2020). COVID-19 in South Africa. *Global epidemiology*, 2, 100034. <https://doi.org/10.1016/j.gloepi.2020.100034>.
- [71] Affi, P.O. (2018). Sensitivity Analysis of the SEIR Epidemic Compartment Model, *Int. J. Sci. Res.* 7(12), 352-357.
- [72] van den Driessche, P., & Watmough, J. (2002). Reproduction numbers and sub-threshold endemic equilibria for compartmental models of disease transmission. *Mathematical biosciences*, 180, 29–48. [https://doi.org/10.1016/s0025-5564\(02\)00108-6](https://doi.org/10.1016/s0025-5564(02)00108-6).
- [73] Witbooi, P. J., Maku-Vyambwera, S., Nsuami, M. U. (2023). Control and elimination in an SEIR model for the disease dynamics of COVID-19 with vaccination[J]. *AIMS Mathematics*, 8(4): 8144-8161. <https://doi.org/10.3934/math.2023411>.
- [74] Todorov, E. (2006). Optimal control theory. *Bayesian brain: probabilistic approaches to neural coding*, 268-298. <https://doi.org/10.7551/mitpress/9780262042383.003.0012>.
- [75] Lenhart, S., & Workman, J.T. (2007). *Optimal Control Applied to Biological Models (1st ed.)*. Chapman and Hall/CRC press. <https://doi.org/10.1201/9781420011418>.
- [76] Lenhart, S. M., & Yong, J. (1992). Optimal control for degenerate parabolic equations with logistic growth, preprint of Institute for mathematics and its application. *University of Minnesota, USA, 1064*.
- [77] Witbooi P. J. (2021). An SEIR model with infected immigrants and recovered emigrants. *Advances in difference equations*, 2021(1), 337. <https://doi.org/10.1186/s13662-021-03488-5>.
- [78] Tilahun, G. T., Demie, S., & Eyob, A. (2020). Stochastic model of measles transmission dynamics with double dose vaccination. *Infectious Disease Modelling*, 5, 478–494. <https://doi.org/10.1016/j.idm.2020.06.003>.
- [79] Vyambwera, S. M., & Witbooi, P. (2021). A Two-Group Model of TB in a Crowded Environment. *Appl. Math*, 15(4), 523-532. <http://doi.org/10.18576/amis/150415>.

- [80] Nyabadza, F., Chiyaka, C., Mukandavire, Z., & Hove-Musekwa, S. D. (2010). Analysis of an HIV/AIDS model with public-health information campaigns and individual withdrawal. *Journal of Biological Systems*, 18(2), 357-375. <https://doi.org/10.1142/S0218339010003329>.
- [81] World Health Organization, South African population timeline from 20 July 2020 until 2 November 2020. <https://covid19.who.int/region/afro/country/za> (Accessed on 31 August 2022).
- [82] Son, H. (2018). *Analysis and Optimal control of deterministic Vector-Borne diseases model*. [PhD Dissertation, Department of Mathematics and Statistics, Auburn University]. <http://hdl.handle.net/10415/6294>.
- [83] Rangkuti, Y. M., & Landong, A. (2022, February). Sensitivity analysis of SEIR epidemic model of Covid 19 spread in Indonesia. In *Journal of Physics: Conference Series* (Vol. 2193, No. 1, p. 012092). IOP Publishing. <https://doi.org/10.1088/1742-6596/2193/1/012092>.
- [84] Jassat, W., Mudara, C., Ozougwu, L., Tempia, S., Blumberg, L., Davies, M. A., Pillay, Y., Carter, T., Morewane, R., Wolmarans, M., von Gottberg, A., Bhiman, J. N., Walaza, S., Cohen, C., & DATCOV author group. (2021). Difference in mortality among individuals admitted to hospital with COVID-19 during the first and second waves in South Africa: a cohort study. *The Lancet. Global health*, 9(9), e1216–e1225. [https://doi.org/10.1016/S2214-109X\(21\)00289-8](https://doi.org/10.1016/S2214-109X(21)00289-8).
- [85] National Institute for Communicable Diseases. (2021). COVID-19 sentinel hospital surveillance update, week 53. <https://www.nicd.ac.za/wp-content/uploads/2021/01/NICD-COVID-19-Weekly-Sentinel-Hospital-Surveillnace-update-Week-53.pdf> (accessed June 15, 2021).
- [86] Stiegler, N., & Bouchard, J. P. (2020). South Africa: Challenges and successes of the COVID-19 lockdown. *Annales medico-psychologiques*, 178(7), 695–698. <https://doi.org/10.1016/j.amp.2020.05.006>.

- [87] Greyling, T., Rossouw, S., & Adhikari, T. (2021). The good, the bad and the ugly of lockdowns during Covid-19. *PloS one*, 16(1), e0245546. <https://doi.org/10.1371/journal.pone.0245546>.
- [88] Businesstech. South Africa moves to level 2 lockdown on Monday - here are the new rules. Available online: <https://businesstech.co.za/news/government/425708/south-africa-moves-to-level-2-lockdown-on-monday-here-are-the-new-rules/> (accessed on 29 September 2022).
- [89] October, K. R., Petersen, L. R., Adebisi, B., Rich, E., & Roman, N. V. (2021). COVID-19 Daily Realities for Families: A South African Sample. *International journal of environmental research and public health*, 19(1), 221. <https://doi.org/10.3390/ijerph19010221>.
- [90] Moonasar, D., Pillay, A., Leonard, E., Naidoo, R., Mngemane, S., Ramkrishna, W., Jamaloodien, K., Lebeso, L., Chetty, K., Bamford, L., Tanna, G., Ntuli, N., Mlisana, K., Madikizela, L., Modisenyane, M., Engelbrecht, C., Maja, P., Bongweni, F., Furumele, T., Mayet, N., ... Pillay, Y. (2021). COVID-19: lessons and experiences from South Africa's first surge. *BMJ Global Health*, 6(2):e004393. <https://doi.org/10.1136/bmjgh-2020-004393>.
- [91] Mukumbang, F. C., Ambe, A. N., & Adebisi, B. O. (2020). Unspoken inequality: how COVID-19 has exacerbated existing vulnerabilities of asylum-seekers, refugees, and undocumented migrants in South Africa. *International journal for equity in health*, 19(1), 141. <https://doi.org/10.1186/s12939-020-01259-4>.
- [92] Shen, Z. H., Chu, Y. M., Khan, M. A., Muhammad, S., Al-Hartomy, O. A., & Higazy, M. (2021). Mathematical modeling and optimal control of the COVID-19 dynamics. *Results in physics*, 31, 105028. <https://doi.org/10.1016/j.rinp.2021.105028>.
- [93] Pontryagin, L.S., Boltyanskii, V.G., et al. (1962) The Mathematical Theory of Optimal Processes. *Interscience Publishers John Wiley & Sons, Inc.*, New York-London, Translated from the Russian by K.N., Tiriogoff.

- [94] LYAPUNOV, A. M. (1992). The general problem of the stability of motion, *International Journal of Control*, 55(3), 531-534, <https://doi.org/10.1080/00207179208934253>.
- [95] Mwalili, S., Kimathi, M., Ojiambo, V., Gathungu, D., & Mbogo, R. (2020). SEIR model for COVID-19 dynamics incorporating the environment and social distancing. *BMC research notes*, 13(1), 352. <https://doi.org/10.1186/s13104-020-05192-1>.
- [96] Khalil, H.K., Choi, J. (Spring 2010). *Lecture 10: ME/ECE 859-Nonlinear Systems and Control (The Invariance Principle)* [PowerPoint slides]. Michigan State University: <https://www.egr.msu.edu/classes/me859/jchoi/2010/lecture/index.html>.
- [97] Silva, C. J., & Torres, D. F. (2013). Optimal control for a tuberculosis model with re-infection and post-exposure interventions. *Mathematical biosciences*, 244(2), 154–164. <https://doi.org/10.1016/j.mbs.2013.05.005>.
- [98] World Health Organization, Framework for a Public Health Emergency Operations Centre 24 November 2015 Handbook. <https://www.who.int/publications/i/item/framework-for-a-public-health-emergency-operations-centre>. (Accessed on 21 December 2023).
- [99] Minister Zweli Mkhize reports first case of Coronavirus Covid-19. <https://www.gov.za/news/media-statements/minister-zweli-mkhize-reports-first-case-coronavirus-covid-19-05-mar-2020>. (Accessed on 21 December 2023).
- [100] President Ramaphosa announces a nationwide lockdown. <https://www.sanews.gov.za/south-africa/president-ramaphosa-announces-nationwide-lockdown>. (Accessed on 21 December 2023).
- [101] Blumberg, L., Jassat, W., Mendelson, M., & Cohen, C. (2020). The COVID-19 crisis in South Africa: Protecting the vulnerable. *South African medical journal = Swid-Afrikaanse tydskrif vir geneeskunde*, 110(9), 825–826. <https://doi.org/10.7196/SAMJ.2020.v110i9.15116>.

- [102] South African Government. About alert system 2020. <https://www.gov.za/covid-19/about/about-alert-system>. (Accessed on 21 December 2023).
- [103] Africa, S. S. (2017). Mid-year population estimates, 2017. *Pretoria: Statistics South Africa*.
- [104] Migration Data in the Southern African Development Community (SADC). <https://www.migrationdataportal.org/regional-data-overview/southern-africa>. (Accessed on 21 December 2023).



Listing 1: code for sensitivity indices of R_0

```

1 n=14;
2 n1=(n+1)*7; %Timeline from 20 July 2020 until 2 November 2020
   as seen
3           %on World Health Organization https://covid19.who
   .int/region/afro/country/za (Accessed on 31
   August 2022)
4 P0=59308690; %South African population in 2020 as seen
5           %on Worldometer https://www.worldometers.info/
   world-population/south-africa-population/ (
   Accessed 01/09/2022)
6 beta=0.08/P0; betaB=1.25*beta;%beta=(0.9)*(0.78)/P0; %
   Transmission rate from S to I due to contact via I/A
7 alpha=0.3*beta; b=0; %0.000007; % 0.1*0.15/P0; %alpha=(0.05)*
   beta/P0; %Transmission rate from S to I due to contact
   with P
8 mu=1/(65*365); %Mortality *rate
9 deltaI=0.0002; %Death rate due to Covid-19
10 deltaA=0.0001; %Death rate due to Covid-19
11 omegaI=0.15; omegaA=2*omegaI; %Recovery rate from I pool ***
12 g=0.1; %Proportion of symptomatic infectious persons
13 B1=200; B1B=0; %Rate of influx of asymptomatic migrants, 0.3
   and above
14 gammaI=0.05; %Infection rate from P to I
15 gammaA=0.005; %Infection rate from P to A
16 theta=1/4;
17 C=0.02; %Proportion of interaction with P
18 v=0; %vaccination rate
19 dt=1; %Time step (days)

```

```

20 S=zeros(1,n1+1); %Susceptible values
21 I=zeros(1,n1+1); %Symptomatic infected values
22 A=zeros(1,n1+1); %Asymptomatic Infected values
23 R=zeros(1,n1+1); %Recovered values
24 P=zeros(1,n1+1); %Density values of pathogens in environment
25 NewC=zeros(1,n1+1);
26 tt=zeros(1,n);
27 t=zeros(1,n1+1);
28 S(1)=0.995*P0;
29 I(1)=171000;
30 A(1)=17000;
31 R(1)=0;
32 P(1)=2000;
33
34 %%Calculations
35 %Recovery rate from A pool
36 B0=P0*mu; %Constant inflow of susceptibles
37 B2=(omegaA*B1)*mu; B2B=(omegaA*B1B)*mu; %Departing rate from
    R pool
38 mu0=(mu+v);
39 mu1=(mu+deltaI+omegaI);
40 mu2=(mu+deltaA+omegaA);
41 obsC=[69090/7, 49898/7, 30465/7,23392/7, 15506/7, 14333/7,
    11330/7, 11442/7, 9842/7, 10218/7, 11180/7,11235/7,
    12115/7, 11206/7,10454/7];
42 tt(1)=4; t(1)=0;
43 for i=1:n1
44     t(i+1)=t(i)+1;
45 end

```

```

46 for i=1:n
47     tt(i+1)=tt(i)+7;
48 end
49
50
51 for j=1:n1
52     New=(alpha*S(j)*P(j))/(1+C*P(j))+beta*S(j)*(I(j)+A(j))
           /(1+b*I(j));
53     NewC(j)=New +B1 ;
54     dS=(B0-New-mu0*S(j))*dt; %Change in S
55     S(j+1)=S(j)+dS; %Current S values
56
57     dI=((1-g)*New-mu1*I(j))*dt; %Change in I
58     I(1+j)=I(j)+dI; %Current I values
59
60     dA=(B1+g*New-mu2*A(j))*dt; %B1*(1-1/j)
61     A(j+1)=A(j)+dA; %Current A values
62
63     dR=(v*S(j)+omegaI*I(j)+omegaA*A(j)-mu*R(j)-B2)*dt; %
           Change in R
64     R(1+j)=R(j)+dR; %Current R values
65     P(1+j)=P(j)+(gammaI*I(j)+gammaA*A(j)-theta*P(j))*dt;
66 end
67     I0=I;
68     I0(n1+1)=I(n1);
69     NewC(n1+1)=NewC(n1);
70     BRN=B0*((1-g)*mu2*(beta*theta+alpha*gammaI)+g*mu1*(beta*
           theta+alpha*gammaA))/(mu0*theta*mu1*mu2);
71

```



```

72 %BRN,
73 %figure
74 %plot(t,NewC, 'r'), hold on
75 %plot(tt,obsC,'*'), hold off
76 %legend('Model','Observed 7d ave.')
77 %grid on
78 %grid minor
79 %xlabel('Time in days')
80 %ylabel('Number of new cases')
81 %plot(t,I0,'k'), hold on
82 %plot(tt,obsC,'*'), hold off
83 %legend('Model')
84 %grid on
85 %grid minor
86 %xlabel('Time in days')
87 %ylabel('Number of Active Cases')
88
89 %%% normalized-forward sensitivity indices of R0%%
90 falpha=alpha*((1-g)*(mu+gammaI*(deltaA+omegaA)+g*gammaA*(mu+
      deltaI)))/((1-g)*mu2*(beta*theta+alpha*gammaI)+g*mu1*(beta
      *theta+alpha*gammaA));
91
92 fg=g*(beta*theta*(mu1-mu2)-(gammaI*mu1-gammaA*mu2))/((1-g)*
      mu2*(beta*theta+alpha*gammaI)+g*mu1*(beta*theta+alpha*
      gammaA));
93
94 fbeta=beta*theta*((1-g)*mu2+g*mu1)/((1-g)*mu2*(beta*theta+
      alpha*gammaI)+g*mu1*(beta*theta+alpha*gammaA));
95

```

96 $f_{\gamma I} = \alpha \mu_2 \gamma I (1-g) / ((1-g) \mu_2 (\beta \theta + \alpha \gamma I) + g \mu_1 (\beta \theta + \alpha \gamma A));$

97

98 $f_{\gamma A} = g \alpha \mu_1 \gamma A / ((1-g) \mu_2 (\beta \theta + \alpha \gamma I) + g \mu_1 (\beta \theta + \alpha \gamma A));$

99

100 $f_{\delta I} = -\delta I (\mu_1 \mu (\beta \theta + \alpha \gamma A) + \mu_2 (\beta \theta + \alpha \gamma I) (2\mu + \delta A \omega A)) / ((1-g) \mu_2^2 \mu_1 (\beta \theta + \alpha \gamma I) + g \mu_1^2 \mu_2 (\beta \theta + \alpha \gamma A));$

101

102 $f_{\delta A} = -\delta A (\mu_1 g (\beta \theta + \alpha \gamma A) (\delta I + \omega I) - \mu_2 \mu (1-g) (\beta \theta + \alpha \gamma I)) / ((1-g) \mu_2^2 \mu_1 (\beta \theta + \alpha \gamma I) + g \mu_1^2 \mu_2 (\beta \theta + \alpha \gamma A));$

103

104 $f_{\omega I} = -\omega I (\mu_1 \mu g (\beta \theta + \alpha \gamma A) + \mu_2 (1-g) (\beta \theta + \alpha \gamma I) (2\mu + \delta A \omega A)) / ((1-g) \mu_2^2 \mu_1 (\beta \theta + \alpha \gamma I) + g \mu_1^2 \mu_2 (\beta \theta + \alpha \gamma A));$

105

106 $f_{\omega A} = \omega A (\mu_2 \mu (1-g) (\beta \theta + \alpha \gamma I) - \mu_1 g (\beta \theta + \alpha \gamma A) (\delta I + \omega I)) / ((1-g) \mu_2^2 \mu_1 (\beta \theta + \alpha \gamma I) + g \mu_1^2 \mu_2 (\beta \theta + \alpha \gamma A));$

107

108 $f_{\theta} = (\mu_2 (1-g) (\beta \theta \mu_1 \mu_2 - (\beta \theta + \alpha \gamma I) (\mu \mu_1 + \mu_2 (\delta I + \omega I))) + \mu_1 g (\beta \theta \mu_1 \mu_2 - (\beta \theta + \alpha \gamma A) (\mu \mu_1 + \mu_2 (\delta I +$

```

109      omegaI)))))/((1-g)*mu2^2*mu1*(beta*theta+alpha*gammaI)+g*
110      mu1^2*mu2*(beta*theta+alpha*gammaA));
111
112      fv=-v*(mu2*(1-g)*(beta*theta+alpha*gammaI)*(mu*mu1+mu2*(
113      deltaI+omegaI)))-v*(mu1*g*(beta*theta+alpha*gammaA)*(mu*
114      mu1+mu2*(deltaI+omegaI)))/(mu0*((1-g)*mu2^2*mu1*(beta*
115      theta+alpha*gammaI)+g*mu1^2*mu2*(beta*theta+alpha*gammaA))
116      );
117
118      fmu=mu*(mu2*(1-g)*(beta*theta+alpha*gammaI)*(mu0*mu1-(mu*(3*
119      mu+2*v)+(deltaI+omegaI)*(2*(2*mu+v)+(deltaA+omegaA)))))+mu1
120      *g*(beta*theta+alpha*gammaA)*(mu0*mu2-(mu*(3*mu+2*v)+(
121      deltaI+omegaI)*(2*(2*mu+v)+(deltaA+omegaA)))))/(mu0*((1-g)
122      *mu2^2*mu1*(beta*theta+alpha*gammaI)+g*mu1^2*mu2*(beta*
123      theta+alpha*gammaA)));
124
125      %print -depsc sensitivityofbrn
126      %print -depsc numberofactivecases1111

```

Listing 2: code for COVID-19 model 1

```

1  clc; close all; clear all;
2
3  graphics_toolkit('gnuplot')
4
5  n=14;
6  n1=(n+1)*7; %Timeline from 20 July 2020 until 2 November 2020
7              as seen
8              %on World Health Organization https://covid19.who
9              .int/region/afro/country/za (Accessed on 31

```

```

August 2022)
8 P0=59308690; %South African population in 2020 as seen
9      %on Worldometer https://www.worldometers.info/
      world-population/south-africa-population/ (
      Accessed 01/09/2022)
10 beta=0.08/P0; betaB=1.25*beta;%beta=(0.9)*(0.78)/P0; %
      Transmission rate from S to I due to contact via I/A
11 alpha=0.3*beta; b=0; %0.000007; % 0.1*0.15/P0; %alpha=(0.05)*
      beta/P0; %Transmission rate from S to I due to contact
      with P
12 mu=1/(65*365); %Mortality *rate
13 deltaI=0.0002; %Death rate due to Covid-19
14 deltaA=0.0001; %Death rate due to Covid-19
15 omegaI=0.15; omegaA=2*omegaI; %Recovery rate from I pool ***
16 g=0.1; %Proportion of symptomatic infectious persons
17 B1=200; B1B=0; %Rate of influx of asymptomatic migrants, 0.3
      and above
18 gammaI=0.05; %Infection rate from P to I
19 gammaA=0.005; %Infection rate from P to A
20 theta=1/4;
21 C=0.02; %Proportion of interaction with P
22 v=0; %vaccination rate
23 dt=1; %Time step (days)
24 S=zeros(1,n1+1); %Susceptible values
25 I=zeros(1,n1+1); %Symptomatic infected values
26 A=zeros(1,n1+1); %Asymptomatic Infected values
27 R=zeros(1,n1+1); %Recovered values
28 P=zeros(1,n1+1); %Density values of pathogens in environment
29 NewC=zeros(1,n1+1);

```

```

30 tt=zeros(1,n);
31 t=zeros(1,n1+1);
32 S(1)=0.995*P0;
33 I(1)=171000;
34 A(1)=17000;
35 R(1)=0;
36 P(1)=2000;
37
38 %%Calculations
39 %Recovery rate from A pool
40 B0=P0*mu; %Constant inflow of susceptibles
41 B2=(omegaA*B1)*mu; B2B=(omegaA*B1B)*mu; %Departing rate from
    R pool
42 mu0=(mu+v);
43 mu1=(mu+deltaI+omegaI);
44 mu2=(mu+deltaA+omegaA);
45 obsC=[69090/7, 49898/7, 30465/7,23392/7, 15506/7, 14333/7,
    11330/7, 11442/7, 9842/7, 10218/7, 11180/7,11235/7,
    12115/7, 11206/7,10454/7];
46 tt(1)=4; t(1)=0;
47 for i=1:n1
48     t(i+1)=t(i)+1;
49 end
50 for i=1:n
51     tt(i+1)=tt(i)+7;
52 end
53
54
55 for j=1:n1

```



```

56     New=(alpha*S(j)*P(j))/(1+C*P(j))+beta*S(j)*(I(j)+A(j))
        /(1+b*I(j));
57     NewC(j)=New +B1 ;
58     dS=(B0-New-mu0*S(j))*dt; %Change in S
59     S(j+1)=S(j)+dS; %Current S values
60
61     dI=((1-g)*New-mu1*I(j))*dt; %Change in I
62     I(1+j)=I(j)+dI; %Current I values
63
64     dA=(B1+g*New-mu2*A(j))*dt; %B1*(1-1/j)
65     A(j+1)=A(j)+dA; %Current A values
66
67     dR=(v*S(j)+omegaI*I(j)+omegaA*A(j)-mu*R(j)-B2)*dt; %
        Change in R
68     R(1+j)=R(j)+dR; %Current R values
69     P(1+j)=P(j)+(gammaI*I(j)+gammaA*A(j)-theta*P(j))*dt;
70 end
71 I0=I;
72 I0(n1+1)=I(n1);
73 NewC(n1+1)=NewC(n1);
74 BRN=B0*((1-g)*mu2*(beta*theta+alpha*gammaI)+g*mu1*(beta*
        theta+alpha*gammaA))/(mu0*theta*mu1*mu2);
75
76 BRN ,
77 figure
78 hold on;
79 plot(t,NewC, 'r','LineWidth',1);
80 plot(tt,obsC,'*'), hold off
81 legend('Model','Observed 7d ave.')

```

```

82 grid on
83 grid minor
84 xlabel('Time in days')
85 ylabel('Number of new cases')
86
87 %figure
88 %hold on;
89 %plot (t ,I0 , 'k', 'LineWidth', 1);
90 %plot (tt ,obsC , '* ') , hold off
91 %legend ('Model')
92 %grid on
93 %grid minor
94 %xlabel ('Time in days')
95 %ylabel ('Number of Active Cases')
96
97 print -depsc numberofnewcases1234578
98 %print -depsc  numberofactivecases1111119

```

Listing 3: code for COVID-19 model 2

```

1 clc; close all; clear all;
2
3 graphics_toolkit('gnuplot')
4
5 n=14;
6 n1=(n+1)*7; %Timeline from 20 July 2020 until 2 November 2020
   as seen
7
   %on World Health Organization https://covid19.who.int/region/afro/country/za (Accessed on 31
   August 2022)

```

```

8 P0=59308690; %South African population in 2020 as seen
9           %on Worldometer https://www.worldometers.info/
           world-population/south-africa-population/(
           Accessed 01/09/2022)
10 beta=0.08/P0; kk=1; betaB=(1+kk)*beta;%beta=(0.9)*(0.78)/P0;
           %Transmission rate from S to I due to contact via I/A
11 alpha=0.3*beta; b=0; %0.000007; % 0.1*0.15/P0; %alpha=(0.05)*
           beta/P0; %Transmission rate from S to I due to contact
           with P
12 mu=1/(65*365); %Mortality *rate
13 deltaI=0.0002; %Death rate due to Covid-19
14 deltaA=0.0001; %Death rate due to Covid-19
15 omegaI=0.15; omegaA=2*omegaI; %Recovery rate from I pool ***
16 g=0.1; %Proportion of symptomatic infectious persons
17 B1=200; B1B=0; %Rate of influx of asymptomatic migrants, 0.3
           and above
18 gammaI=0.05; %Infection rate from P to I
19 gammaA=0.005; %Infection rate from P to A
20 theta=1/4;
21 C=0.02; %Proportion of interaction with P
22 v=0; %vaccination rate
23 dt=1; %Time step (days)
24 S=zeros(1,n1+1); %Susceptible values
25 I=zeros(1,n1+1); %Symptomatic infected values
26 A=zeros(1,n1+1); %Asymptomatic Infected values
27 R=zeros(1,n1+1); %Recovered values
28 P=zeros(1,n1+1); %Density values of pathogens in environment
29 NewC=zeros(1,n1+1);
30 tt=zeros(1,n);

```

```

31 t=zeros(1,n1+1);
32 S(1)=0.995*P0;
33 I(1)=171000;
34 A(1)=17000;
35 R(1)=0;
36 P(1)=2000;
37
38 %%Calculations
39 %Recovery rate from A pool
40 B0=P0*mu; %Constant inflow of susceptibles
41 B2=(omegaA*B1)*mu; B2B=(omegaA*B1B)*mu; %Departing rate from
    R pool
42 mu0=(mu+v);
43 mu1=(mu+deltaI+omegaI);
44 mu2=(mu+deltaA+omegaA);
45 obsC=[69090/7, 49898/7, 30465/7,23392/7, 15506/7, 14333/7,
    11330/7, 11442/7, 9842/7, 10218/7, 11180/7,11235/7,
    12115/7, 11206/7,10454/7];
46 tt(1)=4; t(1)=0;
47 for i=1:n1
48     t(i+1)=t(i)+1;
49 end
50 for i=1:n
51     tt(i+1)=tt(i)+7;
52 end
53
54
55 for j=1:15
56     New=(alpha*S(j)*P(j))/(1+C*P(j))+beta*S(j)*(I(j)+A(j))

```

```

        /(1+b*I(j));
57     NewC(j)=New +B1 ;
58     dS=(B0-New-mu0*S(j))*dt; %Change in S
59     S(j+1)=S(j)+dS; %Current S values
60
61     dI=((1-g)*New-mu1*I(j))*dt; %Change in I
62     I(1+j)=I(j)+dI; %Current I values
63
64     dA=(B1+g*New-mu2*A(j))*dt; %B1*(1-1/j)
65     A(j+1)=A(j)+dA; %Current A values
66
67     dR=(v*S(j)+omegaI*I(j)+omegaA*A(j)-mu*R(j)-B2)*dt; %
        Change in R
68     R(1+j)=R(j)+dR; %Current R values
69     P(1+j)=P(j)+(gammaI*I(j)+gammaA*A(j)-theta*P(j))*dt;
70 end
71
72 for j=16:n1
73     New=(alpha*S(j)*P(j))/(1+C*P(j))+(1+kk*((j-16)/n1)^(0.5)
        )*beta*S(j)*(I(j)+A(j))/(1+b*I(j));
74     NewC(j)=New +B1 ;
75     dS=(B0-New-mu0*S(j))*dt; %Change in S
76     S(j+1)=S(j)+dS; %Current S values
77
78     dI=((1-g)*New-mu1*I(j))*dt; %Change in I
79     I(1+j)=I(j)+dI; %Current I values
80
81     dA=(B1+g*New-mu2*A(j))*dt; %B1*(1-1/j)
82     A(j+1)=A(j)+dA; %Current A values

```



```

83
84     dR=(v*S(j)+omegaI*I(j)+omegaA*A(j)-mu*R(j)-B2)*dt; %
           Change in R
85     R(1+j)=R(j)+dR; %Current R values
86     P(1+j)=P(j)+(gammaI*I(j)+gammaA*A(j)-theta*P(j))*dt;
87 end
88
89 NewC(16)=(4*NewC(15)+2*NewC(17))/6;
90
91 I0=I;
92 I0(n1+1)=I(n1);
93 NewC(n1+1)=NewC(n1);
94 BRN=B0*((1-g)*mu2*(beta*theta+alpha*gammaI)+g*mu1*(beta*
           theta+alpha*gammaA))/(mu*theta*mu1*mu2);
95 betakk=(1+kk*((n1-16)/n1)^(0.5))*beta;
96 BRNkk=B0*((1-g)*mu2*(betakk*theta+alpha*gammaI)+g*mu1*(
           betakk*theta+alpha*gammaA))/(mu0*theta*mu1*mu2);
97
98 BRN, BRNkk, betakk,
99 figure
100 hold on;
101 plot(t,NewC,'r','LineWidth',1);
102 plot(tt,obsC,'*'), hold off
103 legend('Modified Model','Observed 7d ave.')
104 grid on
105 grid minor
106 xlabel('Time in days')
107 ylabel('Number of new cases')
108

```

```

109 %hold on;
110 %plot(t,IO,'k','LineWidth',1);
111 %plot(tt,obsC,'*'), hold off
112 %legend('Modified Model')
113 %grid on
114 %grid minor
115 %xlabel('Time in days')
116 %ylabel('Number of Active Cases')
117
118 print -depsc numberOfNewCasesModified3456789
119 %print -depsc numberOfActiveCasesModified111224

```

Listing 4: Optimal Control for COVID-19 model

```

1 clc; close all; clear all;
2
3 graphics_toolkit('gnuplot')
4
5 %Parameters of Runge-Kutta 4th order method
6 test=-1; Keer= -1000; plas=1.0001;
7 t(1)=0; M=105;
8 deltaError = 0.001;
9 t=zeros(1,M+1)
10 h=1;
11 h2=h/2; h6=h/6;
12
13 %Model parameters
14 P0=59308690;
15 beta=(0.08)/P0; betaB=(1.25)*beta; alpha=(0.3)*beta; b=0; mu
    =1/(65*365); deltaI=0.0002; deltaA=0.0001;

```

```

16 C=0.02; omegaI=0.15; omegaA=(2)*omegaI; v=0.054; mu0=(mu+v);
    mu1=(mu+deltaI+omegaI); mu2=(mu+deltaA+omegaA);
17 g=0.1; B0=P0*mu; B1=200; B1B=0; B2=(omegaA*B1)*mu; B2B=(
    omegaA*B1B)*mu; gammaI=0.05; gammaA=0.005; theta=1/4;
18
19 %Weight constants
20 w1=0.08; w2=0.000967; w3=0.0528; w4=0.0421; %w2=0.00006
21
22 %Initial conditions of model
23 S(1)=(0.995).*P0; I(1)=171000; A(1)=17000; R(1)=0; P(1)
    =2000; %I(1)=(0.005).*P0;
24 S=zeros(1,M+1); I=zeros(1,M+1); A=zeros(1,M+1); R=zeros(1,M
    +1); P=zeros(1,M+1);
25
26 %Initial guess of control inputs
27 u1=zeros(1,M+1); u2=zeros(1,M+1);
28
29 %Initial conditions for adjoint equations
30 lambda1=zeros(1,M+1); lambda2=zeros(1,M+1); lambda3=zeros(1,M
    +1); lambda4=zeros(1,M+1); lambda5=zeros(1,M+1);
31 %lambda1(M+1)=0; lambda2(M+1)=0; lambda3(M+1)=0; lambda4(M+1)
    =0; lambda5(M+1)=0;
32
33 %Forward-backward sweep
34 loopcount=0; %Counts the number of loops
35 for i=1:M
36     t(i+1)=t(i)+h;
37 end
38 while(test < 0)

```

```

39 loopcount=loopcount+1;
40
41 Keer=Keer+plas;
42
43     oldu1=u1;
44     oldu2=u2;
45
46     oldS=S;
47     oldI=I;
48     oldA=A;
49     oldR=R;
50     oldP=P;
51
52 oldlambda1=lambda1;
53 oldlambda2=lambda2;
54 oldlambda3=lambda3;
55 oldlambda4=lambda4;
56 oldlambda5=lambda5;
57
58 %Forward sweep
59 for i=1:M
60     %State equations
61     k11=B0-((alpha*S(i)*P(i))/(1+C*P(i)))-(beta*S(i)*(1-u1(i))
        *(I(i)+A(i)))-(mu+v*u2(i))*S(i);
62     k12=((alpha*S(i)*P(i))/(1+C*P(i)))+(beta*S(i)*(1-u1(i))*(I(
        i)+A(i)))-((g*alpha*S(i)*P(i))/(1+C*P(i)))...
63         -(g*alpha*S(i)*(I(i)+A(i)))-mu1*I(i);
64     k13=B1+((g*alpha*S(i)*P(i))/(1+C*P(i)))+(g*alpha*S(i)*(I(i)
        +A(i)))-mu2*A(i);

```

```

65 k14=v*u2(i)*S(i)+omegaI*I(i)+omegaA*A(i)-mu*R(i)-B2;
66 k15=gammaI*I(i)+gammaA*A(i)-theta*P(i);
67
68 %New approximations
69 S(i+1)=S(i)+h*k11;
70 I(i+1)=I(i)+h*k12;
71 A(i+1)=A(i)+h*k13;
72 R(i+1)=R(i)+h*k14;
73 P(i+1)=P(i)+h*k15;
74 end
75
76 %Backward sweep
77 for i=1:M %Initial value to final value
78     j=M+2-i; %Final value to initial value
79
80     %Adjoint equations
81     z11=((alpha*P(j)*(lambda1(j)-lambda2(j)))/(1+C*P(j)))+
82         beta*(1-u2(j))*(I(j)+A(j))*(lambda1(j)-lambda2(j))...
83         +((g*alpha*P(j)*(lambda2(j)-lambda3(j)))/(1+C*P(j))
84         )+g*beta*(I(j)+A(j))*(lambda2(j)-lambda3(j))...
85         +v*u2(j)*(lambda1(j)-lambda4(j))+mu1*lambda1(j);
86
87     z12=-w3+beta*S(j)*(1-u1(j))*(lambda1(j)-lambda2(j))+g*
88         beta*S(j)*(lambda2(j)-lambda3(j))...
89         +mu1*lambda2(j)-omegaI*lambda4(j)-gammaI*lambda5(j)
90         ;
91
92     z13=-w4+beta*S(j)*(1-u1(j))*(lambda1(j)-lambda2(j))+g*
93         beta*S(j)*(lambda2(j)-lambda3(j))...

```



```

89         +mu2*lambda3(j)-omegaA*lambda4(j)-gammaA*lambda5(j)
90         ;
91     z14=mu*lambda4(j);
92
93     z15=((alpha*S(j)*(lambda1(j)-lambda2(j)))/((1+C*P(j))
94         .^2))+((g*alpha*S(j)*(lambda2(j)-lambda3(j)))/((1+C*
95         P(j)).^2))...
96         +theta*lambda5(j);
97
98 %New approximations
99 lambda1(j-1)=lambda1(j)-h*z11;
100 lambda2(j-1)=lambda2(j)-h*z12;
101 lambda3(j-1)=lambda3(j)-h*z13;
102 lambda4(j-1)=lambda4(j)-h*z14;
103 lambda5(j-1)=lambda5(j)-h*z15;
104 end
105
106 %Optimality conditions
107 u1=(beta.*S.*(I+A));
108 u1=(lambda2-lambda1).*u1;
109 u1=u1./((2).*w1);
110 u1= min(max(0, u1), 1);
111 u1=(u1+oldu1)./2;
112
113 u2=(v.*S);
114 u2=(lambda1-lambda4).*u2;
115 u2=u2./((2).*w2);
116 u2= min(max(0, u2), 1);

```

```

115 u2=(u2+oldu2)./2;
116
117 %Absolute error for convergence
118 temp1a=deltaError*sum(abs(u1))-sum(abs(oldu1-u1));
119 temp1b=deltaError*sum(abs(u2))-sum(abs(oldu2-u2));
120 temp1=min(temp1a,temp1b)
121
122 temp2a=deltaError*sum(abs(S))-sum(abs(oldS-S));
123 temp2b=deltaError*sum(abs(I))-sum(abs(oldI-I));
124 temp2c=deltaError*sum(abs(A))-sum(abs(oldA-A));
125 temp2d=deltaError*sum(abs(R))-sum(abs(oldR-R));
126 temp2e=deltaError*sum(abs(P))-sum(abs(oldP-P));
127 temp2=min(min(min(min(temp2a,temp2b),temp2c),temp2d),temp2e);
128
129 temp3a=deltaError*sum(abs(lambda1))-sum(abs(oldlambda1-
    lambda1));
130 temp3b=deltaError*sum(abs(lambda2))-sum(abs(oldlambda2-
    lambda2));
131 temp3c=deltaError*sum(abs(lambda3))-sum(abs(oldlambda3-
    lambda3));
132 temp3d=deltaError*sum(abs(lambda4))-sum(abs(oldlambda4-
    lambda4));
133 temp3e=deltaError*sum(abs(lambda5))-sum(abs(oldlambda5-
    lambda5));
134 temp3=min(min(min(min(temp3a,temp3b),temp3c),temp3d),temp3e);
135
136 %test = min(min([temp1 temp2 temp3 temp4 temp5 temp6 temp7
    temp8 temp9 temp10 ...
137 %temp11]),Keer);

```

```
138 test=max(min(temp3,min(temp2,temp1)), Keer);
139 end
140 test,
141
142 figure
143 plot(t,S)
144 legend('S(t)')
145 grid on
146 grid minor
147 xlabel('Days')
148
149 figure
150 plot(t,I)
151 legend('I(t)')
152 grid on
153 grid minor
154 xlabel('Days')
155
156 figure
157 plot(t,A)
158 legend('A(t)', "location", "east")
159 grid on
160 grid minor
161 xlabel('Days')
162
163 figure
164 plot(t,R)
165 legend('R(t)', "location", "east")
166 grid on
```

```

167 grid minor
168 xlabel('Days')
169
170 figure
171 plot(t,P)
172 legend('P(t)', "location", "east")
173 grid on
174 grid minor
175 xlabel('Days')
176
177 figure
178 plot(t,u1,'b -.', 'LineWidth',1)
179 legend('u1*(t)')
180 grid on
181 grid minor
182 xlabel('Days')
183
184 figure
185 plot(t,u2,'r', 'LineWidth',1)
186 legend('u2*(t)')
187 grid on
188 grid minor
189 xlabel('Days')
190
191 figure
192 plot(t,u1,'b -.', 'LineWidth',1); hold on;
193 plot(t,u2,'r', 'LineWidth',1);
194 legend('u1*(t)', 'u2*(t)', "location", "northeast")
195 grid on

```



```
196 grid minor
197 xlabel('Days')
198
199 %print -depsc asymptomaticinfectiouspopulation.eps
```

